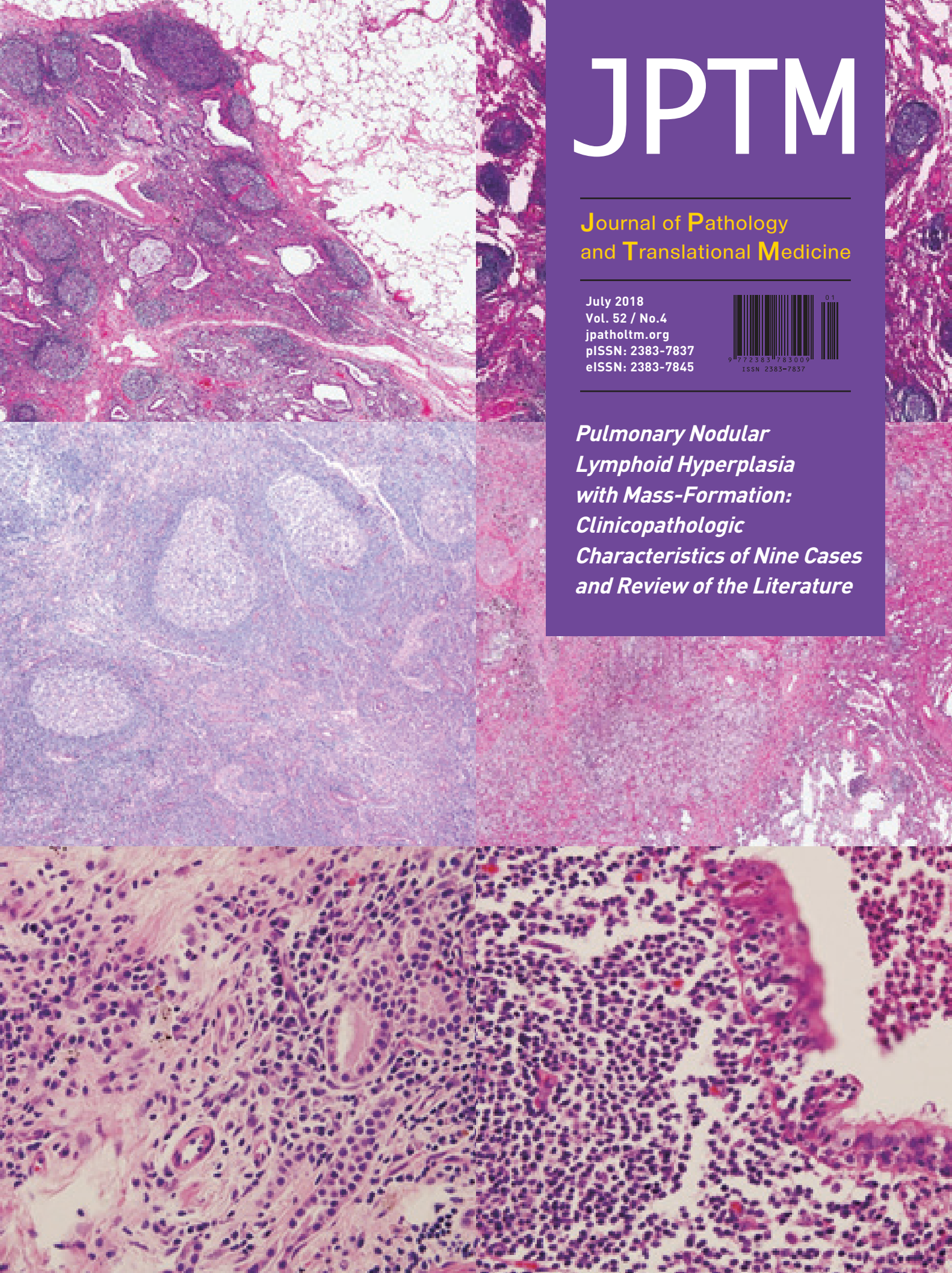

JPTM

Journal of Pathology and Translational Medicine

July 2018
Vol. 52 / No.4
jpatholtm.org
pISSN: 2383-7837
eISSN: 2383-7845

Pulmonary Nodular Lymphoid Hyperplasia with Mass-Formation: Clinicopathologic Characteristics of Nine Cases and Review of the Literature

Journal of Pathology and Translational Medicine

Volume 52 • Number 4 • July 2018 (bimonthly)
Published since 1967
Printed on 11 July 2018 Published on 15 July 2018

J Pathol Transl Med
pISSN: 2383-7837
eISSN: 2383-7845

Aims & Scope

The Journal of Pathology and Translational Medicine is an open venue for the rapid publication of major achievements in various fields of pathology, cytopathology, and biomedical and translational research. The Journal aims to share new insights into the molecular and cellular mechanisms of human diseases and to report major advances in both experimental and clinical medicine, with a particular emphasis on translational research. The investigations of human cells and tissues using high-dimensional biology techniques such as genomics and proteomics will be given a high priority. Articles on stem cell biology are also welcome. The categories of manuscript include original articles, review and perspective articles, case studies, brief case reports, and letters to the editor.

Subscription Information

To subscribe to this journal, please contact the Korean Society of Pathologists/the Korean Society for Cytopathology. Full text PDF files are also available at the official website (http://jpatholtm.org). *Journal of Pathology and Translational Medicine* is indexed by Emerging Sources Citation Index (ESCI), PubMed, PubMed Central, Scopus, KoreaMed, KoMCI, WPRIM, Directory of Open Access Journals (DOAJ), and CrossRef. Circulation number per issue is 700.

Contact the Korean Society of Pathologists/the Korean Society for Cytopathology

Publishers: Jae Bok Park, MD, Hye Kyoung Yoon, MD
Editors-in-Chief: Soon Won Hong, MD, Chong Jai Kim, MD
Published by the Korean Society of Pathologists/the Korean Society for Cytopathology

Editorial Office
Room 1209 Gwanghwamun Officia, 92 Saemunan-ro, Jongno-gu, Seoul 03186, Korea
Tel: +82-2-795-3094 Fax: +82-2-790-6635 E-mail: office@jpatholtm.org

#1508 Renaissancetower, 14 Mallijae-ro, Mapo-gu, Seoul 04195, Korea
Tel: +82-2-593-6943 Fax: +82-2-593-6944 E-mail: office@jpatholtm.org

Printed by iMiS Company Co., Ltd. (JMC)
Jungang Bldg. 18-8 Wonhyo-ro 89-gil, Yongsan-gu, Seoul 04314, Korea
Tel: +82-2-717-5511 Fax: +82-2-717-5515 E-mail: ml@smileml.com

Manuscript Editing by InfoLumi Co.
210-202, 421 Pangyo-ro, Bundang-gu, Seongnam 13522, Korea
Tel: +82-70-8839-8800 E-mail: infolumi.chang@gmail.com

Front cover image: Histopathological features of pulmonary nodular lymphoid hyperplasia (Fig. 3). p214.

This journal was supported by the Korean Federation of Science and Technology Societies Grant funded by the Korean Government.

Journal of Pathology and Translational Medicine

J Pathol Transl Med
pISSN: 2383-7837
eISSN: 2383-7845

Volume 52, Number 4, July 2018

CONTENTS

ORIGINAL ARTICLES

CASE REPORTS

CONTENTS CONTINUED

Instructions for Authors for *Journal of Pathology and Translational Medicine* are available at http://jpatholtm.org/authors/authors.php

Journal of Pathology and Translational Medicine 2018; 52: 211-218
https://doi.org/10.4132/jptm.2018.04.27

■ ORIGINAL ARTICLE ■

Pulmonary Nodular Lymphoid Hyperplasia with Mass-Formation: Clinicopathologic Characteristics of Nine Cases and Review of the Literature

Jongmin Sim · Hyun Hee Koh
Sangjoon Choi · Jinah Chu
Tae Sung Kim[1] · Hojoong Kim[2]
Joungho Han

Department of Pathology and Translational Genomics, [1]Department of Radiology, [2]Division of Pulmonary and Critical Care Medicine, Department of Medicine, Samsung Medical Center, Sungkyunkwan University School of Medicine, Seoul, Korea

Received: December 4, 2017
Revised: April 23, 2018
Accepted: April 27, 2018

Corresponding Author
Joungho Han, MD
Department of Pathology and Translational Genomics, Samsung Medical Center, Sungkyunkwan University School of Medicine, 81 Irwon-ro, Gangnam-gu, Seoul 06351, Korea
Tel: +82-2-3410-2765
Fax: +82-2-3410-0025
E-mail: hanjho@skku.edu

Background: Pulmonary nodular lymphoid hyperplasia (PNLH) is a non-neoplastic pulmonary lymphoid disorder that can be mistaken for malignancy on radiography. Herein, we present nine cases of PNLH, emphasizing clinicoradiological findings and histological features. **Methods:** We analyzed radiological and clinicopathological features from the electronic medical records of nine patients (eight females and one male) diagnosed with PNLH. IgG and IgG4 immunohistochemical staining was performed in three patients. **Results:** Two of the nine patients had experienced tuberculosis 40 and 30 years prior, respectively. Interestingly, none were current smokers, although two were ex-smokers. Three patients complaining of persistent cough underwent computed tomography of the chest. PNLH was incidentally discovered in five patients during examination for other reasons. The remaining patient was diagnosed with the disease following treatment for pneumonia. Imaging studies revealed consolidation or a mass-like lesion in eight patients. First impressions included invasive adenocarcinoma and mucosal-associated lymphoid tissue-type lymphoma. Aspergillosis was suspected in the remaining patient based on radiological images. Resection was performed in all patients. Microscopically, the lesions consisted of nodular proliferation of reactive germinal centers accompanied by infiltration of neutrophils and macrophages in various degrees and surrounding fibrosis. Ultimately, all nine patients were diagnosed with PNLH and showed no evidence of recurrence on follow-up. **Conclusions:** PNLH is an uncommon but distinct entity with a benign nature, and understanding the radiological and clinicopathological characteristics of PNLH is important.

Key Words: Pseudolymphoma; Pulmonary nodular lymphoid hyperplasia

Non-neoplastic pulmonary lymphoproliferative disorders include nodular lymphoid hyperplasia, follicular bronchiolitis, lymphocytic interstitial pneumonia, Castleman's disease, and intrapulmonary lymph node.[1-3] The term "pseudolymphoma" was initially proposed in 1963 by Saltzstein[4] in his study on pulmonary lymphoid lesions. Kradin and Mark[5] later suggested the term "pulmonary nodular lymphoid hyperplasia" (PNLH). Abbondanzo *et al*.[6] also suggested that PNLH consisted of reactive pulmonary lesions ranging from follicular hyperplasia to diffuse hyperplasia of the bronchus-associated lymphoid tissue.[7]

On microscopy, PNLH is composed of reactive nodular lymphoid proliferation that forms one or more pulmonary masses.[2,6-8] However, the other lymphoproliferative lesions mentioned above should be considered, especially malignant lymphomas. Diagnosis can be made using hematoxylin and eosin (H&E) staining of slides with the addition of immunohistochemical (IHC) staining for CD3, CD20, and Ki-67. If necessary, kappa and light chain IHC staining and/or an immunoglobulin heavy chain (IgH) gene rearrangement test can be performed in cases with polyclonal results.[6-9]

PNLH is a benign, reactive, and uncommon lesion.[6,7,10] In the present study, the histopathological features and radiological findings in the resected lungs of nine patients diagnosed with PNLH were evaluated.

MATERIALS AND METHODS

Case selection and clinical data

The electronic medical records of Samsung Medical Center were searched for lung specimens of patients diagnosed with PNLH between January 2012 and September 2017. We excluded

pISSN 2383-7837
eISSN 2383-7845

lymphoid interstitial pneumonia and other lymphoproliferative disorders that were not nodular or reactive. Clinical characteristics of patients were also retrieved from the electronic medical records, including age, sex, chief complaint, past and/or current history, smoking history, and radiological findings. The present study protocol was reviewed and approved by the Institutional Review Board (IRB) of Samsung Medical Center (IRB No. 2017-10-055-011). Formal written informed consent was not required and was waived by the IRB.

Pathological evaluation

Two pathologists (J. Han and J. Sim) reviewed the slides of selected cases. Primary malignant lymphomas and other lymphoproliferative lesions were excluded. IHC staining with CD3 (A0452, Dako, Glostrup, Denmark), CD20 (L26, Leica, Wetzlar, Germany), and Ki-67 (MIB-1, Dako) was performed in all cases. BCL2 (124, Dako), BCL6 (LN22, Novocastra, Newcastle upon Tyne, UK), and kappa and lambda light chain (Dako) IHC staining was performed in only one patient who showed a diffuse pattern (case 6). Additionally, the IgG4:IgG ratio was assessed using IgG (Dako) and IgG4 (MRQ-44, Cell Marque, Rocklin, CA, USA) antibodies in only three cases which showed plasma cell infiltration (cases 1, 2, and 6). Special staining was performed to confirm the presence of microorganisms. Molecular tests such as IgH gene rearrangement test were not performed in any case.

Table 1. Clinical features of patients with pulmonary lymphoid hyperplasia

No.	Age	Sex	TB	Smoking history	Chief complaint	Site	S/M	Radiology finding	Procedure	Dx	Size (cm)	Follow up (mo)
1	42	F	None	Never	GGO after treatment for pneumonia	LUL	S	Persistent subsegmental consolidation DDx 1) MALT-type lymphoma 2) R/O Organizing pneumonia	Segm	PNLH with post-obstructive change	7	10
2	62	F	40 YA	Never	Cough	RLL	M	Persistent two consolidative lesions R/O malignancy such as MALT-type lymphoma or mucinous adenocarcinoma	Lobe	PNLH with post-obstructive change	5.5	4
3	57	F	30 YA	Never	Cough	LUL	S	Increase in extent of 58 mm subsolid lesion DDx 1) Focal organizing pneumonia 2) Invasive adenocarcinoma 3) MALT-type lymphoma	Segm	PNLH with post-obstructive change	4.9	
4	59	F	None	Never	Incidentally found when work-up for angina	LLL	S	Lesion showing air-crescent sign with peribronchail bronchiectasis R/O Aspergilloma	Segm	PNLH with post-obstructive change	1.2	15
5	79	F	None	Never	Cough	LUL	S	A 33-mm-sized ill-defined mass-like lesion R/O Lung cancer	Wedge	PNLH with post-obstructive change	3.3	4
6	50	F	None	Never	Incidentally found on follow up for SLE	LLL	S	A 45-mm growing poorly-defined consolidative mass lesion DDx 1) Mucinous adenocarcinoma 2) Organizing pneumonia, less likely	Wedge	PNLH with post-obstructive change	4.5	18
7	39	F	None	Ex 10 YA stop	Incidentally found	LLL	S	Wide ground-glass opacity lesion DDx 1) Invasive adenocarcinoma 2) Pneumonia	Lobe	PNLH with post-obstructive change	4.5	4
8	69	F	None	Never	Incidentally found on health-exam	RUL	S	A 14-mm-sized oval nodular lesion DDx 1) Benign nodule, more likely 2) invasive adenocarcinoma due to faint uptake on PET	Segm	PNLH with post-obstructive change	1.4	3
9	59	M	None	Ex 2 YA	Incidentally found on follow-up for emphysema	RLL	S	A 18-mm irregular nodular lesion with strong enhancement DDx 1) Focal organizing pneumonia 2) Hypervascular lung cancer	Wedge	PNLH with post-obstructive change	2	3

TB, tuberculosis; S, solitary; M, multiple; Dx, diagnosis; F, female; GGO, ground glass opacity; LUL, left upper lobe; DDx, differential diagnosis; MALT, mucosa-associated lymphoid tissue; R/O, rule out; Segm, segmentectomy; PNLH, pulmonary nodular lymphoid hyperplasia; YA, years ago; RLL, right lower lobe; Lobe, lobectomy; LLL, left lower lobe; Wegde, wedge resection; SLE, systemic lupus erythematosus; EX, ex-smoker; RUL, right upper lobe; PET, positron emission tomography.

https://doi.org/10.4132/jptm.2018.04.27

RESULTS

Clinical and radiological findings

Table 1 shows the clinicopathological characteristics of the nine patients (eight females and one male). The mean age was 57.3 years (range, 39 to 79 years). Two patients (patients 2 and 3) had a history of tuberculosis 40 and 30 years prior, respectively. Seven patients had never smoked, and the other two patients were ex-smokers who stopped smoking 20 and 2 years prior, respectively; none of the patients were current smokers. Three patients were diagnosed with cough symptoms, and five were accidentally discovered during an examination for other reasons, including angina, emphysema, health examination, and systemic lupus erythematosus. The remaining patient was identified after treatment for pneumonia. Only one patient (patient 6) had several autoimmune antibody tests. Antinuclear antibody titer was 1:40 with a nuclear pattern. Negative results were obtained for several autoimmune antibodies, including anti-Sjogren's syndrome A, anti-Sjogren's syndrome B, anti-ribonucleoprotein, anti-Sm, and anti-neutrophil cytoplasmic antibodies. The lesions were solitary in eight patients and multiple in one patient (patient 2). Most radiological findings were persistent and/or slow-growing consolidation lesions (Fig. 1). In eight patients, the possibility of primary lymphoma or primary lung cancer was suspected based on radiological findings. One patient (patient 4) was suspected of aspergilloma based on radiological images. Recurrence, previous disease, or new lesions were not observed in any patient during the 3–18 months of radiological follow-up.

Pathological features

Although gross images were not available in four patients, soft-to-firm and well-circumscribed lesions were observed in most cases on gross examination. An infiltrative mass-like lesion mimicking invasive lung cancer was observed on one image (Fig. 2A).

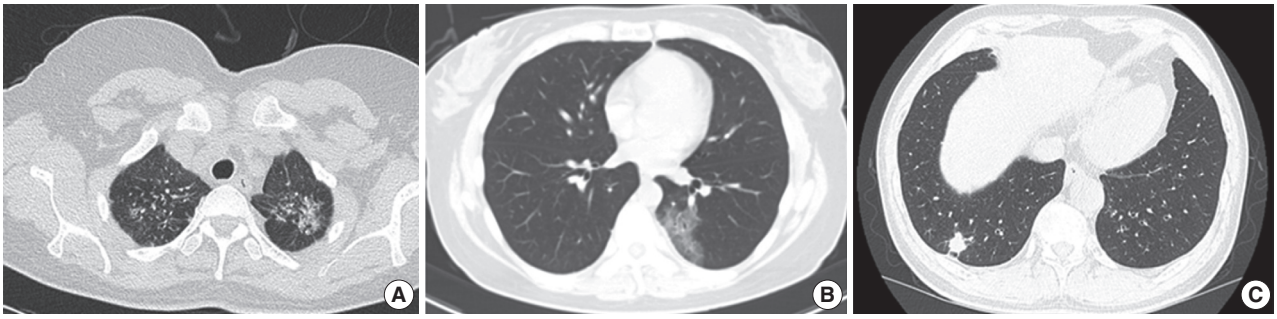

Fig. 1. Radiological images (chest computed tomography) of three patients before surgery. (A) Image from patient 3 shows the extent of a 58-mm subsolid lesion in the lingular division of the left upper lobe. (B) Image from patient 7 shows a wide ground-glass opacity lesion in the superior segment of the left lower lobe. (C) Image from patient 9 shows an 18-mm irregular nodular lesion with strong enhancement in the posterior basal segment of the right lower lobe.

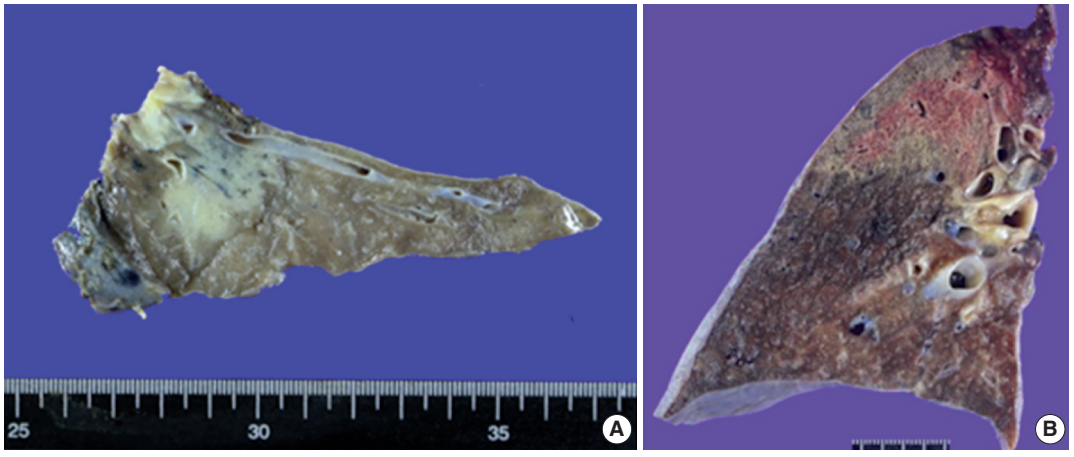

Fig. 2. Gross findings of pulmonary nodular lymphoid hyperplasia. (A) Gross image from patient 3 shows a relatively well-circumscribed grayish-white mass-forming lesion with firm consistency. (B) Gross image from patient 7 displays a well-defined lesion with soft-to-firm consistency.

The remaining four patients showed a relatively well-defined lesion with soft-to-firm consistency (Fig. 2B).

Based on microscopy, the lesions were relatively well-defined with a nodular pattern. Although six of nine patients had well-marginated and regular borders (Fig. 3A), three had a relatively well-demarcated, irregular borders (Fig. 3B). Four cases showed a nodular pattern (Fig. 3B), and the other five showed a mixed diffuse and nodular pattern (Fig. 3C, D). Each lesion was composed of polymorphous lymphoid cells, reactive germinal centers, and infiltration of a variety of neutrophils, plasma cells, and macrophages without a carcinoma component. No Dutcher bodies or invasion of the pleura were present in any case. In addition, three cases showed moderate neutrophilic infiltration with a few macrophages. In contrast, moderate to marked infiltration of macrophages with rare neutrophilic infiltration was observed in five cases. The remaining one showed marked infiltration of neutrophils and macrophages. The degree of fibrosis was variable. Three cases showed rare or mild fibrosis (Fig. 3A, B), and the remaining six displayed moderate to marked fibrosis (Fig. 3D). However, the pattern of fibrosis was not storiform in any case. Obliterative arteritis or phlebitis suggesting IgG4-related disease was not detected in any patient. The amount of plasma cell infiltration also varied from scattered to dense. The plasma cell infiltration was in a scattered pattern in three cases and moderate to marked in six cases (Fig. 3E). Two patients had mild lymphoepithelial lesions which were not extensive or destructive (Fig. 3F). Microscopic features are summarized in Table 2.

IHC staining for B cells showed numerous B cells within reactive follicles in all cases (Fig. 4A). IHC staining for CD3 displayed many T cells in interfollicular areas and occasional T cells within reactive follicles (Fig. 4B). A high proliferative activity (Ki-67 index) was observed in reactive follicles (Fig. 4C), dividing dark and light zones. Although two cases showed a diffuse pattern, diffuse B-cell infiltration which is a characteristic of extranodal marginal zone lymphoma of mucosal-associated lymphoid tissue (MALT)-type lymphoma was not identified by CD3 and CD20 IHC staining (Fig. 4D, E). Additionally, BCL2 and BCL6 IHC staining confirmed inter-follicular lymphoid cells and germinal centers (Fig. 4F, G). Moreover, kappa and lambda light chain IHC staining did not reveal any monoclonality (Fig. 4H, I).

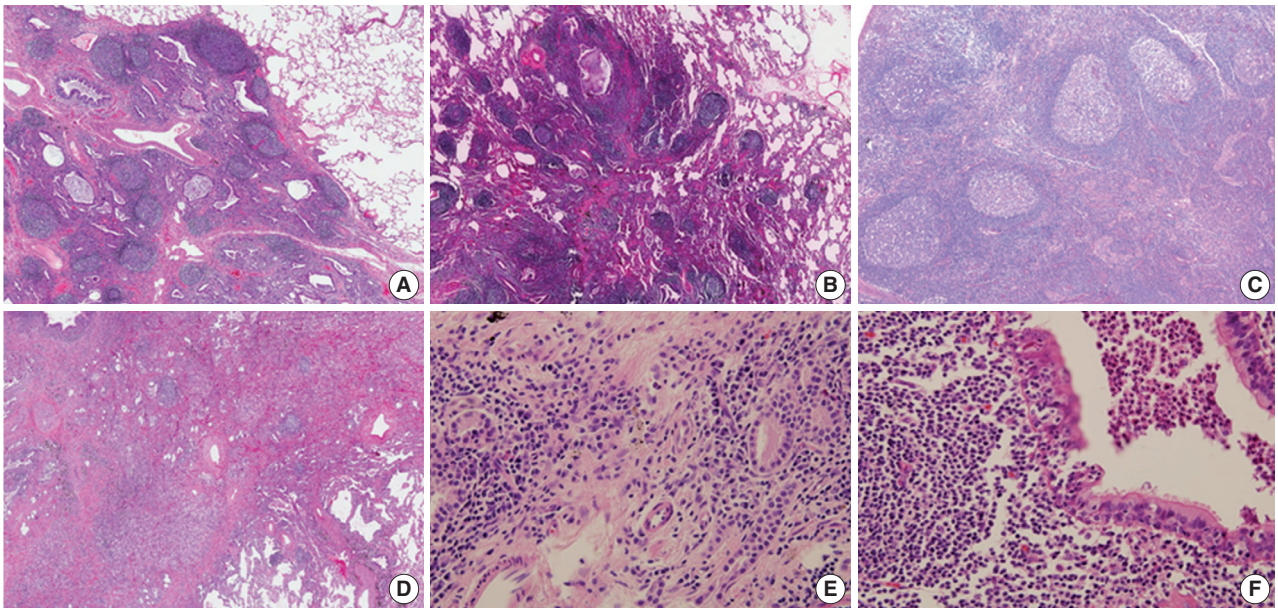

Fig. 3. Histopathological features on hematoxylin and eosin slides of pulmonary nodular lymphoid hyperplasia. (A) In patient 2, a well-circumscribed lesion was observed. The lesion consisted of reactive germinal centers with septal fibrosis, moderate infiltration of neutrophils, and a few macrophages. (B) In patient 4, the lesion was relatively well-defined with irregular borders and rare fibrosis. The lesion was composed of reactive germinal centers with marked infiltration of macrophages. A fungal ball was present in the bronchus at the upper portion of the image and was confirmed using Grocott's methenamine silver stain and Periodic acid–Schiff stain (not shown). (C) In patient 6, the lesion was composed of scattered reactive germinal centers with moderate infiltration of macrophages. No fibrous septum was present. (D) In patient 5, a relatively well-demarcated lesion with irregular border was observed. The lesion consisted of a few reactive germinal centers with fibrosis and marked infiltration of macrophages. (E) In patient 4, the lesion showed moderate infiltration of plasma cells between germinal centers. However, storiform fibrosis or obliterative phlebitis was not detected. (F) Patient 1 showed a mild form of lymphoepithelial lesion. However, the lesion was not extensive or destructive, suggesting extranodal marginal zone lymphoma of mucosal-associated lymphoid tissue.

https://doi.org/10.4132/jptm.2018.04.27

Thus, PNLH was diagnosed as such. In all patients, molecular tests such as IgH gene rearrangement test were not required to differentiate malignant lymphomas. Patient 4 showed an aspergillus species that was confirmed by Grocott's methenamine silver stain and periodic acid–Schiff stain (not shown). The IgG4:IgG ratio was less than 0.2 in three patients, which was not compatible

Table 2. Histologic characteristics of patients with pulmonary lymphoid hyperplasia

No.	Border	Location	Pattern	Germinal centers	Lymphoepithelial lesions	Fibrosis	Plasma cell	Neutrophils	Histiocytes	Other findings
1	Well-defined	Subpleural	Nodular	Present	Present	+	++	++	+++	-
2	Well-defined	Subpleural	Diffuse	Present	Not definite	+	+	++	+	-
3	Irregular	Subpleural	Nodular	Present	Not definite	-	++	+	+	-
4	Irregular	Subpleural	Nodular	Present	Not definite	-	+	-	++	Aspergillosis
5	Well-defined	Subpleural	Diffuse	Present	Not definite	++	+++	-	+++	-
6	Well-defined	Subpleural	Diffuse	Present	Present	-	+++	-	+	-
7	Well-defined	Subpleural	Diffuse	Present	Not definite	+	+	+	++	-
8	Well-defined	Subpleural	Nodular	Present	Not definite	++	+++	+	++	-
9	Irregular	Subpleural	Diffuse	Present	Not definite	++	++	-	++	-

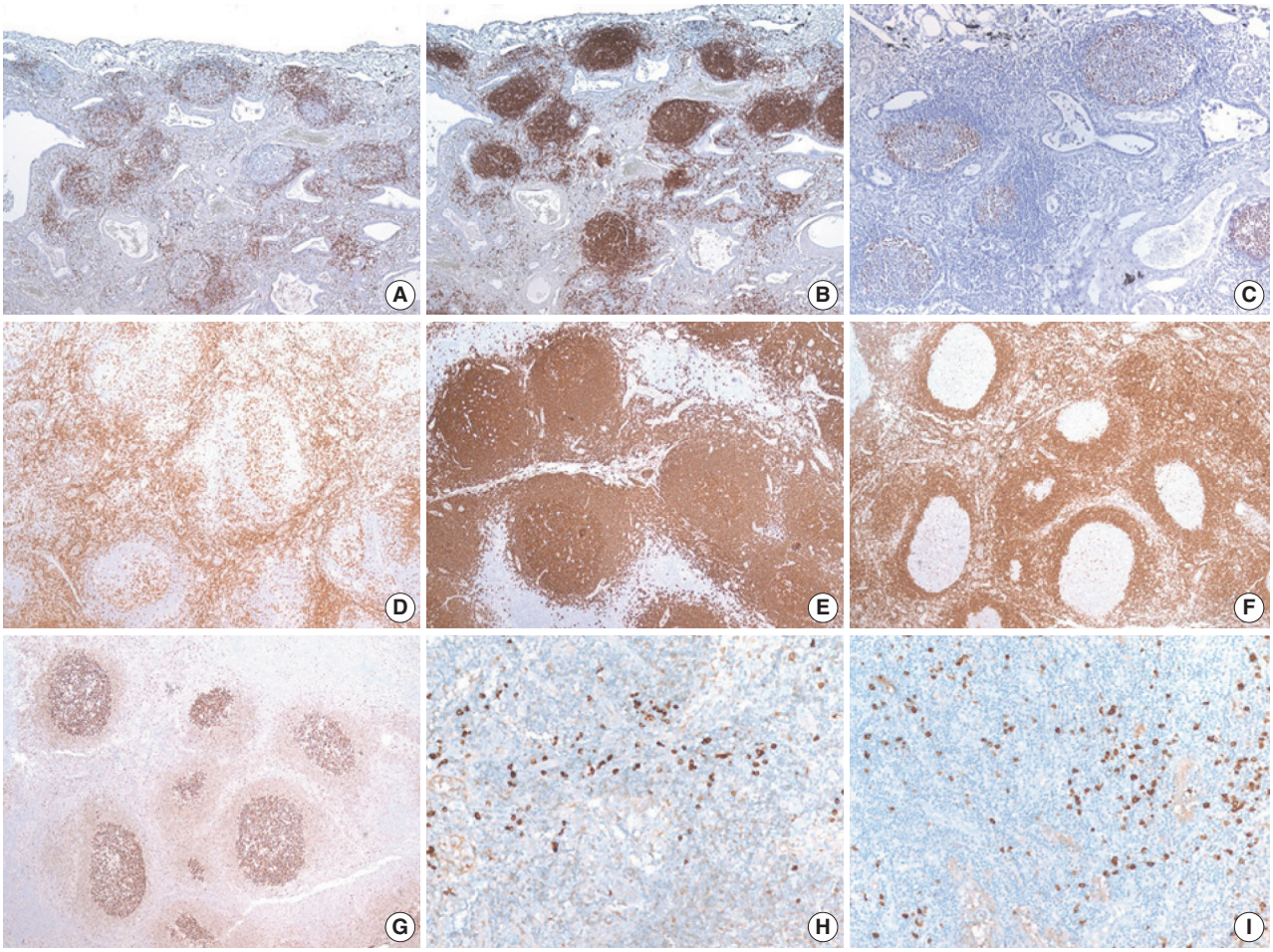

Fig. 4. Immunohistochemical (IHC) results of pulmonary nodular lymphoid hyperplasia. IHC staining using CD20 (A) and CD3 (B) showed that the lesion in patient 2 had several well-preserved germinal centers with mixed inter-follicular T-cells. (C) Ki-67 IHC staining showed high proliferative activity in the germinal center. IHC staining using CD3 (D) and CD20 (E) showed an inter-follicular T-cell zone and germinal center in the lesion in patient 6, confirming a diffuse pattern. (F, G) Additionally, the inter-follicular and germinal centers were IHC stained with BCL2 and BCL6. (H, I) IHC staining of kappa and lambda light chains indicated a polyclonal population.

with IgG4-related disease (Fig. 5).

DISCUSSION

We reviewed clinicopathological features of nine PNLH patients. Based on radiological findings, eight patients were suspected to have a malignancy such as adenocarcinoma or MALT-type lymphoma, and one showed a solid mass-forming lesion on gross examination. However, histological findings on H&E staining showed benign reactive lesions. Non-extensive lymphoepithelial lesions were present in two patients. However, extensive lymphoepithelial lesion, Dutcher bodies, or pleural invasion were not observed. Additional IHC staining for CD3, CD20, and Ki-67 showed no evidence of malignancy. Only one case showed a diffuse pattern; additional staining was required to distinguish the lesion from MALT-type lymphoma. IHC staining of kappa and lambda light chain indicated a polyclonal population. Molecular testing such as IgH gene rearrangement test was not performed in any case.

PNLH is usually asymptomatic and in most cases is found incidentally during examination for other reasons. As mentioned above, PNLH is a benign lesion typically diagnosed histologically using H&E-stained slides.[2,3,6,9] Based on histological analysis, PNLH is composed of reactive germinal centers with a nodular pattern and is mainly located in the subpleural area. Fibrosis and infiltration of other inflammatory cells are variable. Lymphoepithelial lesions with lymphocytes infiltrating the bronchial epithelium can occur;[10] however, no pleural or bronchus invasion is observed.[6,10] Although presence of a single lesion is common, the clinical course of solitary and multiple lesions is similar. Based on radiological findings, PNLH appears as a consolidation or mass-like lesion and cannot be easily distinguished from lung cancer or malignant lymphoma, especially when the size increases during follow-up.[7] Differential diseases include lymphoid interstitial pneumonia, follicular bronchitis, and MALT-type lymphoma.[2,8,9,11] Lymphoid interstitial pneumonia infiltrates the lungs as a whole and does not form a germinal center. MALT-type lymphoma also presents with a diffuse pattern with monotonous lymphoid cells. Dutcher bodies, pleural invasion, and bronchus invasion are common in MALT-type lymphoma. IHC staining and/or IgH gene rearrangement test indicate a monoclonal population. The key features of PNLH and MALT-type lymphoma are summarized in Table 3.

In 2000, Abbondanzo *et al*.[6] reported clinicopathological features of 14 patients with PNLH. They demonstrated that PNLH was mainly asymptomatic, incidentally found on radiological imaging or due to complaints of cough, and often observed as a mass on radiological imaging. Although most patients presented with a single mass smaller than 3 cm, others were as large as 5 cm. Histological analysis showed that PNLH has germinal centers with a nodular pattern, sometimes accompanied by fibrosis. Lymphoepithelial lesions, pleural plaques, or bronchial cartilage involve-

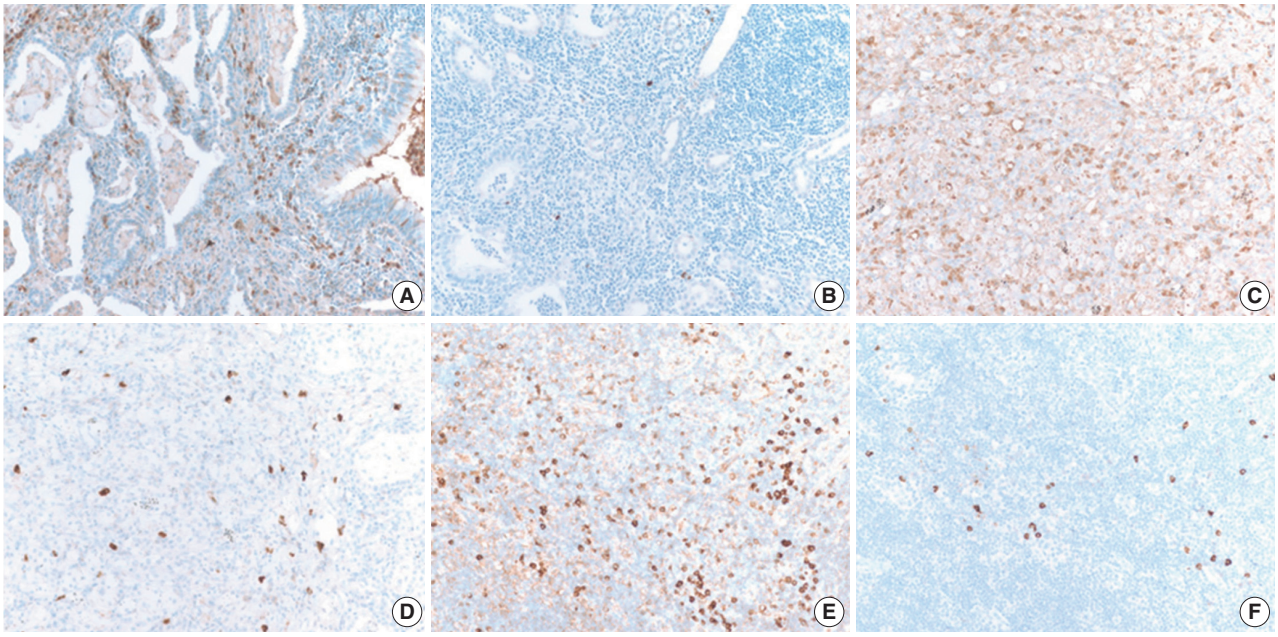

Fig. 5. IgG4:IgG ratio of pulmonary nodular lymphoid hyperplasia. The IgG4:IgG ratio varied in this study. The ratio in case 1 was less than 0.1 (A, IgG; B, IgG4). The ratios in case 5 (C, IgG; D, IgG4) and case 6 (E, IgG; F, IgG4) were approximately 0.1–0.2, which is not compatible with IgG4-related disease.

 https://doi.org/10.4132/jptm.2018.04.27

Table 3. Key features of pulmonary nodular hyperplasia and extranodal marginal zone lymphoma of mucosa-associated lymphoid tissue (MALT)

	Pulmonary nodular lymphoma hyperplasia	Extranodal marginal zone lymphoma of MALT
Clinical feature	Usually asymptomatic	Often asymptomatic Cough and dyspnea
Radiographic finding	Single or multiple (rare), mass or mass-like area of consolidation	Single or multiple, mass and/or areas of consolidation
Histologic feature		
Growth pattern	Nodular pattern	Diffuse or nodular pattern
Component	Mixed cell population, reactive germinal center, and fibrosis	Small lymphocytes which indistinguishable from mature lymphocytes Often monocytoid B-cells May be follicular colonization
Lymphoepithelial lesion	Rare, often	Common
Ducther body	Absent	Common with plasmacytoid differentiation
Pleural or bronchus invasion	Absent	Frequent
Ancillary test		
Immunohistochemistry	Reactive pattern, having well preserved germinal center High proliferative activity in germinal center	Diffuse pattern in B-cell marker Low proliferative activity
IgH gene rearrangement test	Polyclonal	Monoclonal

ment was not observed. However, Begueret *et al*.[10] demonstrated that PNLH could also have lymphoepithelial lesions. They further found the lymphoepithelial lesions in MALT-type lymphoma were $CD20^+/CD43^+$, in contrast to $CD3^+/CD43^+$ or $CD20^+/CD43^-$ lesions in lymphoid hyperplasia. Moreover, they found no intralymphatic extension in lymphoid hyperplasia.

In 2013, Guinee *et al*.[12] reported that the number of IgG4-positive plasma cells was significantly higher in PNLH than in other lesions. Their study included six patients with PNLH, nine patients with MALT-type lymphoma, eight patients with intrapulmonary lymphoma, eight patients with follicular bronchitis, and four patients with lymphoid interstitial pneumonia. They demonstrated that the IgG4/IgG ratio in PNLH was significantly higher than in other lesions. Moreover, two of six PNLH patients had an IgG4/IgG ratio greater than 0.4. However, in 2017, Bois *et al*.[13] reported that the ratio in 26 PNLH patients was not higher than that in controls. The control group in their study included two patients with diffuse lymphoid hyperplasia without nodularity, five patients with usual interstitial pneumonia and increased lymphoplasmacytic infiltrates, and two patients with thoracic lymphadenopathy. In addition, they found that PNLH had a low IgG4/IgG ratio that did not suggest IgG4-related disease and reported no evidence of Epstein-Barr virus infection. In our study, IgG and IgG4 IHC staining results were available in three patients. Similar to the previous results, there was no evidence of IgG4-related disease in those patients. Whether PNLH is associated with IgG4-related disease requires further evaluation with a greater number of patients.

Interstitial lung disease (ILD) may be the first presentation of connective tissue diseases (CTDs); up to 15% of patients initially diagnosed with idiopathic nonspecific interstitial pneumonia (NSIP) have an underlying systemic autoimmune rheumatic disease upon further evaluation.[14,15] The most common histological pattern in patients with CTD is NSIP.[14] However, no evidence of ILD except PNLH was found in the systemic lupus erythematosus patient included in this study. Moreover, on radiological analysis, ILD was not evident. PNLH in patients with Sjogren's syndrome was previously reported.[16] To determine whether PNLH is associated with CTD requires further studies with a larger cohort.

In addition, we observed that PNLH could have various degrees of fibrosis as well as neutrophil and macrophage. Patients with PNLH could possibly be diagnosed using some of the organizing pneumonia spectrum as a post-obstructive change due to mass formation. Moderate to marked infiltration of neutrophils with rare macrophage infiltration could represent a relatively early phase of organizing pneumonia, while numerous macrophages and surrounding fibrosis with rare neutrophil infiltration are more likely to indicate progression of organizing pneumonia.

In conclusion, we report a mass-like or consolidative lesion in nine patients with PNLH. Differential diagnosis of PNLH includes MALT-type lymphoma and other benign lymphoproliferative disorders. Although molecular tests were not performed, meticulous pathological examination can aid in diagnosing PNLH with confidence.

ORCID

Jongmin Sim: https://orcid.org/0000-0002-7106-1279

Hyun Hee Koh: https://orcid.org/0000-0003-2050-3564
Sangjoon Choi: https://orcid.org/0000-0003-2108-0575
Jinah Chu: https://orcid.org/0000-0001-9050-084X
Tae Sung Kim: https://orcid.org/0000-0001-7512-0283
Hojoong Kim: https://orcid.org/0000-0001-9207-0433
Joungho Han: https://orcid.org/0000-0003-4424-7008

Conflicts of Interest

No potential conflict of interest relevant to this article was reported.

REFERENCES

1. Travis WD, Galvin JR. Non-neoplastic pulmonary lymphoid lesions. Thorax 2001; 56: 964-71.
2. Guinee DG Jr. Update on nonneoplastic pulmonary lymphoproliferative disorders and related entities. Arch Pathol Lab Med 2010; 134: 691-701.
3. Yi E, Aubry MC. Pulmonary pseudoneoplasms. Arch Pathol Lab Med 2010; 134: 417-26.
4. Saltzstein SL. Pulmonary malignant lymphomas and pseudolymphomas: classification, therapy, and prognosis. Cancer 1963; 16: 928-55.
5. Kradin RL, Mark EJ. Benign lymphoid disorders of the lung, with a theory regarding their development. Hum Pathol 1983; 14: 857-67.
6. Abbondanzo SL, Rush W, Bijwaard KE, Koss MN. Nodular lymphoid hyperplasia of the lung: a clinicopathologic study of 14 cases. Am J Surg Pathol 2000; 24: 587-97.
7. Sirajuddin A, Raparia K, Lewis VA, *et al*. Primary pulmonary lymphoid lesions: radiologic and pathologic findings. Radiographics 2016; 36: 53-70.
8. Poletti V, Ravaglia C, Tomassetti S, *et al*. Lymphoproliferative lung disorders: clinicopathological aspects. Eur Respir Rev 2013; 22: 427-36.
9. Arcadu A, Moua T, Yi ES, Ryu JH. Lymphoid interstitial pneumonia and other benign lymphoid disorders. Semin Respir Crit Care Med 2016; 37: 406-20.
10. Begueret H, Vergier B, Parrens M, *et al*. Primary lung small B-cell lymphoma versus lymphoid hyperplasia: evaluation of diagnostic criteria in 26 cases. Am J Surg Pathol 2002; 26: 76-81.
11. Tashtoush B, Okafor NC, Ramirez JF, Smolley L. Follicular bronchiolitis: a literature review. J Clin Diagn Res 2015; 9: OE01-5.
12. Guinee DG Jr, Franks TJ, Gerbino AJ, Murakami SS, Acree SC, Koss MN. Pulmonary nodular lymphoid hyperplasia (pulmonary pseudolymphoma): the significance of increased numbers of IgG4-positive plasma cells. Am J Surg Pathol 2013; 37: 699-709.
13. Bois MC, Sekiguchi H, Ryu JH, Yi ES. No definite clinical features of immunoglobulin G4-related disease in patients with pulmonary nodular lymphoid hyperplasia. Hum Pathol 2017; 59: 80-6.
14. Atzeni F, Gerardi MC, Barilaro G, Masala IF, Benucci M, Sarzi-Puttini P. Interstitial lung disease in systemic autoimmune rheumatic diseases: a comprehensive review. Expert Rev Clin Immunol 2018; 14: 69-82.
15. Mittoo S, Gelber AC, Christopher-Stine L, Horton MR, Lechtzin N, Danoff SK. Ascertainment of collagen vascular disease in patients presenting with interstitial lung disease. Respir Med 2009; 103: 1152-8.
16. Song MK, Seol YM, Park YE, et al. Pulmonary nodular lymphoid hyperplasia associated with Sjogren's syndrome. Korean J Intern Med 2007; 22: 192-6.

Journal of Pathology and Translational Medicine 2018; 52: 219-225
https://doi.org/10.4132/jptm.2018.05.16

ORGINAL ARTICLE

Endobronchial Smooth Muscle Tumors: A Series of Five Cases Highlighting Pitfalls in Diagnosis

Tripti Nakra · Aanchal Kakkar
Shipra Agarwal · Karan Madan[1]
Suresh C Sharma[2] · Deepali Jain

Departments of Pathology, [1]Pulmonary Medicine, and [2]Otorhinolaryngology, All India Institute of Medical Sciences, New Delhi, India

Received: April 17, 2018
Revised: May 14, 2018
Accepted: May 15, 2018

Corresponding Author
Deepali Jain, MD, DNB, FIAC
Department of Pathology, All India Institute of Medical Sciences, New Delhi 110029, India
Tel: +91-9868895112
Fax: +91-11-26588663
E-mail: deepalijain76@gmail.com

Background: Primary endobronchial smooth muscle tumors (SMTs), which are extremely rare, include endobronchial leiomyomas and leiomyosarcomas. Clinically, SMTs present with signs and symptoms of bronchial obstruction, and lack specific radiological findings. Thus, histopathological examination is required for accurate diagnosis as well as for tumor grading. We examined the histomorphological and immunohistochemical features of endobronchial SMTs and highlighted pitfalls in diagnosis, particularly when using small biopsies. **Methods:** Cases of primary endobronchial SMTs diagnosed at our Institute over the last 6 years (2012–2017) were retrieved from the departmental archives. Histopathological features and immunohistochemistry performed for establishing the diagnosis were reviewed. **Results:** Five cases of SMTs occurring in endobronchial locations were identified. These included three cases of leiomyoma, and two cases of leiomyosarcoma. The age distribution of patients ranged from 13 to 65 years. Leiomyomas showed more consistent staining with smooth muscle markers (smooth muscle actin, desmin, and smooth muscle myosin heavy chain), while tumors of higher grade showed variable, focal staining, leading to erroneous diagnosis, especially on small biopsies. **Conclusions:** The diagnosis of endobronchial SMTs relies on histopathological examination, for both confirmation of smooth muscle lineage and determination of the malignant potential of the lesion. Appropriate immunohistochemical panels including more than one marker of smooth muscle differentiation are extremely valuable for differential diagnosis from morphological mimics, which is necessary for instituting appropriate management.

Key Words: Endobronchial; Leiomyoma; Leiomyosarcoma; Smooth muscle tumor; Immunohistochemistry

Primary bronchopulmonary mesenchymal tumors are rare. Among these, the most frequent are smooth muscle tumors (SMTs), which include leiomyomas and leiomyosarcomas (LMS).[1] They are believed to arise from the peri-bronchiolar/interstitial smooth muscle, or rarely from smooth muscle of arteriolar walls.[2] Leiomyomas constitute 2% of benign lung tumors, and are more commonly located in lung parenchyma (51%), while endobronchial and tracheal leiomyomas account for 33% and 16%, respectively.[2] LMS accounts for less than 0.5% of primary pulmonary malignancies, and approximately one-third of primary sarcomas of the lung.[3] Only a few cases of endobronchial localization of LMS have been reported in the literature.[3]

Patients with endobronchial SMTs present with symptoms reflecting partial or complete obstruction of the affected bronchus, including wheezing, orthopnea, hemoptysis, or changes in the lung distal to the obstruction, such as recurrent pneumonia and subsequent bronchiectasis.[4] SMTs have been observed in patients with human immunodeficiency virus infections, as well as other immunosuppressed conditions. Coinfection with Epstein-Barr virus (EBV) may play a role in the development of these tumors. AIDS-related EBV-associated SMTs have been reported in endobronchial locations as well.[5] Imaging per se does not help much in the diagnosis of SMTs as there are no pathognomonic features to differentiate SMTs from more common endobronchial tumors.[4] Thus, histopathological examination is required for accurate diagnosis as well as for tumor grading, as the prognosis of SMTs depends upon the grade and degree of differentiation of the tumor. Complete surgical resection is the favored treatment modality for SMTs, irrespective of tumor grade. We describe five cases of endobronchial SMTs and their clinicoradiopathological features, and highlight difficulties in differential diagnosis.

MATERIALS AND METHODS

Cases of primary endobronchial SMTs diagnosed at our institution over a period of 6 years (2012–2017) were retrieved from

pISSN 2383-7837
eISSN 2383-7845

the departmental archives. Clinical, radiological, and treatment details were collected from the hospital medical record system and by telephonic conversation. Hematoxylin and eosin stained slides were retrieved, and histopathological features, as well as immunohistochemistry performed for establishing the diagnosis, were reviewed. Immunostaining for EBV–latent membrane protein 1 (LMP1) was performed in all cases. Approval from the Institute Ethics Committee (IEC no. 404/02.09.2016), All India Institute of Medical Sciences, was obtained to conduct this retrospective study on archival patient samples and thus, informed consent was waived due to the retrospective nature of this study.

RESULTS

Five cases of SMTs occurring in endobronchial locations were identified from the records, including one previously published case.[6] These included three cases of leiomyoma and two cases of LMS. In all cases, the tumor was excised through transtracheal or transbronchial approaches. Clinical presentation, radiological findings, and clinical diagnoses are summarized in Table 1. Patient 1 underwent bronchoscopy (Fig. 1) and biopsy at our institution, after which a diagnosis of leiomyoma was made. He subsequently underwent a lobectomy at a private hospital. Patient 4 underwent a biopsy, after which a diagnosis of inflammatory myofibroblastic tumor (IMT) was made. This was followed by

Table 1. Clinical features, imaging findings and pathological diagnosis of five cases of SMTs

Case No.	Age (yr)/ Sex	Clinical presentation	Imaging	Bronchoscopy	Clinical diagnosis	Pathology diagnosis	Management and outcome
1	13/M	Cough, hemoptysis ×3 mo	Intraluminal soft tissue mass of 3.5 cm in RMB	Mass lesion in RMB	Benign tumor	Leiomyoma	Excision; symptom-free at 5 yr
2	18/M	Non-smoker; dyspnea, cough, fever ×8 mo	1 cm endotracheal growth with calcification	Lower tracheal growth arising from postero- lateral wall of RMB	Benign tumor	Leiomyoma	Excision; symptom-free at 7 mo
3	65/M	Smoker; hemoptysis SOB×4 days	Intraluminal nodule of 0.5 cm in LMB	LMB nodule	Tuberculosis vs. malignancy	Leiomyoma	Excision; symptom-free at 4 mo
4	28/F	Dyspnea, hemoptysis ×1 yr	RMB tumor of 3.5 cm with carina involvement and right lung collapse	Endobronchial lobulated growth occluding the RMB just distal to carina	Inflammatory myofibroblastic tumor	LMS	Radiotherapy 30 cycles/60 Gy, after which patient is asymptomatic for 8 mo
5	57/F	Non-smoker; chest pain×1 yr; h/o ATT	5.1 cm mass in lower lobe of right lung	Intrabronchial growth	Lung carcinoma with bone and liver metastases	LMS	Chemotherapy 9 cycles; marked reduction in size at 9 mo

SMT, smooth muscle tumor; M, male; RMB, right main bronchus; SOB, shortness of breath; LMB, left main bronchus; F, female; LMS, leiomyosarcoma; h/o, history of; ATT, anti-tubercular treatment.

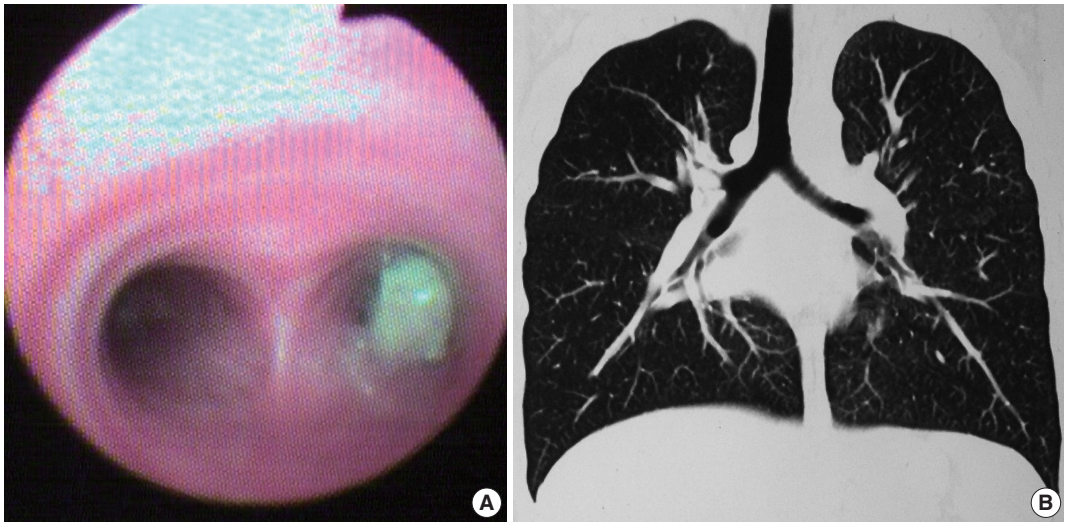

Fig. 1. Clinical and radiological features in patient 1. (A) Flexible bronchoscopic image showing an endoluminal mass in the right main bronchus. (B) Coronal computed tomography reconstructed image showing a mass lesion in the right main bronchus (case 1).

https://doi.org/10.4132/jptm.2018.05.16

excision of the tumor repeated thrice due to the presence of residual disease. For patient 5 only a biopsy was performed, as she presented with an endobronchial mass with multiple metastases to the bone and to both lobes of the liver, suggesting a primary in an endobronchial location. Detailed clinical workups did not reveal any evidence of primary extrapulmonary malignancy in any of the cases.

Cases 1, 2, and 3

Histopathological examination showed squamous metaplasia of the lining bronchial epithelium in cases 1 and 2. The subepithelium showed a sparsely cellular spindle cell tumor with cells arranged in short and long intersecting fascicles (Fig. 2A). The cells had abundant eosinophilic cytoplasm, and ovoid nuclei with homogeneous chromatin (Fig 2B). Paranuclear vacuoles were noted focally. The cells did not show nuclear atypia or mitotic figures; necrosis was also absent. Case 1 showed few inflammatory cells, including lymphocytes and histiocytes, interspersed between tumor cells. Areas of myxoid change, hyalinization, calcification, and mast cells were noted in case 2 (Fig. 2C, D). Immunohistochemical features are summarized in Table 2.

Cases 4 and 5

Microscopic examination (Figs. 3, 4) showed tissue fragments with metaplastic squamous epithelial lining. The subepithelium revealed the presence of cellular spindle cell tumor, with cells arranged in short and long intersecting fascicles. The tumor cells were plump with moderate amounts of pale to brightly

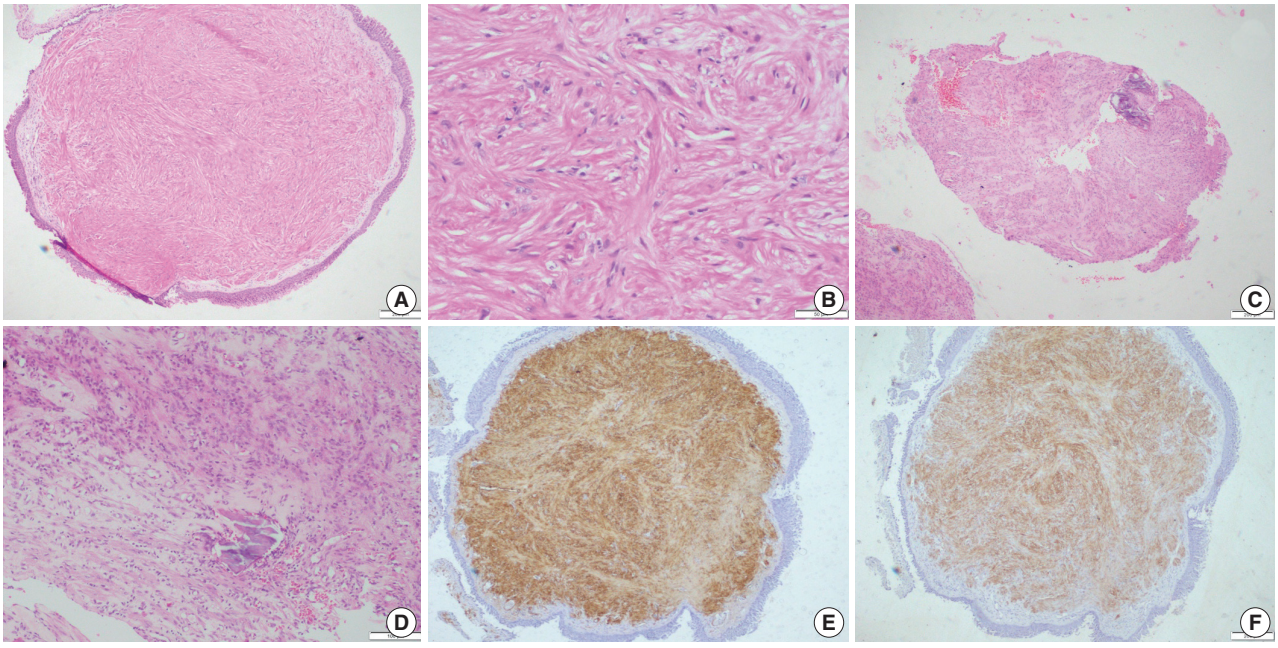

Fig. 2. Leiomyoma. (A) Photomicrographs of case 3 show bronchial epithelium with a sub-epithelial spindle cell tumor arranged in fascicles. (B) Tumor cells have abundant cytoplasm and ovoid nuclei with homogeneous chromatin. (C, D) Areas of hyalinization and calcification are noted in case 2. Immunohistochemistry shows diffuse smooth muscle actin (E) and desmin positivity (F).

Table 2. Immunohistochemical features of five cases of endobronchial smooth muscle tumors

Case No.	SMA	Desmin	SMMHC	Pan-CK	EMA	S-100	HMB-45	ALK-1	EBV-LMP1	MIB-1 LI (%)	Final diagnosis
1	Diffuse+	Diffuse+	Diffuse+	Negative	Negative	Negative	Negative	Negative	Negative	1–2	LM
2	Diffuse+	Focal+	Diffuse+	Negative	Negative	Negative	Negative	Negative	Negative	1–2	LM
3	Diffuse+	Diffuse+	Diffuse+	Negative	Negative	Negative	Negative	Negative	Negative	1	LM
4	Focal+	Focal+	Focal+	Negative	Negative	Focal+	Negative	Negative	Negative	8–10	LMS
	Focal+	Diffuse+	Focal+	Negative	Negative	Negative	Negative	Negative	Negative	8–10	-
	Negative	Focal+	Focal+	Negative	Negative	Focal+	Negative	Negative	Negative	10	
5	Diffuse+	Focal+	Diffuse+	Negative	Focal+	Negative	Negative	Negative	Negative	10	LMS

SMA, smooth muscle actin; SMMHC, smooth muscle myosin heavy chain; CK, cytokeratin; EMA, epithelial membrane antigen; HMB-45, human melanoma black 45; EBV, Epstein-Barr virus; LMP1, latent membrane protein; LM, leiomyoma; LMS, leiomyosarcoma.

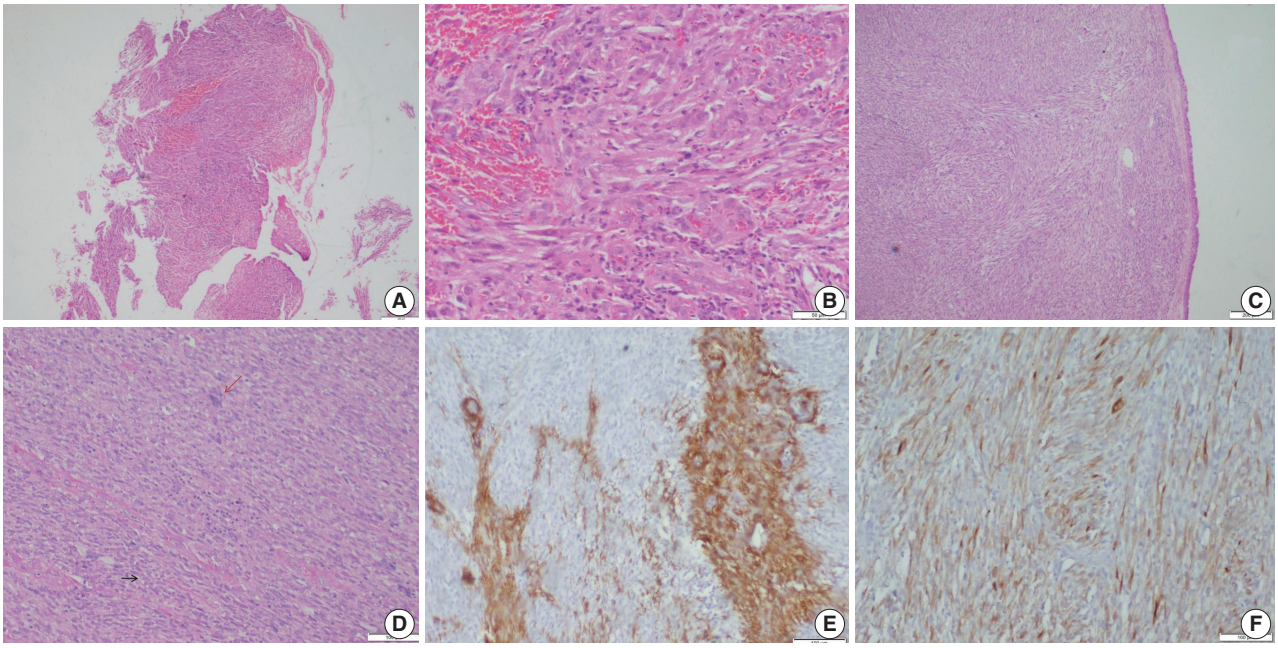

Fig. 3. Leiomyosarcoma. (A, B)Photomicrographs of the first biopsy from case 4 show small fragments of spindle cell tumor with mild to moderate nuclear pleomorphism and interspersed inflammatory cells; diagnosed as inflammatory myofibroblastic tumor. (C) Excision biopsy showed bronchial epithelium with a cellular spindle cell tumor in the sub-epithelial region. (D) Tumor cells have pale to bright eosinophilic cytoplasm, paranuclear vacuoles (black arrow) with interspersed inflammatory cells and pleomorphic tumor giant cells (red arrow). Immunohistochemistry shows focal positivity for smooth muscle actin (E) and desmin (F).

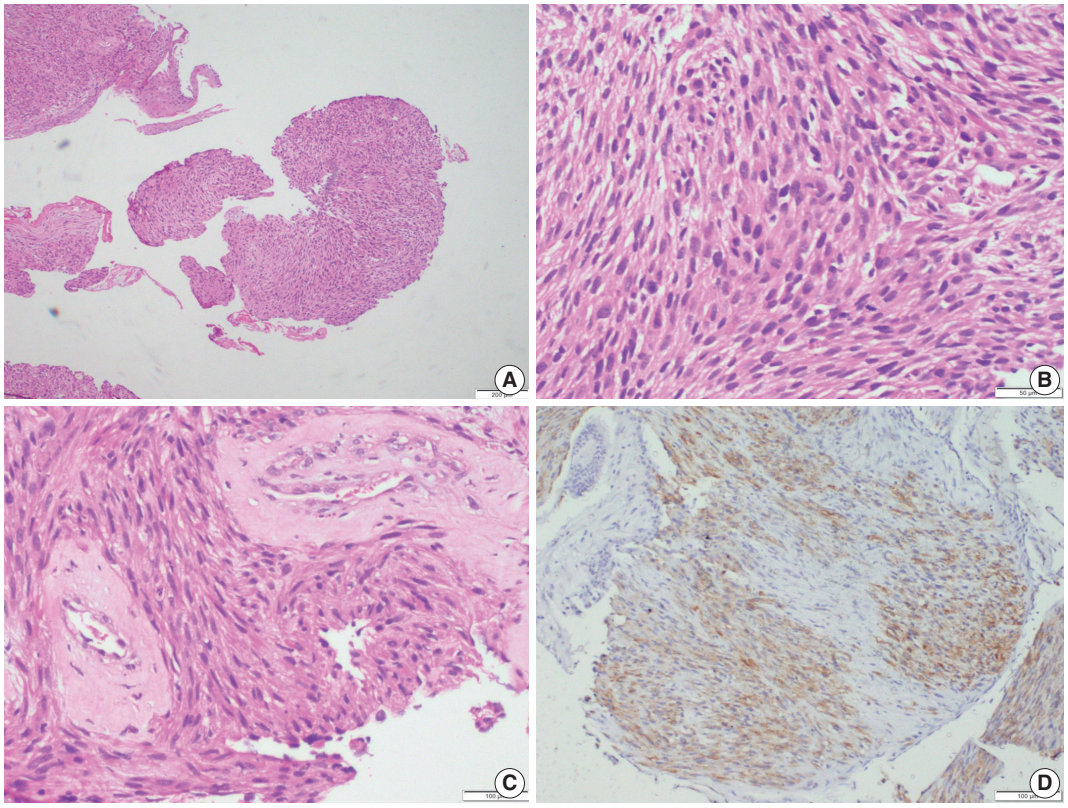

Fig. 4. Leiomyosarcoma. Photomicrographs of case 5 show multiple fragments of tumor tissue displaying a cellular spindle cell tumor (A) with moderate amounts of eosinophilic cytoplasm, ovoid, hyperchromatic nuclei, paranuclear vacuoles, and mitotic figures (B); perivascular hyalinization is noted (C). (D) Immunohistochemistry shows focal desmin positivity.

https://doi.org/10.4132/jptm.2018.05.16

eosinophilic cytoplasm, had ovoid to elongated vesicular nuclei with small conspicuous nucleoli, and occasionally demonstrated paranuclear vacuoles. There was moderate nuclear pleomorphism, and a mitotic count of 6–7/10 high-power field (HPF) in case 5. A few hyalinized blood vessels and focal myxoid changes were also noted. The first biopsy in case 4 revealed mostly fibrin, acute inflammatory exudate, and a tiny fragment from a spindle cell tumor displaying moderate nuclear pleomorphism, with prominent nucleoli, and an occasional mitotic figure (Fig. 3A, B). The presence of many interspersed inflammatory cells led to a diagnosis of IMT, a more common mesenchymal neoplasm in this location, although anaplastic lymphoma kinase 1 was negative. Paranuclear vacuoles were not evident in the initial biopsy, obscuring the correct diagnosis. Subsequent excision biopsies (Fig. 3C–F) showed a cellular spindle cell tumor with similar tumor morphology to case 5. In addition, there was moderate to marked nuclear pleomorphism, with pleomorphic tumor giant cells intimately admixed with a complement of more uniform-appearing spindle cells. Few eosinophils, mast cells, and plasma cells were also identified scattered among the tumor cells. Mitotic figures varied from 1–2/10 HPF. Necrosis was not seen in either of the cases. Both cases showed variable immunostaining patterns, even in separate biopsies from the same patient (Table 2).

DISCUSSION

The supporting fibroconnective tissues of the trachea and bronchi can give rise to a variety of benign and malignant mesenchymal tumors. However, these are far less common than epithelial tumors.[7] Primary SMTs of the respiratory tract are extremely rare, with leiomyomas comprising approximately 2% of benign lung tumors[7] and LMS accounting for less than 0.5% of malignant primary lung tumors. However, LMS is the most frequent primary lung sarcoma.[3] SMTs can occur along the tracheo-bronchial tree, or within the lung parenchyma.[4] Approximately one-third of pulmonary leiomyomas have endobronchial locations.[2] Most primary pulmonary LMSs are intraparenchymal, with direct extension to the bronchi giving rise to an endobronchial component.[7] The primary endobronchial form of LMS is exceptional, with only 16 adult cases having been documented to date.[3,8] Tracheobronchial leiomyomas occur most commonly in the fourth decade of life, although one-third of reported patients are younger than 20 years of age,[9] and affect both sexes equally.[10] LMSs also occur in middle aged patients, but with a slight male predominance.[3] In our series, the patients demonstrated wide age distributions of 13 to 65 years for leiomyoma and 28 to 57 years for LMS. Contrary to published data,[3,10] leiomyomas were seen only in males, and LMS only in female patients in our series.

Presenting symptoms of endobronchial SMTs are based on the degree of bronchial obstruction, with the most common being coughing, followed by hemoptysis and wheezing.[10] Radiologically, atelectasis is the most frequent finding, although normal imaging, solitary round mass, pneumonic infiltration, unilateral emphysema, and hyperlucency due to air trapping distal to the obstructed bronchus may also be seen on chest radiographs. Calcification has also been reported in leiomyomas,[4] as seen in one of our cases. Definitive diagnosis can be achieved by direct visualization of the lesion by bronchoscopy, followed by biopsy and histopathological characterization.[2] As metastatic pulmonary sarcomas are more common than primary sarcomas, it is necessary to rule out metastases from extrapulmonary sites before establishing a diagnosis of primary pulmonary LMS. Similarly, the possibility of a benign metastasizing leiomyoma should be excluded by the absence of previous surgical history or radiological evidence of a mass at any other site, as done in all our cases.

Differentiation in pulmonary LMS can range from low, intermediate, and high grade. Low-grade tumors recapitulate smooth muscle cell differentiation with low mitotic rates (< 3/10 HPF) as well as absence of cellular atypia, necrosis, and hemorrhage. Intermediate-grade tumors have increased cellularity, with mild to moderate nuclear atypia, and brisk mitotic activity (3–8/10 HPF). High-grade LMS show marked increases in cellularity, nuclear pleomorphism, high mitotic activity (average 8–12 mitoses/10 HPF), abundant necrosis, and hemorrhaging.[11] Primary pulmonary LMS can show a wide spectrum of differentiation with presence of necrosis, cytological atypia, and mitoses.[1] Well-defined criteria for these tumors at endobronchial locations have not been described, and therefore the diagnoses in our cases were based on the criteria discussed above. Diagnoses of intermediate grade LMS of were rendered on the basis of increased cellularity and nuclear pleomorphism in case 4, and increased mitotic activity in case 5.

Upon immunohistochemistry, benign and low grade malignant tumors are more likely to show immunoreactivity for smooth muscle markers, such as smooth muscle actin (SMA), h-caldesmon, and desmin, while high-grade or less differentiated tumors may be negative for all muscle markers, and may require ultrastructural examination to confirm the diagnosis.[11] In our cases as well, leiomyomas showed more consistent staining with smooth muscle markers (SMA, desmin, and smooth muscle myosin heavy chain), while LMSs showed variable, focal staining, leading to erroneous diagnoses, especially on small biopsies.

Several benign and malignant neoplasms enter the differential diagnosis, and can be distinguished by appropriate immunohistochemical stains. They include spindle cell or sarcomatoid carcinoma (positive for epithelial markers), IMT (less cellular, with collagen- rich stroma, prominent plasma cell infiltration, and ALK1 positivity in approximately 50% of cases), monophasic spindle cell synovial sarcoma (CD99 positive), malignant peripheral nerve sheath tumor (S-100 positive), gastrointestinal stromal tumor (CD117 and DOG1 positive), and spindle cell melanoma (human melanoma black 45 positive). The use of more than one smooth muscle marker is recommended in differential diagnostic immunohistochemical panels due to such variable staining, particularly in high grade malignant SMTs.

SMTs arising in immunocompetent patients are not associated with EBV.[5] None of the patients included in this study had a history of AIDS or immunosuppression. On immunohistochemistry, all cases were immunonegative for EBV-LMP1, thus excluding diagnoses of EBV-associated SMT.

Bronchoscopic interventions have shown good results for the resection of endobronchial leiomyoma, and a variety of techniques like electrocautery, argon plasma coagulation, cryotherapy, and Nd:YAG laser can be used for this purpose.[12] The prognosis of these tumors is excellent after complete resection, although rare recurrences have been documented in the literature.[13,14] Kim *et al*.[9] reported that respiratory tract leiomyomas may show an iceberg growth pattern with both intra- and extra-luminal tumor components, and bronchoscopic removal of the visible intraluminal part only may be responsible for local recurrences.

The prognosis of LMS depends on tumor grade and degree of differentiation.[11] Other variables such as size of the tumor, stage at presentation, and completeness of resection also affect survival.[12] The only curative therapy for primary LMS of the lung is radical resection. However, sleeve lobectomy, pneumonectomy, or carinal resection may be necessary to complete resection and prolong survival, depending on the anatomic location and size of the tumor.[8] Survival following excision of these tumors is better than that for a primary lung carcinoma.[15] Chemotherapy has been suggested in cases with metastases; however, it lacks efficacy, resulting in only partial response.[3] In our series, patient 5 is currently receiving chemotherapy due to distant metastases, and patient 4 received 30 cycles/60 Gy of radiotherapy due to the presence of residual tumor following resection. Among the 16 previously reported cases of endobronchial LMSs, 13 were alive after a minimum follow-up period of 5 months.[3,8] However, in a larger series of parenchymal LMSs, these tumors have been seen to result in comparatively worse prognosis.[16,17]

To conclude, endobronchial SMTs are extremely rare tumors with typically favorable outcomes, depending on degree on differentiation. Accurate diagnosis relies on histopathological examination, for both confirmation of smooth muscle lineage and for determining the malignant potential of the lesion. An appropriate immunohistochemical panel, which includes more than one marker of smooth muscle differentiation, is extremely valuable for differential diagnosis from their morphological mimics, and is necessary for instituting appropriate management.

ORCID

Aanchal Kakkar: https://orcid.org/0000-0002-4303-1099
Shipra Agarwal: https://orcid.org/0000-0001-7037-4444
Karan Madan: https://orcid.org/0000-0002-5330-6391
Deepali Jain: https://orcid.org/0000-0001-5315-9814

Conflicts of Interest

No potential conflict of interest relevant to this article was reported.

REFERENCES

1. Dacic S, Elmberger G. Other mesenchymal tumours. In: Travis WD, Brambilla E, Burke AP, Marx A, Nicholson AG, eds. WHO classification of tumours of lung, pleura, thymus and heart. Lyon: IARC Press, 2015; 132-3.
2. Swarnakar R, Sinha S. Endobronchial leiomyoma: a rare and innocent tumour of the bronchial tree. Lung India 2013; 30: 57-60.
3. Elouazzani H, Zouaidia F, Jahid A, Bernoussi Z, Mahassini N. Primary endobronchial leiomyosarcoma of the lung: clinical, gross and microscopic findings of two cases. J Clin Imaging Sci 2012; 2: 35.
4. Cardenas-Garcia J, Lee-Chang A, Chung V, Shim C, Factor S, Tibb A. Bronchial leiomyoma, a case report and review of literature. Respir Med Case Rep 2014; 12: 59-62.
5. Purgina B, Rao UN, Miettinen M, Pantanowitz L. AIDS-related EBV-associated smooth muscle tumors: a review of 64 published cases. Patholog Res Int 2011; 2011: 561548.
6. Awasthi A, Dubey S, Sabhikhi AK, Bal S. Primary endobronchial myxoid leiomyoma in a child: an unusual case report and review of literature. Indian J Pathol Microbiol 2016; 59: 87-9.
7. Litzky L. Epithelial and soft tissue tumors of the tracheobronchial tree. Chest Surg Clin N Am 2003; 13: 1-40.
8. Lee MC, Hsu CP, Hsia JY. Surgical treatment of endobronchial leiomyosarcoma with right main bronchus total obstruction: a case report. Ann Thorac Cardiovasc Surg 2008; 14: 105-8.

9. Kim YK, Kim H, Lee KS, *et al*. Airway leiomyoma: imaging findings and histopathologic comparisons in 13 patients. AJR Am J Roentgenol 2007; 189: 393-9.
10. Dmello D, Javed A, Espiritu J, Matuschak GM. Endobronchial leiomyoma: case report and literature review. J Bronchology Interv Pulmonol 2009; 16: 49-51.
11. Moran CA, Suster S. Tumors of the lung and pleura. In: Fletcher CD, ed. Diagnostic histopathology of tumors. New York: Churchill Livingstone, 2013; 207-45.
12. Vaz AP, Magalhães A, Bartosch C, Fernandes G, Marques A. Primary endobronchial leiomyoma: endoscopic laser resection. Rev Port Pneumol 2011; 17: 228-31.
13. Kwon YS, Kim H, Koh WJ, *et al*. Clinical characteristics and efficacy of bronchoscopic intervention for tracheobronchial leiomyoma. Respirology 2008; 13: 908-12.
14. Harris PF, Maness GM, Ward PH. Leiomyoma of the larynx and trachea: case reports. South Med J 1967; 60: 1223-7.
15. Lee SH, Shim JJ, Shin JS, *et al*. Primary endobronchial leiomyosarcoma: diagnosis following expectoration of tumor fragment. Respiration 2001; 68: 99-102.
16. Attanoos RL, Appleton MA, Gibbs AR. Primary sarcomas of the lung: a clinicopathological and immunohistochemical study of 14 cases. Histopathology 1996; 29: 29-36.
17. Janssen JP, Mulder JJ, Wagenaar SS, Elbers HR, van den Bosch JM. Primary sarcoma of the lung: a clinical study with long-term follow-up. Ann Thorac Surg 1994; 58: 1151-5.

Journal of Pathology and Translational Medicine 2018; 52: 226-231
https://doi.org/10.4132/jptm.2017.11.12

■ CASE STUDY ■

Hepatocellular Carcinoma Arising in a Huge Hepatocellular Adenoma with Bone Marrow Metaplasia

Hyo Jeong Kang[1,2] · Hui Jeong Jeong[1]
So-Woon Kim[1] · Eunsil Yu[1,3]
Young-Joo Lee[4] · So Yeon Kim[5]
Jihun Kim[1]

[1]Departments of Pathology and [2]Physiology, [3]Asan Liver Center, Departments of [4]Surgery and [5]Radiology, Asan Medical Center, University of Ulsan College of Medicine, Seoul, Korea

Received: September 8, 2017
Revised: October 30, 2017
Accepted: November 12, 2017

Corresponding Author
Jihun Kim, MD, PhD
Department of Pathology, Asan Medical Center, University of Ulsan College of Medicine, 88 Olympic-ro 43 gil, Songpa-gu, Seoul 05505, Korea
Tel: +82-2-3010-4556
Fax: +82-2-472-7898
E-mail: Jihunkim@amc.seoul.kr

Hepatocellular adenoma (HCA) is the most common type of benign liver tumor, and its major complication is malignant transformation to hepatocellular carcinoma (HCC). Here, we report a case of HCC arising in HCA with bone marrow metaplasia in a 24-year-old Korean woman who presented with abdominal discomfort. A huge liver mass was found on abdominal ultrasonography. She underwent surgical hepatic resection, and the resected specimen was entirely involved by a 20-cm-sized tumor. Histological review revealed a well differentiated HCC arising from inflammatory HCA with β-catenin nuclear positivity and bone marrow metaplasia that contained hematopoietic cells. This case was unique because malignant transformation, inflammatory type HCA, β-catenin nuclear staining, and bone marrow metaplasia were simultaneously observed. Additionally, it should be noted that a large HCA with β-catenin activation can undergo malignant transformation and should be surgically resected in a timely manner.

Key Words: Carcinoma, hepatocellular; Adenoma, liver cell; Bone marrow metaplasia; β-catenin

Hepatocellular adenoma (HCA) is the most common benign liver neoplasm that can arise from hepatocytes. Oral contraceptives (OCPs) are the main predisposing factors to the development of HCA; however, other associations, such as obesity, have been more recently recognized.[1,2] HCA represents a heterogeneous group of tumors that differ in histology, immunophenotype, molecular pathogenesis, and biological behavior. Based on these factors, HCAs can be sub-classified into the following four major groups: HNF1α-inactivated HCA, β-catenin activated HCA, inflammatory HCA, and unclassified HCA.[2-5] Approximately 10% of inflammatory HCA cases coexist with a β-catenin mutation.[2,4] The most important complications of HCAs are hemorrhage and malignant transformation to hepatocellular carcinoma (HCC).[6] Although the overall risk of malignant transformation has not been well defined, according to previous reports, 4%–8% of resected HCA have undergone malignant transformation.[6] Risk factors for HCC from HCA include male sex, androgen use, large tumor size (> 5 cm), and β-catenin-activated subtype.[4,6] Bone marrow metaplasia has been very rarely reported in primary liver tumors; indeed, only four such cases have been reported to date.[7-10] Here, we report for the first time in Korea a case of HCC arising from a β-catenin–activated inflammatory HCA with bone marrow metaplasia in a young woman who had not taken OCPs.

CASE REPORT

A 24-year-old woman was admitted to an outside hospital presenting with abdominal discomfort. She was referred to Asan Medical Center and was found to have a huge liver mass that was detected by abdominal ultrasonography. The diagnosis of pre-operative liver biopsy performed by an outside hospital was HCA. Her medical and family histories were unremarkable. She had never taken OCPs and had a body mass index of 21.48 kg/m^2. Hepatitis B surface (HBs) antigen, anti-HBs antibody, and anti–hepatitis C virus antibody were all negative. A complete blood count and serum chemistry tests, including coagulation and liver function tests, were normal except for elevated

pISSN 2383-7837
eISSN 2383-7845

levels of gamma glutamyl transferase (111 IU/L; normal range, 8 to 61 IU/L). Serum tumor marker of prothrombin induced by vitamin K absence-II (PIVKA-II) levels were markedly elevated (2,964 mAU/mL; normal range, ≤40 mAU/mL). α-Fetoprotein levels were slightly elevated (11.1 ng/mL; normal range, ≤7.0 ng/mL), while those of serum carcinoembryonic antigen (0.9 ng/mL; normal range, ≤5 ng/mL) and carbohydrate antigen 19-9 (3.8 U/mL; normal range, ≤37 U/mL) were within normal limits. A dynamic liver and pelvis computerized tomography (CT) scan revealed a 20 cm hypervascular mass occupying segments 4, 5, and 8 of the liver (Fig. 1A). An enhanced CT image exhibited high attenuation during the arterial phase and decreasing attenuation during the portal and delayed phases. The lesion showed heterogeneous foci of hemorrhage, necrosis, fat, and calcification. An experienced radiologist (S.Y.K.) interpreted the lesion as a huge HCA and suspected a partly malignant transformation. The patient underwent segmentectomy and partial hepatectomy to remove the lesion. Macroscopically, the resected specimen was filled with a well circumscribed 19.9×18.4×7.9-cm solid mass, and its cut surface showed a heterogeneous yellow-brown color, multinodular growth, partly cystic degeneration, hemorrhage, and necrosis (Fig. 1B). Microscopically, the lesion exhibited typical features of a HCA and was characterized by well differentiated hepatocytes arranged in thin cords or sheets with bland cytology and abundant eosinophilic cytoplasm (Fig. 2A). The parenchyma showed dilated sinusoids, occasionally with large aberrant arteries, and multifocal inflammation composed of lymphocytes, neutrophils, and eosinophils (Fig. 2A, B). Immunohistochemical stains of HCA cells showed diffuse positivity of liver fatty acid binding protein, serum amyloid A (Fig. 2C), C-reactive protein (Fig. 2D), and glutamine synthetase (Fig. 2E) antibodies and partial nuclear positivity for β-catenin antibody (Fig. 2F), suggesting an inflammatory HCA with β-catenin activation. Although this case showed histologically typical features of inflammatory HCA without histological features of other subtypes, it coexisted with β-catenin nuclear positivity, suggesting a β-catenin–activated inflammatory HCA. It was difficult to grossly distinguish the area of malignant transformation. However, multiple malignant foci were found microscopically that occupied less than 10% of the total tumor area. These malignant foci were all well differentiated HCC that partially resembled the surrounding HCA but also showed nuclear hyperchromasia and pleomorphism and thickened trabeculae (Fig. 2G). Glutamine synthetase showed stronger expression in the HCC area than in the HCA area, and heat shock protein-70 (Fig. 2H) and glypican 3 (Fig. 2I) were positive in the HCC area. As is typical of HCC, reticulin loss (Fig. 2J) and diffuse CD34 expression on sinusoidal cells (Fig. 2K) were observed. The Ki-67 labeling index of the HCC area (15%) was significantly increased compared with that of the HCA area (< 2%) (Fig. 2L). Corresponding to visible calcification regions in the CT scan were areas of bone marrow metaplasia (Fig. 3A) that were characterized by mature lamellar bone forming trabeculae intermingled with fat tissue that contained myeloid and erythroid cells (Fig. 3B, C). The patient was discharged 10 days after surgery and showed no evidence of recurrence at the last follow up visit 23 months after surgery.

This study was approved by the Institutional Review Board of Asan Medical Center with a waiver of informed consent (IRB No.2017-0679).

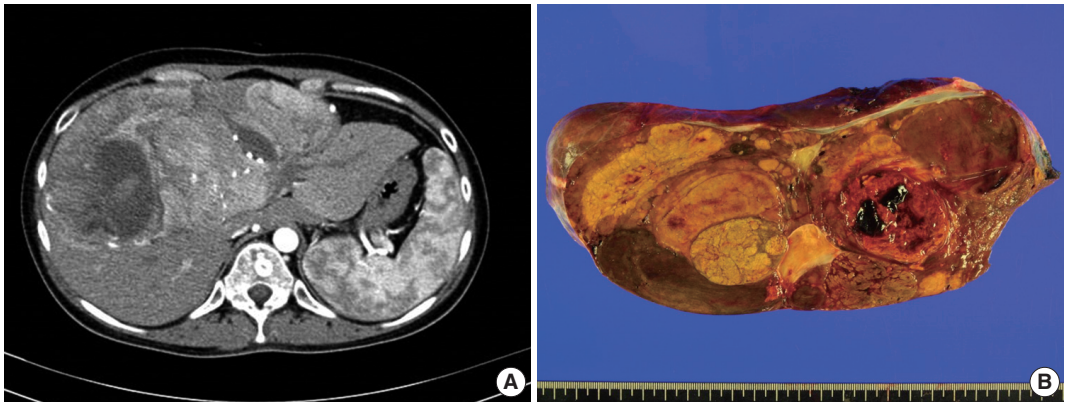

Fig. 1. Imaging and gross pathological findings. (A) Dynamic liver and pelvis computed tomography shows an enlarged liver with a huge, well-defined, hypervascular mass in segments 4, 5, and 8 of the liver during arterial phase. (B) The surface of a slice from a surgically resected specimen reveals a heterogeneously yellow-brown color and multinodular growth with partly cystic degeneration that contained hemorrahge and necrosis.

DISCUSSION

HCA is an uncommon benign liver neoplasm composed of hepatocytes and typically develop in a non-cirrhotic liver. It primarily occurs in young to middle-aged women with a history of OCP use. Estrogen or exogenous androgen use for medical purposes

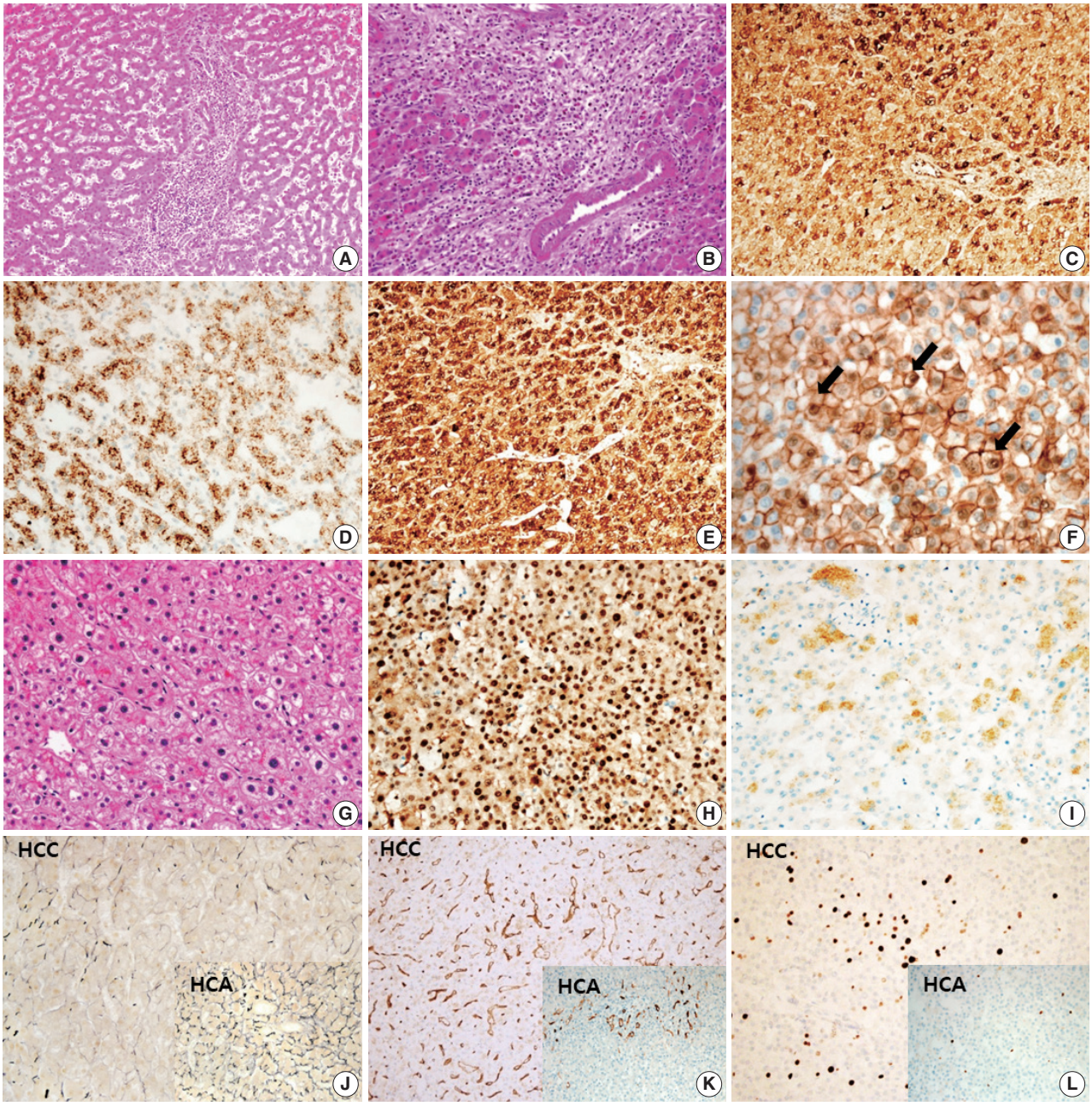

Fig. 2. Microscopic and immunohistochemical findings of hepatocellular adenoma (HCA), inflammatory type with β-catenin activation (A–F) and hepatocellular carcinoma (HCC) (G–L). (A) Dilated sinusoids and intratumoral inflammation in the portal tract-like areas are observed in the parenchyma. (B) Large aberrant arteries with infiltration of variable inflammatory cells including lymphocytes, neutrophils, and eosinophils are occasionally observed. Tumor cells show diffuse cytoplasmic expression of serum amyloid A (C), C-reactive protein (D), and glutamine synthetase (E). (F) Nuclear β-catenin expression (arrows) is observed in several tumor cells. (G) Nuclear atypia and thick trabeculae are observed in the HCC component. (H) Heat shock protein-70 is strongly and diffusely positive. (I) Glypican 3 is partially positive. (J) Loss of reticulin is observed in the HCC component, whereas reticulin staining is preserved in the HCA (inset). (K) CD34 expression on sinusoidal cells is strong and diffuse in HCC but is patchy in HCA (inset). (L) The Ki-67 labeling index of the HCC area is significantly increased compared with that of HCA (inset).

https://doi.org/10.4132/jptm.2017.11.12

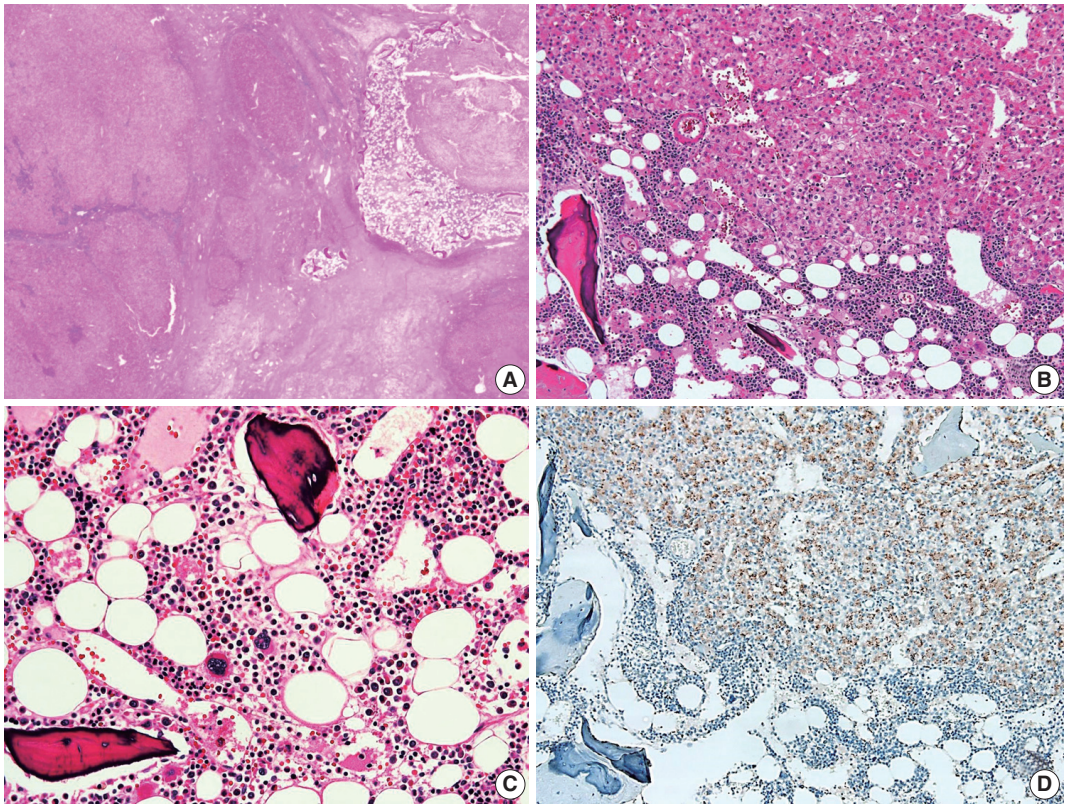

Fig. 3. Histological findings of bone marrow metaplasia. (A) Bone marrow metaplasia is observed in the inner hepatocellular adenoma. (B, C) Bone marrow metaplasia is characterized by mature lamellar bone that formed trabeculae intermingled with fat tissue containing erythroblasts, myeloblasts, and megakaryocytes. (D) Tumor cells near the bone marrow metaplasia shows positivity for epithelial cell adhesion molecule immunohistochemical staining.

is also a recognized risk factor for HCA. Additionally, rarely HCA is found in children and is association with other conditions such as glycogen storage disease, galactosemia, tyrosinemia, familial polyposis coli, Fanconi anemia, and hepatic iron overload with β-thalassemia.[11,12] It has recently been reported that the incidence of HCA is increasing in males and non-OCP individuals. Additionally, there is a trend towards increasing cases of multiple HCAs. This may primarily be a consequence of the higher prevalence of obesity and metabolic syndrome, rather than an effect of OCPs, which have been considered to be the main cause for the development of HCA.[1,13,14] Interestingly, the woman with HCA in this study had a huge mass at a young age, and she showed no history of OCP use or genetically determined metabolic disease.

Malignant transformation of HCA is the main reason for surgical treatment. It is important to identify factors that increase the risk of malignancy. However, HCA is difficult to distinguish from HCC because of its similar imaging characteristics and histopathological features.[6] Several studies have indicated that high risk groups of patients having an increased risk of malignant alteration from HCA display larger tumors (> 5 cm), have a history of androgen or anabolic steroid intake, are male, and are patients with glycogen storage disease.[12,15-19] HCA has recently been roughly classified into four subgroups according to genotype-phenotype based analysis. Moreover, β-catenin–activated HCA represents a well-known factor for an increased risk of malignant transformation compared with the other subtypes.[17] In our present case, although the patient was a young woman who had only abdominal discomfort without any symptoms related to malignancy the large tumor size and high level of PIVKA-II could predict the possibility of malignant transformation from HCA. Therefore, a rapid assessment of mass removal was performed to prevent intraperitoneal hemorrhage, rupture, malignant progression, or metastasis. Within the surgically resected specimen, partially malignant transformation was confirmed by histological and immunohistochemical examination. Nuclear accumulation of β-catenin antibody was detected in areas corresponding to malignant foci by immunohistochemistry, which was consistent with an association with malignant transformation in HCA.

A notable feature of this case was the presence of bone marrow

Table 1. Overview of cases of HCA and HCC with bone marrow metaplasia

Study	Year	Age (yr)	Sex	Diagnosis	Associated disease	Size (cm)	Bone marrow metaplasia	
							Fat component	Hematopoietic cells
Moriura *et al*.[9]	1996	34	Male	HCA (×2)	GSD type 1a	Up to 12	Present	Absent
Ramacciato *et al*.[10]	2006	58	Male	HCA	Absent	14	Present	Present
Copin *et al*.[7]	2015	42	Female	HCC	Absent	No mention	Present	Present
Iguchi *et al*.[8]	2016	46	Female	HCC arising in HCA (multiple)	GSD type I	Up to 10	Present	Present
Present case	2017	24	Female	HCC arising in HCA	Absent	20	Present	Present

HCA, hepatocellular adenoma; HCC, hepatocellular carcinoma; GSD, glycogen storage disease.

metaplasia in the inner HCA. Bone or osteoid formation has been found in special types of primary liver tumors, especially hepatoblastoma. However, bone marrow metaplasia with hematopoietic cells is extremely rare in primary liver tumors in adults, especially in cases of HCA or HCC. Only four cases have been reported in the English literature in which areas of bone marrow metaplasia were found in HCC or HCA (Table 1). According to a review of the literature, this represents the first case report of HCC arising from HCA with complete bone marrow metaplasia consisting of both fat components and hematopoietic cells in an adult younger than 30 years old. It has been previously demonstrated that bone marrow-derived stem cells can differentiate into hepatic progenitor cells that may play a role in liver tumor development.[10,20] In this present case, hepatic progenitor cells with epithelial cell adhesion molecule expression (Fig. 3D) were observed around bone marrow metaplasia but were less frequent or not detected in areas far from bone marrow metaplasia.

In conclusion, we report a case of HCC arising from inflammatory HCA with β-catenin activation. Two important points of this case are that malignant transformation in huge HCA can occur in a young woman without risk factors such as use of OCP or genetic metabolic diseases and that complete bone marrow metaplasia can occur in HCA. This case report emphasizes that a large HCA can show malignant transformation, even in a young woman, and that these tumors should be promptly, surgically resected.

ORCID

Jihun Kim: https://orcid.org/0000-0002-8694-4365

Conflicts of Interest

No potential conflict of interest relevant to this article was reported.

REFERENCES

1. Chang CY, Hernandez-Prera JC, Roayaie S, Schwartz M, Thung SN. Changing epidemiology of hepatocellular adenoma in the United States: review of the literature. Int J Hepatol 2013; 2013: 604860.
2. Bioulac-Sage P, Sempoux C, Balabaud C. Hepatocellular adenoma: classification, variants and clinical relevance. Semin Diagn Pathol 2017; 34: 112-25.
3. Bioulac-Sage P, Balabaud C, Zucman-Rossi J. Subtype classification of hepatocellular adenoma. Dig Surg 2010; 27: 39-45.
4. Margolskee E, Bao F, de Gonzalez AK, *et al*. Hepatocellular adenoma classification: a comparative evaluation of immunohistochemistry and targeted mutational analysis. Diagn Pathol 2016; 11: 27.
5. Chu HH, Moon WS. β-catenin activated hepatocellular adenoma. Clin Mol Hepatol 2013; 19: 185-9.
6. Stoot JH, Coelen RJ, De Jong MC, Dejong CH. Malignant transformation of hepatocellular adenomas into hepatocellular carcinomas: a systematic review including more than 1600 adenoma cases. HPB (Oxford) 2010; 12: 509-22.
7. Copin P, Ronot M, Vilgrain V. Hepatocellular carcinoma with osseous metaplasia and bone marrow elements. Clin Gastroenterol Hepatol 2015; 13: e26-7.
8. Iguchi T, Yamagata M, Sonoda T, *et al*. Malignant transformation of hepatocellular adenoma with bone marrow metaplasia arising in glycogen storage disease type I: a case report. Mol Clin Oncol 2016; 5: 599-603.
9. Moriura S, Kuroda M, Kimura A, *et al*. Case report: hepatic adenoma with bone marrow metaplasia in a patient with glycogen storage disease type 1a. J Gastroenterol Hepatol 1996; 11: 556-9.
10. Ramacciato G, Nigri GR, Aurello P, *et al*. Giant hepatic adenoma with bone marrow metaplasia not associated with oral contraceptive intake. World J Surg Oncol 2006; 4: 58.
11. Vaithianathan R, Philipchandran, Selvambigai G, Jayaganesh P. Spontaneous hepatocellular adenoma in paediatric age group: case report. J Clin Diagn Res 2013; 7: 2962-3.
12. Velazquez I, Alter BP. Androgens and liver tumors: Fanconi's anemia and non-Fanconi's conditions. Am J Hematol 2004; 77: 257-67.
13. Stueck AE, Qu Z, Huang MA, Campreciós G, Ferrell LD, Thung SN. Hepatocellular carcinoma arising in an HNF-1alpha-mutated

adenoma in a 23-year-old woman with maturity-onset diabetes of the young: a case report. Semin Liver Dis 2015; 35: 444-9.
14. Hirata E, Shimizu S, Umeda S, *et al*. Hepatocyte nuclear factor 1alpha-inactivated hepatocellular adenomatosis in a patient with maturity-onset diabetes of the young type 3: case report and literature review. Nihon Shokakibyo Gakkai Zasshi 2015; 112: 1696-704.
15. Dokmak S, Paradis V, Vilgrain V, *et al*. A single-center surgical experience of 122 patients with single and multiple hepatocellular adenomas. Gastroenterology 2009; 137: 1698-705.
16. Gorayski P, Thompson CH, Subhash HS, Thomas AC. Hepatocellular carcinoma associated with recreational anabolic steroid use. Br J Sports Med 2008; 42: 74-5.
17. Zucman-Rossi J, Jeannot E, Nhieu JT, *et al*. Genotype-phenotype correlation in hepatocellular adenoma: new classification and relationship with HCC. Hepatology 2006; 43: 515-24.
18. Franco LM, Krishnamurthy V, Bali D, *et al*. Hepatocellular carcinoma in glycogen storage disease type Ia: a case series. J Inherit Metab Dis 2005; 28: 153-62.
19. Terkivatan T, de Wilt JH, de Man RA, *et al*. Indications and long-term outcome of treatment for benign hepatic tumors: a critical appraisal. Arch Surg 2001; 136: 1033-8.
20. Herzog EL, Chai L, Krause DS. Plasticity of marrow-derived stem cells. Blood 2003; 102: 3483-93.

Journal of Pathology and Translational Medicine 2018; 52: 232-237
https://doi.org/10.4132/jptm.2018.05.17

■ CASE STUDY ■

Combined Hepatocellular Carcinoma and Neuroendocrine Carcinoma with Ectopic Secretion of Parathyroid Hormone: A Case Report and Review of the Literature

Hyun Jung Kwon · Ji-Won Kim[1]
Haeryoung Kim[2] · YoungRok Choi[3]
Soomin Ahn

Department of Pathology and [1]Division of Hematology and Medical Oncology, Department of Internal Medicine, Seoul National University Bundang Hospital, Seongnam; [2]Department of Pathology, Seoul National University Hospital, Seoul; [3]Department of Surgery, Seoul National University Bundang Hospital, Seongnam, Korea

Received: April 16, 2018
Accepted: May 15, 2018

Corresponding Author
Soomin Ahn, MD
Department of Pathology, Seoul National University Bundang Hospital, 82 Gumi-ro 173beon-gil, Bundang-gu, Seongnam 13620, Korea
Tel: +82-31-787-3379
Fax: +82-31-787-4012
E-mail: suminy317@gmail.com

Primary combined hepatocellular carcinoma (HCC) and neuroendocrine carcinoma is a rare entity, and so is hypercalcemia due to ectopic parathyroid hormone (PTH) secretion by tumor. A 44-year old man with hepatitis B virus associated chronic liver disease presented with a hepatic mass. Hemihepatectomy discovered the mass as combined HCC and poorly differentiated cholangiocarcinoma. During adjuvant chemoradiation therapy, he presented with nausea, and multiple systemic metastases were found. Laboratory tests revealed hypercalcemia with markedly elevated PTH and neuron specific enolase. Parathyroid scan showed normal uptake in parathyroid glands, suggestive of ectopic PTH secretion. Subsequently, immunohistochemistry of neuroendocrine marker was performed on the primary lesion, and confirmed the neuroendocrine differentiation in non-HCC component. The patient died 71 days after surgery. This report may suggest the possibility of ectopic PTH secretion by neuroendocrine carcinoma of hepatic origin causing hypercalcemia. Caution for neuroendocrine differentiation should be exercised when diagnosing poorly differentiated HCC.

Key Words: Combined; Liver; Carcinoma, hepatocellular; Carcinoma, neuroendocrine

Primary neuroendocrine carcinoma (NEC) in the liver is a rare entity that behaves aggressively. Primary hepatocellular carcinoma (HCC) with a NEC component is very rare, consisting of about 0.46% of primary hepatic tumors.[1] Eighteen cases of primary combined or collided NEC and HCC have been reported in English literature to this date.[1-14] None of these cases had paraneoplastic syndromes or proved to be functional.

Hypercalcemia is a well-known paraneoplastic metabolic condition associated with many malignancies.[15] In HCC, hypercalcemia accounts for 7.8% of the paraneoplastic syndromes.[16] While primary hyperparathyroidism is the most common cause for hypercalcemia without malignancies, hypercalcemia can occur in association with malignancies through other mechanisms. Most of the malignancies associated with hypercalcemia proved to be caused by parathyroid hormone (PTH)–related peptide (PTHrP).[17] Metastasis of the malignancies to the bone can also cause osteolysis leading to hypercalcemia.[17] Only rare cases are considered to be a result of ectopic PTH production by the tumors.

Here, we present a rare case of combined hepatic NEC and HCC with malignancy associated hypercalcemia caused by ectopic PTH production. Previously reported primary mixed HCC and NEC cases and ectopic PTH-producing HCC cases are also summarized and discussed.

CASE REPORT

A 44-year-old man presented with a hepatic mass discovered during a regular abdominal ultrasound for hepatitis B virus associated chronic liver disease. The chronic liver disease was diagnosed 9 years ago and the patient was on Tenofovir. Laboratory findings showed elevated white blood cells (17,000/μL), mildly elevated aspartate aminotransferase (4 IU/L), alanine transaminase (22 IU/L), and normal calcium and phosphate levels. Computed tomographic scan identified one huge mass in segment

pISSN 2383-7837
eISSN 2383-7845

(S) 8 and the other small mass in S6, with thrombi in right portal and hepatic veins. No other systemic lesion was found. The patient underwent right hemihepatectomy with partial diaphragm resection and lymph node dissection.

On pathological examination, the cut section of S8 revealed a yellow-whitish mass measuring 10.5×8.0 with irregular margins and necrosis. The mass in S6 was a yellowish multinodular mass that measured 1.3×1.0. Tumor thrombosis was noted in the right portal vein, and cirrhosis was observed in the non-neoplastic liver. Histologically, the main mass in S8 consisted of two components; a dominant poorly differentiated carcinoma component (60%) composed of small tumor cells with enlarged vesicular irregular nuclei, high nuclear to cytoplasmic ratio, large nucleoli, and frequent mitoses, and multiple foci of typical HCC component (40%) showing trabecular architecture and grade 2 nuclei (Fig. 1). The tumor penetrated the Glisson's capsule directly invading the diaphragm and showed extensive necrosis and microvessel invasion. The poorly differentiated carcinoma component was focally positive for cytokeratin (CK) 7 and negative for α-fetoprotein, hepatocyte, glypican-3, and CK19 immunohistochemistry, and was interpreted as poorly differentiated cholangiocarcinoma component. The pathologic diagnosis of S8 mass was combined HCC and cholangiocarcinoma. The other mass in S6 showed typical histologic features of HCC. There was no metastasis in 22 lymph nodes.

The patient subsequently received adjuvant concurrent chemoradiation therapy (CCRT) of one cycle of 5-flourouracil chemotherapy and two cycles of 5 fx radiation. On postoperative day 59, he visited the emergency room for nausea and vomiting. Laboratory results showed elevated levels of total calcium (13.2 mg/dL; normal range, 8.8 to 10.5), ionized calcium (2.3 mmol/L; normal range, 1.05 to 1.35), blood urea nitrogen (33 mg/dL; normal range, 10 to 26), and creatinine (2.16 mg/dL; normal range, 0.7 to 1.4) with normal to low levels of phosphate. Further evaluation of hypercalcemia revealed markedly increased PTH (3,859 by enzyme-linked immunosorbent assay; normal range, 15 to 65), and neuron-specific enolase (101.04 ng/mL; normal range, 0 to 16.3). Parathyroid scan was performed to exclude primary hyperparathyroidism, which showed no abnormality. Whole body positron emission tomography revealed multiple hypermetabolic lesions in the liver and whole skeleton, and biopsy of an osteolytic lesion involving a left rib discovered metastatic poorly differentiated carcinoma. Only the poorly differentiated carcinoma component, not the HCC component, was identified in the metastatic lesion. Regarding hypercalcemia, elevated PTH could not be explained with bone metastasis or PTHrP, and hypercalcemia persisted despite management. Finally, ectopic PTH production by the tumor was suggested as the cause of hypercalcemia.

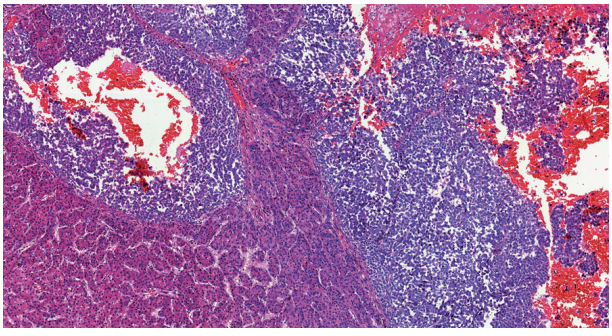

Fig. 1. Representative histologic image of the main hepatic mass.

Meanwhile, the clinician in charge enquired to the pathologist of the presence of NEC component in the tumor based on the possibility that ectopic hormone could be secreted by NEC, the rapid progression of the tumor and the elevated neuron-specific enolase level. Subsequent immunohistochemistry of neuroendocrine markers and PTH were performed on both primary (S8 mass) and metastatic tumor specimens. CD56 stained positive while chromogranin and synaptophysin were focally positive in the poorly differentiated area on both specimens, implying neuroendocrine differentiation (Fig. 2). The component with typical HCC morphology was negative for all three markers (Fig. 2). There was no immunoreactivity for PTH on either specimen. Symptomatic treatment including continuous renal replacement therapy was applied for the acute renal failure induced by hypercalcemia. However, the patient expired of disease progression 2 months after diagnosis.

This study was approved by the Institutional Review Board of Seoul National University Bundang Hospital (IRB No. B-1801-442-702), and patient consent was waived.

DISCUSSION

Primary combined HCC and NEC is very rare. The initial pathologic diagnosis of this case was combined HCC and cholangiocarcinoma because its poorly differentiated component bore little resemblance to typical NEC morphology. However, with clinical suspicion, immunohistochemistry revealed multifocal areas within the poorly differentiated component that stained positive for neuroendocrine markers. Therefore, we classified it as combined HCC and NEC.

The clinical characteristics of the 18 reported cases of primary mixed HCC and NEC are summarized in Table 1. Most cases

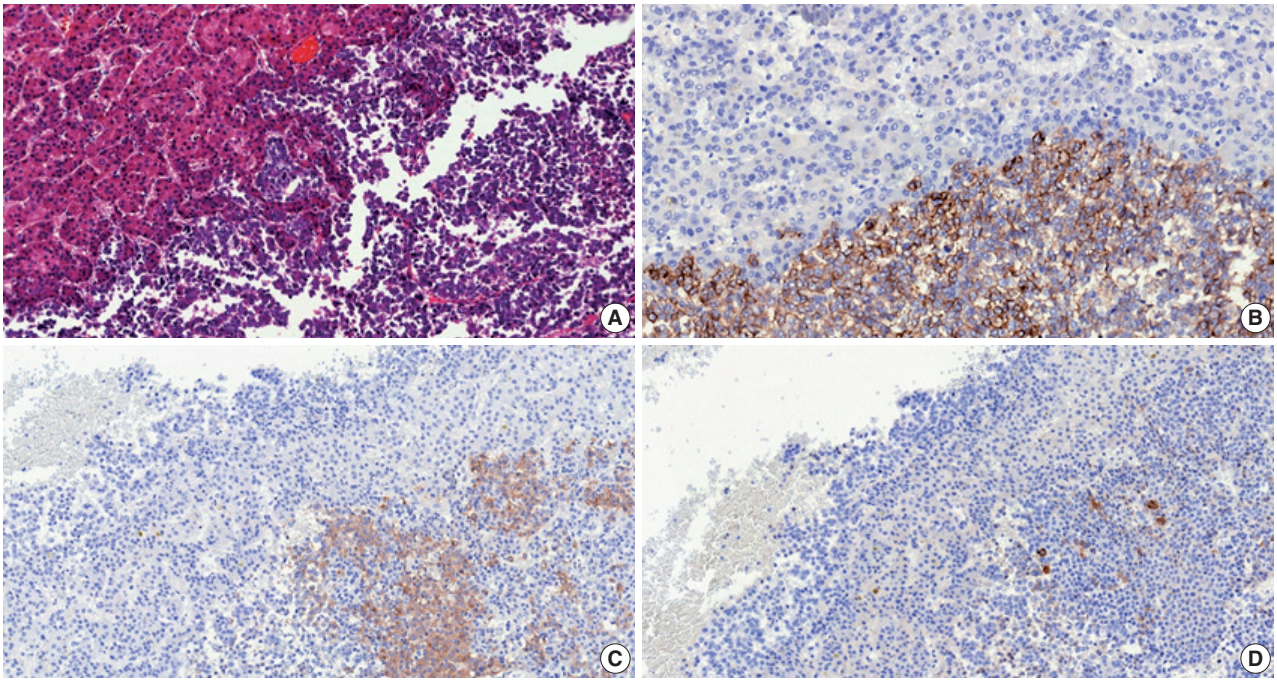

Fig. 2. (A) The main hepatic tumor consists of neuroendocrine carcinoma (right side) and hepatocellular carcinoma (left side) components. On immunohistochemistry, the neuroendocrine carcinoma component is focally positive for CD56 (B), chromogranin (C), and synaptophysin (D).

were associated with chronic hepatitis B or C. The reported carcinomas have been classified to two types according to its spatial histologic arrangement. Combined types have a transition zone in which HCC and NEC intermingle with each other whereas collision types show clear separation of the histologically different components, usually by fibrous septa. In our case, the HCC was tightly intermingled with the NEC component, their borders almost indiscernible due to transition zones. Therefore, we classified it as combined HCC and NEC.

Primary mixed HCC and NEC generally tend to have a poorer prognosis than conventional HCC.[1] Of the 18 cases summarized, eight patients experienced recurrence, six patients died within the year of operation from the disease, and only two patients were confirmed to be alive 2 years after surgery (Table 1). Remarkably, in the cases with biopsy-confirmed metastasis, the NEC component was solely found in all occasions, similar to the presenting case. This indicates that the NEC component acts more aggressively, which has a much poorer prognosis than primary HCC.[1] Therefore, it is important to identify the neuroendocrine component and assure proper treatment be given to the patient.

None of the reported combined HCC-NEC described paraneoplastic syndrome or ectopic hormone production. To our knowledge, our case may be the first to report primary mixed HCC and NEC associated with malignancy-related hypercalcemia caused by ectopic PTH production. The patient had multiple bone metastases, and one of which was histologically confirmed. In hypercalcemia caused by osteolytic lesions or PTHrP produced by tumors, however, PTH levels are usually suppressed.[15] It led us to favor ectopic PTH production to be the cause for hypercalcemia than bone metastasis or PTHrP, even though serum PTHrP level was not available.

The prevalence of hypercalcemia accounts for 7.8% of the paraneoplastic syndromes observed in HCC, and is associated with short survival.[16] Ectopic PTH production has been reported in only three HCC cases (Table 2) and not in any primary hepatic NEC case. All three cases performed PTH immunohistochemistry on their biopsy specimens which were negative. Our case also showed negative results. These findings, rather than acting as counter-evidence of hormone production, may suggest that the tumor cells do not store PTH but secrete it into circulation soon after synthesis.[18,19] We were not able to perform genetic analysis or RNA sequencing for PTH mRNA. As hypercalcemia developed during adjuvant CCRT, comparison of intact PTH levels of before and after the operation or CCRT was impossible. However, in our case, the patient developed hypercalcemia with elevated intact PTH as the metastatic lesions formed. Considering that the metastatic component was NEC, it may be possible to suggest that the intact PTH was synthesized by the NEC cells.

Primary hepatic NEC has poor prognosis, and the NEC component of primary mixed HCC and NEC behaves aggressively.

https://doi.org/10.4132/jptm.2018.05.17

Table 1. Summary of previously reported primary mixed hepatocellular and neuroendocrine carcinoma cases

	Age (yr)/ sex	Chronic hepatitis type	Tumor size (cm)	Nodal metastasis	Type	Ectopic hormone production	Clinical course	Treatment	Survival
Barsky *et al*.[2]	43/M	B	Large	Negative	Combined	None	-	Chemotherapy (doxorubicin, 5-fluorouracil)	Dead (26 mo)
Artopoulos and Destuni[3]	69/M	B	10	Negative	Combined	None	-	Surgery	Not given
Ishida *et al*.[4]	72/M	C	3	Positive (NEC)	Collision	None	-	Surgery	Not given
Yamaguchi *et al*.[5]	71/M	C	4.1	Negative	Combined	None	Recurred (5 mo, bone)	Surgery	Alive (F/U 5 mo)
Garcia *et al*.[6]	50/M	C	5.3	Negative	Collision	None	Recurred (4 mo, liver)	Surgery → recur: chemotherapy (doxorubicin, thalidomide, bevacizumab)	Alive (F/U 16 mo)
Yang *et al*.[7]	65/M	B	7.5	Positive (NEC)	Combined	None	Recurred (3 mo, liver)	Surgery	Dead (12 mo)
Tazi *et al*.[8]	68/M	B	4.0	Positive (NEC)	Collision	None	-	Surgery → chemotherapy (cisplatin, etoposide)	Alive (F/U 28 mo)
Nakanishi *et al*.[9]	76/M	C	3.0	Negative	Combined	None	Recurred (6 mo, bone)	TACE → surgery	Dead (7 mo)
Aboelenen *et al*.[10]	51/M	C	7.5	Negative	Combined	None	-	Surgery	Alive (F/U 6 mo)
Nishino *et al*.[11]	72/M	C	2.5	Negative	Combined	None	Recurred (1 wk, lymph nodes)	Surgery → recur: chemotherapy (cisplatin, etoposide)	Dead (2 mo)
Nomura *et al*.[1]	71/M	C	4.1	Not given	Combined	None	Recurred (liver)	Surgery	Dead (8 mo)
Nomura *et al*.[1]	71/M	C	3.0	Not given	Collision	None	Recurred (liver)	RFA → surgery	Dead (2 mo)
Nomura *et al*.[1]	58/M	B	4.3	Not given	Combined	None	-	Surgery	Alive (F/U 20 mo)
Nomura *et al*.[1]	50/M	B	1.8	Not given	Combined	None	-	Surgery	Alive (F/U 19 mo)
Nomura *et al*.[1]	63/M	C	3.0	Not given	Combined	None	-	IFN → surgery	Alive (24 mo)
Baker *et al*.[12]	76/M	None	5.5	Negative	Collision	None	-	Surgery → chemotherapy (platinum-based)	Alive (F/U not given)
Choi *et al*.[13]	72/M	C	2.5	Negative	Collision	None	Recurred (6 mo, liver)	Surgery → recur: chemotherapy (cisplatin, etoposide)	Alive (F/U 10 mo)
Liu *et al*.[14]	65/M	C	4.3	Positive (NEC)	Collision	None	-	Surgery	Dead (1.3 mo)

M, male; NEC, neuroendocrine carcinoma; F/U, follow-up; TACE, transarterial chemoembolization; RFA, radiofrequency ablation; IFN, interferon therapy.

Table 2. Summary of previously reported hepatocellular carcinoma cases with ectopic PTH production

	Age/ Sex	Chronic hepatitis type	Hepatocellular carcinoma	Initial laboratory findings				Parathyroid lesion	Treatment	Method of ectopic PTH confirmation	Survival
				Calcium (mg/dL)	Intact PTH (pg/mL)	PTHrP (pmol/L)	AFP (ng/mL)				
Koyama *et al.*[20]	83/M	C	Single 8 cm mass	13.0 (8.9–10.1)	360 (15–50)	18.7 (13.8–55.3)	29.348 (0–10)	None	TAE	Venous sampling Decreased serum calcium and intact PTH after TAE	Alive (F/U 24 mo)
Mahoney *et al.*[19]	72/M	None	Multiple large lesions, extending into portal vein	14.5 (8.5–10.5)	92 (12–65)	< 0.7 (< 1.3)	Not given	Parathyroid adenoma	Parathyroid resection and TACE	Sestamibi SPECT scan Immunoradiometric assay and rapid assay	Dead (not given)
Abe *et al.*[18]	73/F	B	Large mass with multiple metastasis	12.9 (8.5–10.5)	99 (< 60)	< 1 (not given)	189.3 (not given)	None	TACE	Decreased serum calcium and intact PTH after TACE	Dead (2 mo)

PTH, parathyroid hormone; PTHrP, PTH-related peptide; AFP, α-fetoprotein; M, male; TAE, transcatheter arterial embolization; F/U, follow-up; TACE, transarterial chemoembolization; SPECT, single-photon emission computed tomographic.

Clinicians and pathologists are advised to take caution for neuroendocrine differentiation when diagnosing poorly differentiated HCC.

Conflicts of Interest

No potential conflict of interest relevant to this article was reported.

REFERENCES

1. Nomura Y, Nakashima O, Akiba J, *et al*. Clinicopathological features of neoplasms with neuroendocrine differentiation occurring in the liver. J Clin Pathol 2017; 70: 563-70.
2. Barsky SH, Linnoila I, Triche TJ, Costa J. Hepatocellular carcinoma with carcinoid features. Hum Pathol 1984; 15: 892-4.
3. Artopoulos JG, Destuni C. Primary mixed hepatocellular carcinoma with carcinoid characteristics: a case report. Hepatogastroenterology 1994; 41: 442-4.
4. Ishida M, Seki K, Tatsuzawa A, *et al*. Primary hepatic neuroendocrine carcinoma coexisting with hepatocellular carcinoma in hepatitis C liver cirrhosis: report of a case. Surg Today 2003; 33: 214-8.
5. Yamaguchi R, Nakashima O, Ogata T, Hanada K, Kumabe T, Kojiro M. Hepatocellular carcinoma with an unusual neuroendocrine component. Pathol Int 2004; 54: 861-5.
6. Garcia MT, Bejarano PA, Yssa M, Buitrago E, Livingstone A. Tumor of the liver (hepatocellular and high grade neuroendocrine carcinoma): a case report and review of the literature. Virchows Arch 2006; 449: 376-81.
7. Yang CS, Wen MC, Jan YJ, Wang J, Wu CC. Combined primary neuroendocrine carcinoma and hepatocellular carcinoma of the liver. J Chin Med Assoc 2009; 72: 430-3.
8. Tazi EM, Essadi I, M'Rabti H, Errihani H. Hepatocellular carcinoma and high grade neuroendocrine carcinoma: a case report and review of the literature. World J Oncol 2011; 2: 37-40.
9. Nakanishi C, Sato K, Ito Y, *et al*. Combined hepatocellular carcinoma and neuroendocrine carcinoma with sarcomatous change of the liver after transarterial chemoembolization. Hepatol Res 2012; 42: 1141-5.
10. Aboelenen A, El-Hawary AK, Megahed N, *et al*. Right hepatectomy for combined primary neuroendocrine and hepatocellular carcinoma: a case report. Int J Surg Case Rep 2014; 5: 26-9.
11. Nishino H, Hatano E, Seo S, *et al*. Histological features of mixed neuroendocrine carcinoma and hepatocellular carcinoma in the liver: a case report and literature review. Clin J Gastroenterol 2016; 9: 272-9.
12. Baker E, Jacobs C, Martinie J, Iannitti DA, Vrochides D, Swan RZ. Mixed hepatocellular carcinoma, neuroendocrine carcinoma of the liver. Am Surg 2016; 82: 1121-5.
13. Choi GH, Ann SY, Lee SI, Kim SB, Song IH. Collision tumor of hepatocellular carcinoma and neuroendocrine carcinoma involving the liver: case report and review of the literature. World J Gastroenterol 2016; 22: 9229-34.
14. Liu YJ, Ng KF, Huang SC, Wu RC, Chen TC. Composite hepatocellular carcinoma and small cell carcinoma with early nodal metastasis: a case report. Medicine (Baltimore) 2017; 96: e7868.
15. Doyle MA, Malcolm JC. An unusual case of malignancy-related hypercalcemia. Int J Gen Med 2013; 7: 21-7.
16. Huh UY, Kim JH, Kim BH, *et al*. The incidence and clinical significance of paraneoplastic syndromes in patients with hepatocellular carcinoma. Korean J Hepatol 2005; 11: 275-83.
17. Burtis WJ, Wu T, Bunch C, *et al*. Identification of a novel 17,000-dalton

parathyroid hormone-like adenylate cyclase-stimulating protein from a tumor associated with humoral hypercalcemia of malignancy. J Biol Chem 1987; 262: 7151-6.
18. Abe Y, Makiyama H, Fujita Y, Tachibana Y, Kamada G, Uebayashi M. Severe hypercalcemia associated with hepatocellular carcinoma secreting intact parathyroid hormone: a case report. Intern Med 2011; 50: 329-33.
19. Mahoney EJ, Monchik JM, Donatini G, De Lellis R. Life-threatening hypercalcemia from a hepatocellular carcinoma secreting intact parathyroid hormone: localization by sestamibi single-photon emission computed tomographic imaging. Endocr Pract 2006; 12: 302-6.
20. Koyama Y, Ishijima H, Ishibashi A, *et al*. Intact PTH-producing hepatocellular carcinoma treated by transcatheter arterial embolization. Abdom Imaging 1999; 24: 144-6.

Journal of Pathology and Translational Medicine 2018; 52: 238-242
https://doi.org/10.4132/jptm.2017.11.21

■ CASE STUDY ■

Primary Cutaneous Mucinous Carcinoma with Extramammary Paget's Disease: Eccrine or Apocrine?

Sun-Ju Oh · Young-Ok Kim

Department of Pathology, Kosin University Gospel Hospital, Busan, Korea

Received: October 26, 2017
Revised: November 17, 2017
Accepted: November 21, 2017

Corresponding Author
Sun-Ju Oh, MD
Department of Pathology, Kosin University Gospel Hospital, 262 Gamcheon-ro, Seo-gu, Busan 49267, Korea
Tel: +82-51-990-6744
Fax: +82-51-990 3080
E-mail: 10highpowerfield@gmail.com

Primary cutaneous mucinous carcinoma (PCMC) is an uncommon tumor of the sweat gland origin. The occurrence of PCMC is mostly in middle-aged and older patients, with a slight male predominance. Most cases of PCMC arise on the head, with a preference for eyelids. The histogenesis of PCMC, whether eccrine or apocrine, remains controversial. We report a rare case of PCMC with secondary extramammary Paget's disease in the groin of a 75-year-old man, which favored an apocrine origin. Furthermore, based on a review of the literature, we provide several histologic clues that can be used to differentiate PCMC from metastatic mucinous carcinoma.

Key Words: Cutaneous mucinous carcinoma; Skin adnexal tumor; Apocrine carcinoma; Paget's disease, extramammary

Primary cutaneous mucinous carcinoma (PCMC) is a rare sweat gland tumor,[1] whereas the majority of mucinous carcinoma of the skin is metastatic. The common metastasis originates from the gastrointestinal tract and other sites such as the breast, salivary glands, lacrimal glands, nose and paranasal sinuses, bronchi, renal pelvis, and ovary.[2] It occurs mostly in middle-aged and older patients, with a slight male predominance. The histogenesis of PCMC, whether eccrine or apocrine, remains controversial. Several studies have suggested that the neoplasm showed eccrine differentiation,[3-6] while others favored apocrine origin.[7-10]

We report a case of PCMC with extramammary Paget's disease (EMPD), exhibiting the biphasic appearance of pure mucinous carcinoma and poorly differentiated carcinoma that favors apocrine differentiation. In addition, we discuss features that differentiate PCMC and metastatic mucinous carcinoma.

CASE REPORT

A 75-year-old man presented with recurrent pruritic eczema of the penis and scrotum that was refractory to medication of the local dermatologic clinic for one and a half years. The lesion consisted of an erythematous and indurated plaque with ulceration and exudation (Fig. 1A). Review of the patient's history revealed that he underwent right hemicolectomy for adenocarcinoma in the ascending colon when he was 62 years old. He remained under regular follow-up for 13 years, during which no metastases were reported. Examination of skin biopsy from the inguinal folds revealed large cells with clear to eosinophilic cytoplasm that had infiltrated into the epidermis, singly and in clusters (Fig. 1B). The initial histologic diagnosis of the skin biopsy was EMPD. The preoperative instrumental investigations showed no evidence of recurrence on the previous surgical site or other underlying internal malignancy. The patient underwent a mapping biopsy at multiple sites to accurately establish the boundary of the lesion, followed by wide excision and closure of the defect with a skin graft.

The resected perineum and penile shaft showed ill-defined indurated nodules with a firm consistency. The lesion in the overlying epidermis measured 6 cm, with a 1.5-cm-sized mass in the dermis. The cut surface was solid and gray-white with focal mucinous appearance. On histologic examination, the low-power view showed a relatively well-defined mass occupying the dermis and subcutis (Fig. 2B). The overlying epidermis showed irregular epidermal hyperplasia containing scattered large cells arranged singly or in groups, as in the previous skin biopsy,

pISSN 2383-7837
eISSN 2383-7845

suggesting an epidermal pagetoid spread of underlying tumor cells (Fig. 1B). The tumor showed two composite features in which solid nests of poorly differentiated carcinoma were juxtaposed with paucicellular mucinous lakes with floating tumor cell clusters (Fig. 2C). The latter accounted for the majority of the tumor, about 70%, and the rest consisted of poorly differentiated components. Tumor cells in both the mucinous pool and more cellular area revealed the same histological features of abundant eosinophilic cytoplasm and large vesicular nuclei with frequent mitoses up to 7/10 high power field (Fig. 2C, D). *In*

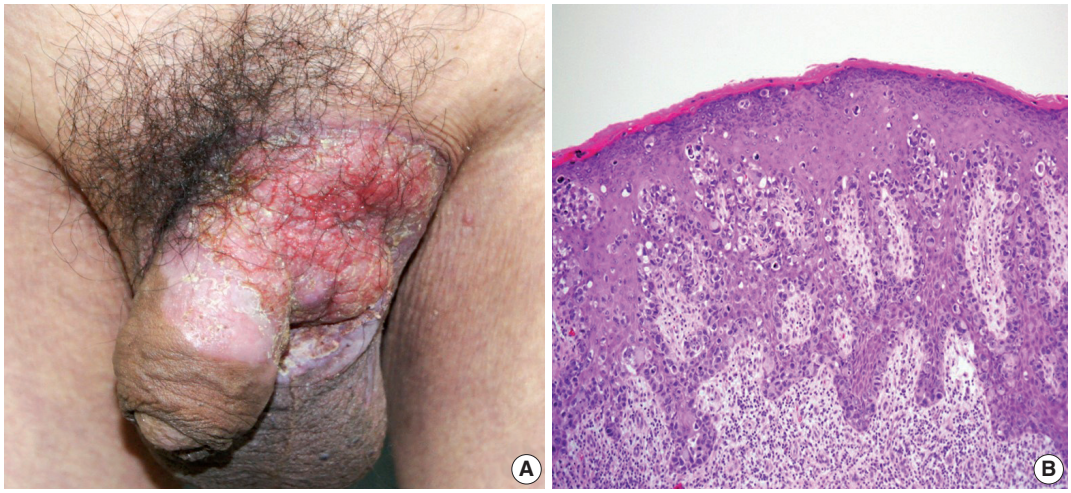

Fig. 1. (A) Erythematous plaque of the left groin with extension to the scrotum and penis. (B) Histology of preoperative skin biopsy revealing extensive involvement of the epidermis by large pagetoid cells with clear or eosinophilic cytoplasm.

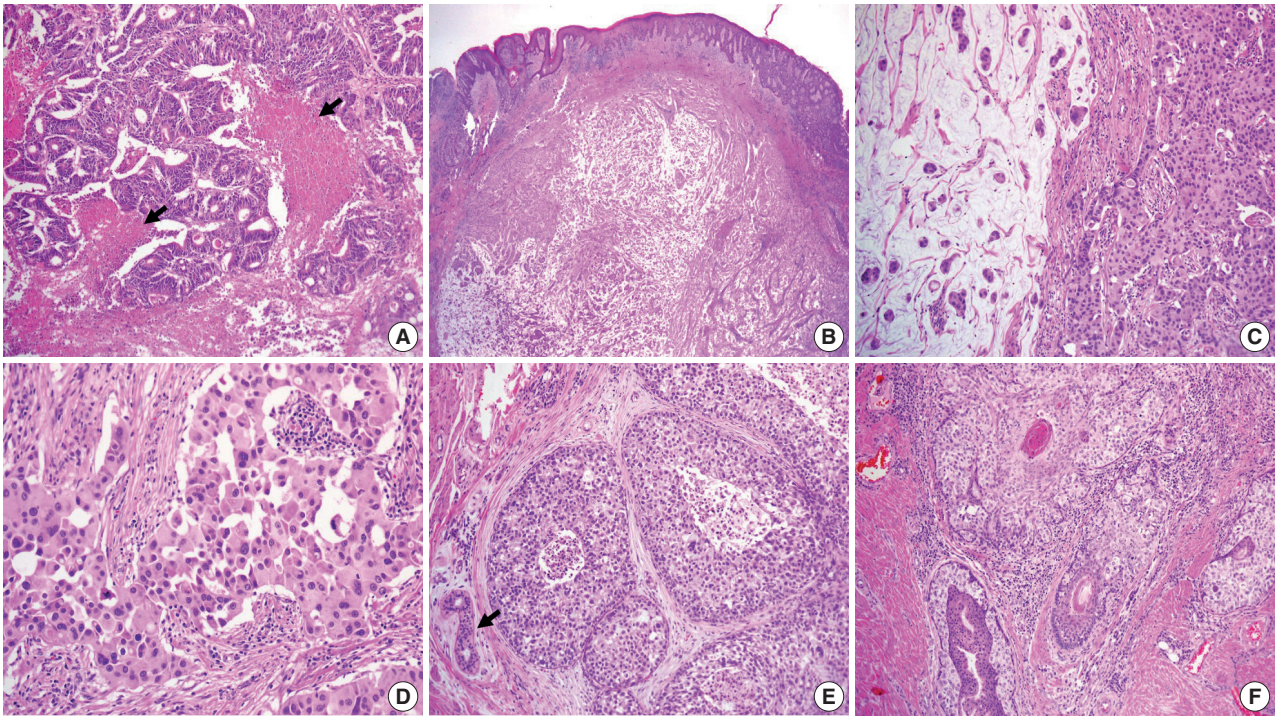

Fig. 2. (A) Moderately differentiated adenocarcinoma of the colon with dirty necrosis (arrows) diagnosed 13 years earlier. (B) Low magnification of the mass in the dermis with epidermal acanthosis due to pagetoid spread of the tumor cells. (C) Mucinous lakes with free-floating tumor nests (left) are juxtaposed with a cellular apocrine carcinoma (right), of which high magnification (D) reveals solid nests of tumor cells with round nuclei and abundant eosinophilic cytoplasm. (E) Comedo-type in situ component is depicted with normal apocrine glands (arrow). (F) Colonization of tumor cells in the hair follicle.

situ lesions similar to ductal carcinoma *in situ* of the breast were also observed (Fig. 2E) with colonization of the hair follicles (Fig. 2F). Overall histology suggested a mucinous carcinoma with minor poorly differentiated components.

Histological differential diagnosis included PCMC and late metastasis of the previously diagnosed colon cancer. Histologic review of the patient's previous colon cancer showed a 4.3-cm moderately differentiated adenocarcinoma with the assigned stage of T3N0M0. The tumor consisted of well-formed or cribriform patterns of tumor glands with frequently observed dirty necrosis (Fig. 2A). There was no mucin production observed in the skin lesion.

Immunohistochemical studies were performed. The Paget's and dermal tumor cells of the skin lesion were positive for cytokeratin (CK) 7, CK20, gross cystic disease fluid protein-15 (GCDFP-15) (Fig. 3A–C), and carcinoembryonic antigen (CEA), but negative for caudal-related homeobox gene 2 (CDX-2). On the other hand, tumor cells of the colon cancer were positive for CK20, CDX-2, CEA, but not gross cystic disease fluid protein 15 or CK7. Additional staining of human epidermal growth factor receptor 2 and estrogen receptor (ER) was observed in the skin lesion (Fig. 3D, E), but the lesion was negative for progesterone receptor (PR). Myoepithelial cells surrounding the carcinoma *in situ* were highlighted by CK5/6 immunostaining (Fig. 3F). The overall immunohistochemical findings of the skin lesion were different from those of colon cancer but similar to those of breast cancer, but similar to those of breast cancer, indicating sweat gland origin. On the basis of these histologic and immunohistochemical findings, the two malignancies were considered to differ in origin, and the present case was a primary mucinous carcinoma of the skin.

Another challenge was to determine whether the minor poorly differentiated components were eccrine or apocrine in origin because there was no clear distinction in histologic and immunohistochemical features. We concluded apocrine differentiation of the lesion due to the location in the groin, where apocrine glands are many in number, and to the resemblance of apocrine carcinoma in the breast even though decapitation secretion was absent. In addition, close approximation and colonization of the hair follicle (Fig. 2F) favored the origin of the follicular-apocrine unit.

The final pathologic diagnosis was PCMC with EMPD showing apocrine differentiation.

This case was approved by the institutional review board (IRB) of Kosin University Gospel Hospital, and informed consent was waived by the IRB (IRB reference number: 2017-10-010).

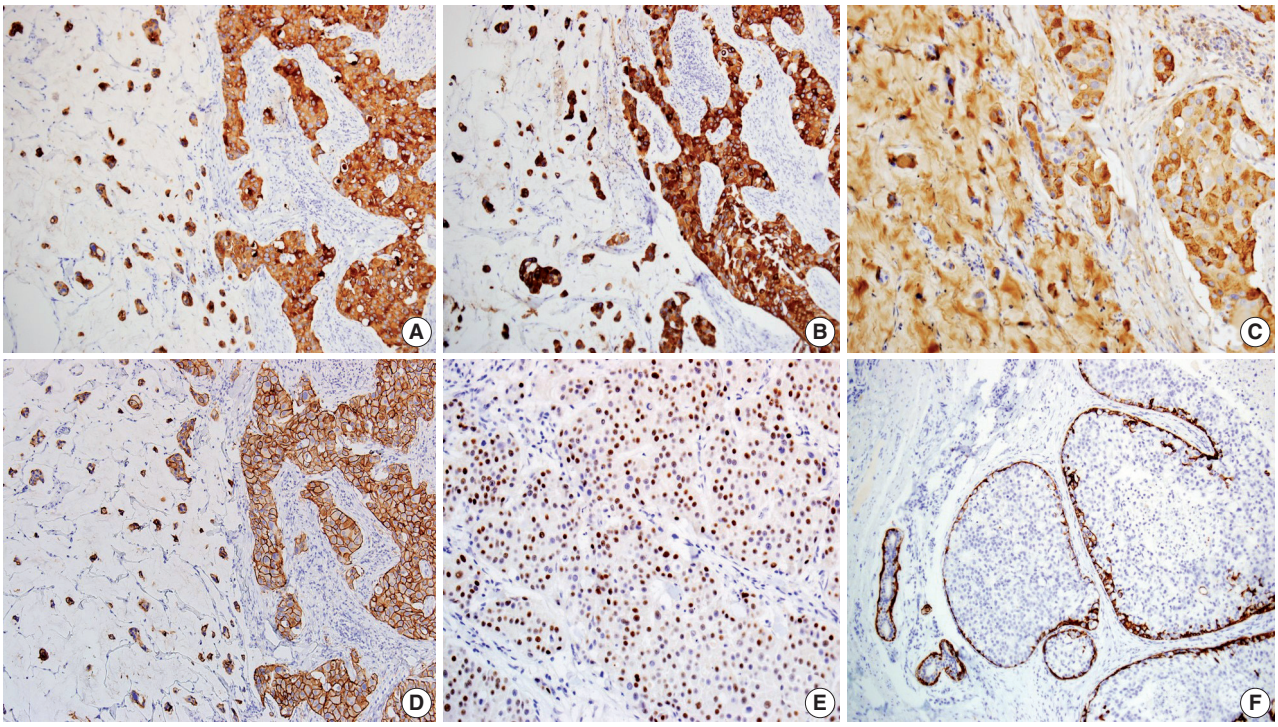

Fig. 3. Immunohistochemical findings of tumor cells showing positivity for cytokeratin (CK) 7 (A), CK20 (B), Gross cystic disease fluid protein 15 (C), human epidermal growth factor receptor 2 (D), and estrogen receptor (E). Myoepithelial cells of *in situ* components and normal apocrine glands highlighted by immunostaining for CK5/6 (F).

https://doi.org/10.4132/jptm.2017.11.21

DISCUSSION

PCMC is an uncommon subtype of sweat gland tumor. Only about 100 cases of PCMC have been reported[1,6] since the first report by Lennox *et al*.[11] in 1952. PCMC shows a slight male predominance and typically affects people aged 50–70 years. The eyelid was most commonly affected, followed by the scalp, face, axilla, chest/abdominal wall, vulva, neck, extremity, canthus, groin, and ear.[6] The primary lesion of PCMC is often solitary, and the size of the neoplasm varies in diameter from about 0.7–8.0 cm.

It is still controversial whether PCMC has eccrine or apocrine differentiation. Determining the eccrine or apocrine differentiation continues to be problematic because there is no clear distinction in histologic and immunohistochemical features. Robson *et al*.[12] suggested that apocrine differentiation was determined when encountering the tumor in its usual anatomic location with numerous apocrine glands and with its propensity for coexistence with follicular tumors, which means it is derived from the follicular-apocrine-sebaceous rather than eccrine axis. The presence of decapitation secretion is also known to be a hallmark of apocrine differentiation. However, some authors[12] described apocrine carcinoma without decapitation secretion, and they relied on the identification of tumor cells with abundant eosinophilic cytoplasm in tumors that arises from a typical location including the axilla or groin, as in the present case.

For PCMC, some authors have favored eccrine differentiation based on immunohistochemical studies and ultrastructural analysis.[3-5] On the other hand, other studies have suggested that PCMC has an apocrine origin.[7-10] Riquena *et al*.[7] suggested an apocrine origin for PCMC because it shows identical histologic features with mucinous carcinoma of the mammary glands, known as modified apocrine glands. Another study reported a case of PCMC coexisting with trichofolliculoma, also providing evidence of apocrine lineage.[9]

The present case revealed EMPD associated with underlying PCMC. EMPD is considered to be an intraepithelial adenocarcinoma typically involving vulvar, perianal, perineal, scrotal, and penile regions.[13] EMPD sometimes occurs secondarily in association with cutaneous adnexal tumors or with internal malignancies. Some authors have shown that vulvar EMPD was associated with adnexal adenocarcinoma in 4% of cases and with a distant malignancy in 20%, while perianal EMPD was associated with adnexal adenocarcinoma in 7% of cases and an internal malignancy in 14% of cases.[14] There have been rare cases of PCMC coexisting with overlying EMPD, as in our case.[15-17] Hurt *et al*.[15] reported two cases of anogenital PCMC with EMPD, describing fibroepithelioma-like change of the overlying epidermis. The authors suggested that the anogenital mucinous carcinoma was associated with the EMPD, which had never been described in extraperineal mucinous carcinoma. To our knowledge, there have been no reports of EMPD coexisting with eccrine carcinoma in the groin. Instead, four cases of apocrine carcinoma with EMPD in this region have been reported in the English literature,[14,18-20] which supports apocrine differentiation.

Another challenge in establishing the diagnosis of PCMC is the exclusion of metastasis from an underlying neoplasm because the majority of mucinous carcinomas in the skin are metastatic. The common metastasis is derived from the gastrointestinal tract, and other sites including the breast, salivary glands, lacrimal glands, nose and paranasal sinuses, bronchi, renal pelvis, and ovary have been reported.[2] There are several histologic criteria and immunohistochemical patterns that can differentiate primary and secondary mucinous carcinomas.[1,2,7] Riquena *et al*.[7] suggested that histologic features such as larger clusters of cohesive neoplastic cells, fewer quantities of mucin, predominance of epithelium over mucin, and the absence of delicate fibrous septa favor metastasis. There have been other reports[1,2] that the presence of an *in situ* component is most useful to establish PCMC especially when discriminating it from cutaneous metastasis of breast mucinous carcinoma. Morphologically, cutaneous and mammary lesions are indistinguishable and have immunophenotypic similarity, both expressing CK7, CEA, GCDFP 15, S-100 protein, ER, and PR. Qureshi *et al*.[2] emphasized *in situ* components assessed by the presence of a myoepithelial cell layer identified by immunohistochemical staining for p63, CK5/6, calponin, and smooth muscle actin. The presence of an *in situ* component defines the neoplasm as primary cutaneous, but its absence does not exclude the diagnosis. A full clinical investigation is required to exclude metastasis and establish the origin. It is less challenging to exclude a metastasis of colorectal origin. Kazakov *et al*.[1] suggested that dirty necrosis, frequently encountered in colorectal metastasis to the ovaries, is a good criterion of cutaneous mucinous carcinoma of intestinal origin. Tumor cells from colorectal adenocarcinoma were CK7–/CK20+ and invariably positive for CDX-2.

The current treatment for PCMC is excision with an at least 1-cm margin, as it is found to be resistant to chemotherapy and radiation.[6] Prognosis is relatively good after complete surgical excision, with rare metastasis to regional lymph nodes.[2] Prophylactic lymph node dissection should be considered in tumors of the axilla, as these have a higher rate of metastasis.[5] Close follow-

up is warranted as local recurrence is frequent at 29.4% in spite of a low metastasis rate and an indolent course. The overall mortality rate is 2%.[6]

In summary, PCMC is an uncommon variant of sweat gland tumor. Our case is a rare PCMC with EMPD. Minor poorly differentiated components were also observed, which suggested apocrine differentiation. However, further studies are required to clarify the histogenesis of PCMC. Clinical differentiation from metastatic mucinous carcinoma is most important, and a careful search for an *in situ* component can be a helpful morphologic finding that identifies the primary nature of the carcinoma in addition to the immunohistochemical panel.

Conflicts of Interest

No potential conflict of interest relevant to this article was reported.

REFERENCES

1. Kazakov DV, Suster S, LeBoit PE, *et al*. Mucinous carcinoma of the skin, primary, and secondary: a clinicopathologic study of 63 cases with emphasis on the morphologic spectrum of primary cutaneous forms: homologies with mucinous lesions in the breast. Am J Surg Pathol 2005; 29: 764-82.
2. Qureshi HS, Salama ME, Chitale D, *et al*. Primary cutaneous mucinous carcinoma: presence of myoepithelial cells as a clue to the cutaneous origin. Am J Dermatopathol 2004; 26: 353-8.
3. Headington JT. Primary mucinous carcinoma of skin: histochemistry and electron microscopy. Cancer 1977; 39: 1055-63.
4. Wright JD, Font RL. Mucinous sweat gland adenocarcinoma of eyelid: a clinicopathologic study of 21 cases with histochemical and electron microscopic observations. Cancer 1979; 44: 1757-68.
5. Pilgrim JP, Kloss SG, Wolfish PS, Heng MC. Primary mucinous carcinoma of the skin with metastases to the lymph nodes. Am J Dermatopathol 1985; 7: 461-9.
6. Martinez S, Young S. Primary mucinous carcinoma of the skin. Internet J Oncol 2004; 2: 1-7.
7. Requena L, Kiryu H, Ackerman AB. Neoplasms with apocrine differentiation. Philadelphia: Lippincott Williams & Wilkins, 1998; 907-47.
8. Saigal RK, Khanna SD, Chander J. Apocrine gland carcinoma in axilla. Indian J Dermatol Venereol 1971; 37: 177-80.
9. Aso K, Sato N. A case of primary mucinous carcinoma of the skin and trichofolliculoma developed in the same tissue. Jpn J Clin Dermatol 1989; 43: 117-20.
10. Wako M, Nishimaki K, Kawamura N, *et al*. Mucinous carcinoma of the skin with apocrine-type differentiation: immunohistochemical studies. Am J Dermatopathol 2003; 25: 66-70.
11. Lennox B, Pearse AG, Richards HG. Mucin-secreting tumours of the skin with special reference to the so-called mixed-salivary tumour of the skin and its relation to hidradenoma. J Pathol Bacteriol 1952; 64: 865-80.
12. Robson A, Lazar AJ, Ben Nagi J, *et al*. Primary cutaneous apocrine carcinoma: a clinico-pathologic analysis of 24 cases. Am J Surg Pathol 2008; 32: 682-90.
13. Helwig EB, Graham JH. Anogenital (extramammary) Paget's disease: a clinicopathological study. Cancer 1963; 16: 387-403.
14. Pascual JC, Perez-Ramos M, Devesa JP, Kutzner H, Requena L. Extramammary Paget's disease of the groin with underlying carcinoma and fatal outcome. Clin Exp Dermatol 2008; 33: 595-8.
15. Hurt MA, Hardarson S, Stadecker MJ, Santa Cruz DJ. Fibroepithelioma-like changes associated with anogenital epidermotropic mucinous carcinoma: fibroepitheliomatous Paget phenomenon. J Cutan Pathol 1992; 19: 134-41.
16. Taniyama K, Suzuki H, Yamada A, Tahara E. Extramammary Paget's disease with an underlying mucinous adenocarcinoma of the buttocks. Gan No Rinsho 1988; 34: 379-84.
17. Matin RN, Gibbon K, Rizvi H, Harwood CA, Cerio R. Cutaneous mucinous carcinoma arising in extramammary Paget disease of the perineum. Am J Dermatopathol 2011; 33: 705-9.
18. Bowling JC, Powles A, Nasiri N, Searle A, Bunker CB. Spontaneous regression of extramammary Paget's disease after excision of primary apocrine carcinoma, in an immunosuppressed patient. Br J Dermatol 2005; 153: 676-7.
19. Hernandez JM, Copeland EM 3rd. Infiltrating apocrine adenocarcinoma with extramammary pagetoid spread. Am Surg 2007; 73: 307-9.
20. Seo SH, Shin DH, Sung HW. Apocrine carcinoma of the groin possibly associated with extramammary Paget's disease. Ann Dermatol 2011; 23: 519-22.

 https://doi.org/10.4132/jptm.2017.11.21

Journal of Pathology and Translational Medicine 2018; 52: 243-247
https://doi.org/10.4132/jptm.2018.03.27

■ CASE STUDY ■

Recurrent Indeterminate Dendritic Cell Tumor of the Skin

Jin Woo Joo · Taek Chung
Yoon Ah Cho · Sang Kyum Kim

Department of Pathology, Severance Hospital, Yonsei University College of Medicine, Seoul, Korea

Received: September 14, 2017
Revised: March 13, 2018
Accepted: March 27, 2018

Corresponding Author
Sang Kyum Kim, MD, PhD
Department of Pathology, Severance Hospital, Yonsei University College of Medicine, 50-1 Yonsei-ro, Seodaemun-gu, Seoul 03722, Korea
Tel: +82-2-2228-6751
Fax: +82-2-2227-7939
E-mail: NICEKYUMI@yuhs.ac

Indeterminate dendritic cell tumor (IDCT) is a dendritic cell tumor that displays histologic features similar to those of Langerhans cells. The origin of the indeterminate cells may represent precursors of Langerhans cells or skin dendritic cells. IDCT is extremely rare, and tumor progression and predictive factors are not well known. Here, we report a case of a 61-year-old man who presented with a papule on his back and was finally diagnosed with IDCT based on histology and immunohistochemistry. The tumor recurred three months after surgical excision.

Key Words: Indeterminate dendritic cell tumor; Skin tumor; Recurrence

Indeterminate dendritic cell tumor (IDCT) is a proliferative disorder of indeterminate cells that has been reported since the 1980s.[1,2] However, the origin of indeterminate cells is still debated. Indeterminate cells share histological, ultrastructural, and antigenic features of Langerhans cells, but they lack Birbeck granules on electron microscopic examination.[1,2]

The clinical course of IDCT is relatively good. However, associations between IDCT and other hematologic malignancies such as B-cell lymphoma and acute myeloid leukemia have been reported,[3,4] and recurrent IDCT was reported in the oral mucosa,[5] although there are no known prognostic factors. To our knowledge, recurrent IDCT in the skin after surgical resection is extremely rare. We herein describe a case of recurrent IDCT in the skin after surgical excision.

CASE REPORT

A 61-year-old man had started to develop a papule on his back approximately 2 years prior. After 1 year, the papule was removed by laser therapy. However, the patient continued to have multiple papules on his back, and he presented to our hospital. On physical examination, four asymptomatic erythematous papules were observed (Fig. 1A). The largest papule was approximately 2 cm in size (Fig. 1B). Since the patient's brother was diagnosed with acute leukemia, he had blood analyses which showed white blood cell count (WBC) of 3.4×10^9/L, hemoglobin 14.7 g/L, and platelet count 99×10^9/L. The patient underwent surgical excision of the papules. Gross examination of the largest nodule revealed a poorly defined infiltrative whitish mass (1.8×1.3 cm) involving the dermis and subcutis, showing focal hemorrhage and necrosis (Fig. 1C).

Histological evaluation revealed the infiltration of large epithelioid cells with mild to moderate nuclear atypia and large, irregular folded or twisted nuclei with a solid growth pattern (Fig. 2A–C). Proliferative cells with abundant pale eosinophilic cytoplasm were noted. The lesion exhibited frequent mitotic figures (99/10 high-power field) and a few scattered multi-nucleated giant cells (Fig. 2D). Peritumoral lymphocytic infiltration was also observed, with the absence of eosinophilic infiltration. Immunohistochemistry showed that the tumor expressed S100 protein and CD1a, but not Langerin (Fig. 3A–C). The tumor focally expressed CD68 (Fig. 3D), but did not express CD3, CD20, CD21, CD30, CD31, CD34, CD45, CD99, CD163, MPO, c-Kit, Melan A, human melanoma black 45, or smooth muscle actin. The Ki67 labeling index was approximately 70%. In situ hybridization for Epstein-Barr virus encoded RNA was negative

pISSN 2383-7837
eISSN 2383-7845

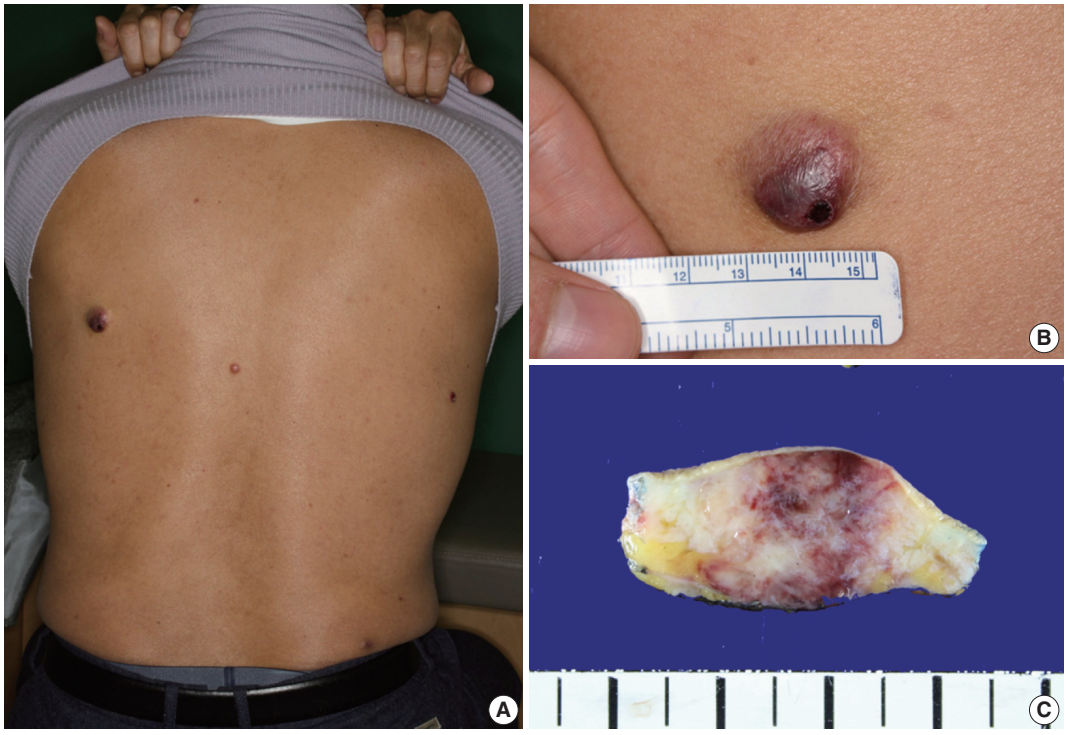

Fig. 1. Physical and gross findings. (A) Four erythematous papules on the patient's back. (B) The largest papule. (C) Gross examination of the largest nodule involving the dermis and subcutis.

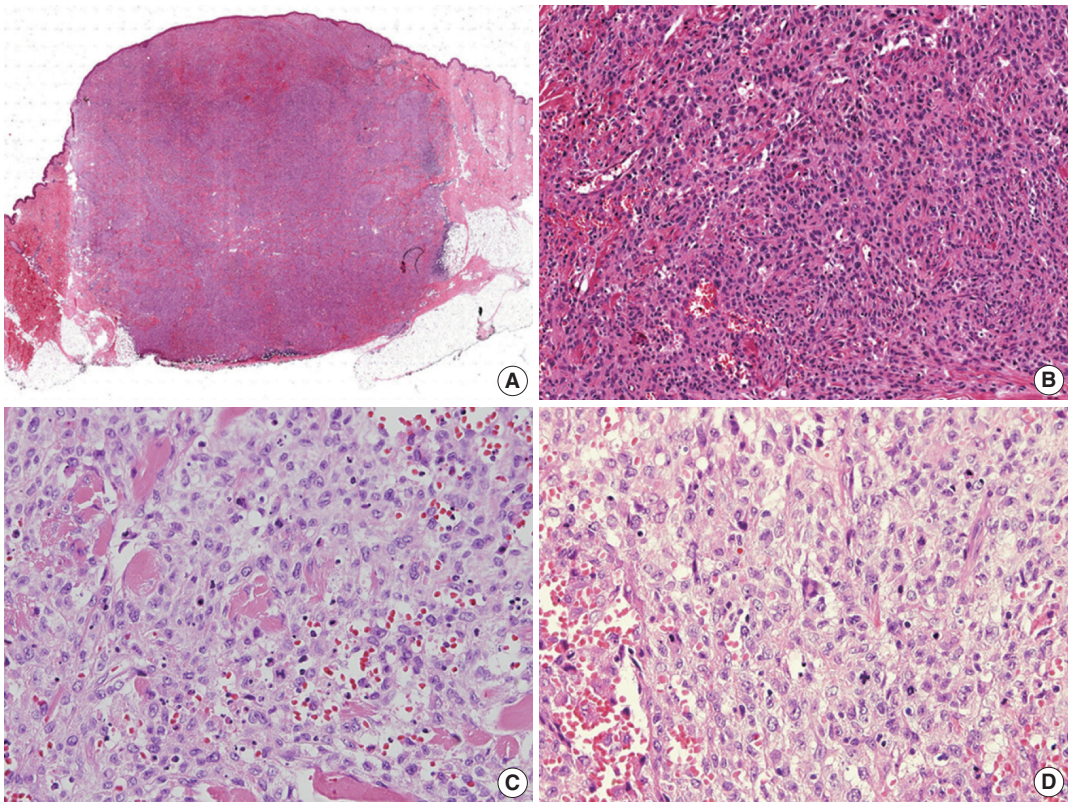

Fig. 2. Histologic findings. (A) Scan power view of the largest nodule. (B) A solid growth of epithelioid cells with infiltrative borders. (C) Epithelioid cells with moderate nuclear atypia and irregular folded nuclei. (D) Frequent mitoses and a few scattered multi-nucleated giant cells.

https://doi.org/10.4132/jptm.2018.03.27

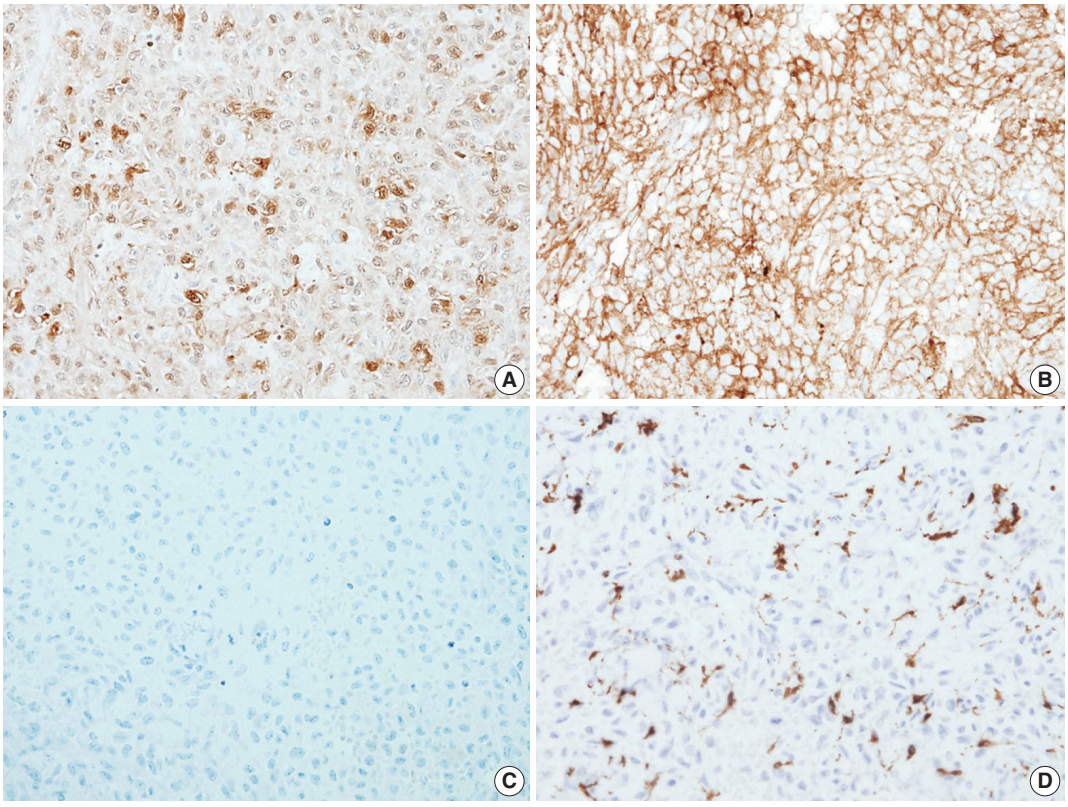

Fig. 3. The immunohistochemical stain results. Immunohistochemical panels of S100 (A), CD1a (B), Langerin (C), and CD68 (D).

and *BRAF* mutation was not identified by the pyrosequencing method. No ultrastructural examination was performed.

Two weeks after the operation, bone marrow examinations were performed because of the patient's low platelet count. A bone marrow aspiration and biopsy showed hypocellular marrow (about 20%) with a slightly increased number of megakaryocytes. The proportion of megakaryocytes showing dysplastic features was increased, but did not meet the diagnostic criteria of myelodysplastic syndrome.

Two months after the bone marrow examinations, a 0.5 cm nodule was found on the patient's left buttock. The nodule was resected, and the tumor exhibited similar histological features as those of the previous specimens. Therefore, we diagnosed this tumor as recurrent IDCT. Three months later, multiple papulonodular skin lesions recurred on the patient's back and anterior chest. We observed these lesions without administering medical therapy. The patient was not examined with whole-body imaging technology for metastasis.

Hematology oncologists suggested that further whole body examinations should be performed because of the repeated recurrence. The latest blood examination results were within normal limits for WBC count, hemoglobin level, and platelet count (WBC 5.81×10^9/L, hemoglobin 11.2 g/dL, and platelet 120×10^9/L). Chest X-ray did not reveal any suspicious metastatic lesions.

Authorization for the use of the case information and materials was obtained from the Institutional Review Board (IRB) of Yonsei University College of Medicine (4-2017-0669). Informed consent was waived because the IRB decided that this retrospective study presented minimal risk to the patient (risk level I).

DISCUSSION

IDCTs are believed to derive from cells with features similar to Langerhans and interdigitating cells.[2] They have morphological and immunological similarities to normal Langerhans cells, but do not contain Birbeck granules.[1,2] Clinically, IDCTs have most often been described in adults, who present with one or more lesions, commonly cutaneous, and rarely in the lymph nodes or spleen.[1] The lesions are usually based in the dermis, occasionally with extension into the epidermis. The clinical course varies widely from spontaneous regression, to rapid progression or stable disease and to recurrence.[1]

Some recent studies suggest that Langerin (CD207) is quite a

useful marker for tumors derived from Langerhans cells, with negative findings in reported IDCTs.[6,7] Wang *et al*.[8] reported on a Langerin-positive Langerhans cell sarcoma (LCS) that did not present with Birbeck granules on ultrastructural examination.[8] This has occurred in some cases of LCS due to damage of Birbeck granules or poorly differentiated tumor cells.[9] In conclusion, Langerin is a very specific marker for distinguishing IDCT from LCS.[7,10] Our case showed typical histologic and immunophenotypic features including Langerin negativity. Therefore, this case is consistent with IDCT, even though an electron microscopic examination was not performed. Li *et al*.[11] also studied IDCT in a 90-year-old man. Although they did not perform an ultrastructural examination, they used the pathologic evaluation and immunohistochemical analysis to diagnose IDCT. The tumor revealed aggressive histologic features such as central necrosis and a high Ki67 proliferation index (35%). Moreover, multiple lymph node metastases were identified by computed tomography scan. The patient underwent radiation therapy, but died three months later due to circulatory and respiratory failure. The study suggested that old age, distant metastases, and a high Ki67 labeling index are potential prognostic factors. In our study, the Ki67 labeling index of the tumor cells was approximately 70%.

Roh *et al*.[12] reported the first case of IDCT in Korea. The patient was a 29-year-old woman who had an erythematous nodule on the flank. Histologically, the nodule exhibited typical IDCT morphology without epidermotropism or eosinophilic microabscess. Unlike our case, this tumor did not present with tumor necrosis or frequent mitoses.

The proper treatment for IDCT has not been standardized because of its rarity. Various treatments of IDCT have been reported, and some therapies such as electron beam therapy and ultraviolet B phototherapy were successful.[13,14] Since most IDCT cases are clinically benign, there is no requirement for aggressive treatment.[15]

A report by Ibrar *et al*.[5] described recurrent multifocal IDCT involving the oral mucosa in an 86-year-old man. The patient initially had a skin lesion in his left temporal scalp. Three months later, multiple skin lesions were identified on the scalp. Finally, the tumors involved the mandible, buccal mucosa, and tongue with lymph node metastasis. This case exhibited a rapidly progressing clinical course and poor prognosis. In contrast, some cases in the literature reported spontaneous regression of IDCTs in skin lesions.[16] In a study by Ratzinger *et al*.,[17] most of the patients who were diagnosed with localized IDCT were completely cured after surgical excision.

Vasef *et al*.[3] reported two cases of IDCT associated with low-grade B-cell malignancies. These cases suggest that B-cell neoplasms might be associated with several histiocytic and dendritic cell tumors. Furthermore, there is a possibility that histiocytic/dendritic cells and B cells share a common precursor.[2] Ventura *et al*.[18] reported a case of indeterminate cell histiocytosis that presented with normal findings on the hematologic examination by bone marrow biopsy at diagnosis. However, 7 months later, the blood examination represented hyperleukocytosis, anemia, and thrombocytopenia. The bone marrow biopsy revealed hypercellularity with extensive blast infiltration. The patient was finally diagnosed with acute monocytic leukemia.

According to a recent study, IDCT cells might contain the *BRAF* mutation.[19] We performed *BRAF* mutation analysis in our case, and the result was negative. The recent study also discovered *ETV3-NCOA2* translocations in a few cases of IDCT,[19] suggesting that IDCTs may have a specific clonal neoplasm.

In our case, the microscopic findings revealed several aggressive features including frequent mitoses, a focal area of necrosis, and a high Ki67 labeling index. This corresponded to the patient's malignant clinical course. We could not rule out the possibility of lymph node metastasis or involvement of other organs.

ORCID

Sang Kyum Kim: https://orcid.org/0000-0003-0768-9923

Conflicts of Interest

No potential conflict of interest relevant to this article was reported.

Acknowledgments

The Basic Science Research Program through the National Research Foundation of Korea (NRF) and was funded by the Ministry of Education (grant number 2016R1D1A1B03931581).

REFERENCES

1. LeBoit PE, Burg G, Weedon D, Serasin A. Pathology and genetics of skin tumours. Lyon: IARC Press, 2006; 220.
2. Rezk SA, Spagnolo DV, Brynes RK, Weiss LM. Indeterminate cell tumor: a rare dendritic neoplasm. Am J Surg Pathol 2008; 32: 1868-76.
3. Vasef MA, Zaatari GS, Chan WC, Sun NC, Weiss LM, Brynes RK. Dendritic cell tumors associated with low-grade B-cell malignancies: report of three cases. Am J Clin Pathol 1995; 104: 696-701.
4. Vener C, Soligo D, Berti E, *et al*. Indeterminate cell histiocytosis in association with later occurrence of acute myeloblastic leukaemia.

Br J Dermatol 2007; 156: 1357-61.
5. Ibrar W, Khurram M, Snower D. Recurrent multifocal indeterminate dendritic cell tumor involving oral mucosa: a rare case report. Am J Clin Pathol 2015; 144(Suppl 2): A316.
6. Zhao G, Luo M, Wu ZY, *et al*. Langerhans cell sarcoma involving gallbladder and peritoneal lymph nodes: a case report. Int J Surg Pathol 2009; 17: 347-53.
7. Chikwava K, Jaffe R. Langerin (CD207) staining in normal pediatric tissues, reactive lymph nodes, and childhood histiocytic disorders. Pediatr Dev Pathol 2004; 7: 607-14.
8. Wang C, Chen Y, Gao C, Yin J, Li H. Multifocal Langerhans cell sarcoma involving epidermis: a case report and review. Diagn Pathol 2012; 7: 99.
9. Ben-Ezra J, Bailey A, Azumi N, *et al*. Malignant histiocytosis X: a distinct clinicopathologic entity. Cancer 1991; 68: 1050-60.
10. Lau SK, Chu PG, Weiss LM. Immunohistochemical expression of Langerin in Langerhans cell histiocytosis and non-Langerhans cell histiocytic disorders. Am J Surg Pathol 2008; 32: 615-9.
11. Li Y, Wang TT, Zhang ZH, Wang L. Aggressive indeterminate dendritic cell tumor mimicking scalp angiosarcoma. Ann Dermatol 2017; 29: 614-7.
12. Roh J, Kim SW, Park CS. Indeterminate dendritic cell tumor: a case report of a rare Langerhans cell lineage disease. J Pathol Transl Med 2016; 50: 78-81.
13. Malhomme de la Roche H, Lai-Cheong JE, Calonje E, Davies M, Morris S, Whittaker SJ. Indeterminate cell histiocytosis responding to total skin electron beam therapy. Br J Dermatol 2008; 158: 838-40.
14. Ishibashi M, Ouchi T, Tanikawa A, Ishiko A. Indeterminate cell histiocytosis successfully treated with ultraviolet B phototherapy. Clin Exp Dermatol 2008; 33: 301-4.
15. Sidoroff A, Zelger B, Steiner H, Smith N. Indeterminate cell histiocytosis: a clinicopathological entity with features of both X- and non-X histiocytosis. Br J Dermatol 1996; 134: 525-32.
16. Contreras F, Fonseca E, Gamallo C, Burgos E. Multiple self-healing indeterminate cell lesions of the skin in an adult. Am J Dermatopathol 1990; 12: 396-401.
17. Ratzinger G, Burgdorf WH, Metze D, Zelger BG, Zelger B. Indeterminate cell histiocytosis: fact or fiction? J Cutan Pathol 2005; 32: 552-60.
18. Ventura F, Pereira T, da Luz Duarte M, Marques H, Pardal F, Brito C. Indeterminate cell histiocytosis in association with acute myeloid leukemia. Dermatol Res Pract 2010; 2010: 569345.
19. Emile JF, Abla O, Fraitag S, *et al*. Revised classification of histiocytoses and neoplasms of the macrophage-dendritic cell lineages. Blood 2016; 127: 2672-81.

Journal of Pathology and Translational Medicine 2018; 52: 248-251
https://doi.org/10.4132/jptm.2017.10.23

■ BRIEF CASE REPORT ■

Sudden Child Death due to Thrombotic Giant Coronary Artery Aneurysms Complicated by Atypical Kawasaki Disease: An Autopsy Case

DongJa Kim · Man-Hoon Han[1] · SangHan Lee[2]

Shinhyunho Pathology Clinic, Daegu; [1]Department of Pathology, Kyungpook National University Hospital, Daegu;
[2]Department of Forensic Medicine, School of Medicine, Kyungpook National University, Daegu, Korea

Kawasaki disease (KD) is an acute, self-limited vasculitis with a specific predilection for the coronary arteries, and it occurs predominantly in infancy and early childhood. Coronary artery complications develop in up to 25% of affected children if the disease is left untreated.[1] Typical KD presents a high swinging fever (often > 39°C) that persists for 5 or more days despite treatment. However, the diagnosis of KD is difficult due to obscure clinical manifestations. The atypical or incomplete form of KD is most common in children younger than 6 months or older than 5 years, and diagnosis is important due to a higher incidence of coronary artery abnormalities.[2] In Korea, there has been limited information on postmortem findings in the pediatric population.[3]

Here, we report an autopsy case of a 23-month-old child with a history of the atypical form of KD, who developed bilateral giant aneurysms of the coronary arteries.

CASE REPORT

A 23-month-old boy collapsed suddenly after taking a bath at home and was transferred to an emergency center. On arrival, he was unresponsive and expired despite intensive resuscitation. Six weeks previously, he had visited a local clinic with complaints of mild fever, general myalgia, and diarrhea. The pediatrician found conjunctival injection and a facial rash. However, oral mucosal changes, such as strawberry tongue and cervical lymphadenopathy, were not present. He was treated under the presumptive diagnosis of upper respiratory infection. A mild fever was persistent even under medical care. There were no specific complaints except that his activity had decreased for several days before the event.

At autopsy, no significant trauma or injury was noted. The patient was underweight at only 15 kg. The heart weighed 140 g, with a smooth epicardium. The pericardial space was filled with 55 mL of yellowish effusion. The right coronary artery (RCA) had three saccular aneurysms, occluded by thrombi, measuring 3.4 cm × 2.0 cm × 1.1 cm, 3.1 cm × 1.7 cm × 1.2 cm, and 0.7 cm × 0.3 cm × 0.3 cm, respectively. The left main coronary artery and the proximal part of the left anterior descending coronary artery (LAD) formed a bilocular aneurysm with a large thrombus, measuring 3.7 cm × 2.0 cm × 1.8 cm (Fig. 1). The left circumflex coronary artery was not dilated. Multiple dark, mottled areas were observed on a cross section of the myocardial wall. The affected area showed various morphologies depending on the duration after the infarction. The posterior wall of the left ventricle (LV) showed several yellow-tan infarct sites, the largest of which measured 1.5 cm × 1.0 cm. The anterior and posterior walls of the right ventricle (RV) showed gray, depressed infarct sites, or gray-white scar lesions, which indicated irreversible myocardial injury accordant to 10 to 14 days. Microscopically, foci of acute coagulative necrosis and contraction bands were seen in the posterior wall of the LV, which usually become detectable in the first four to 12 hours after injury (Fig. 2A). Polymorphonuclear leukocytes infiltrated around the necrotic muscle fibers. Some areas of the posterior wall of the LV showed hemosiderin-laden macrophages and fibrovascular granulation tissue. Histologic findings of the posterior wall of

Corresponding Author
SangHan Lee, MD
Department of Forensic Medicine, School of Medicine, Kyungpook National University, 680 Gukchaebosang-ro, Jung-gu, Daegu 41944, Korea
Tel: +82-53-420-4885, Fax: +82-53-422-4712, E-mail: sanghan1@knu.ac.kr

Received: July 22, 2017 **Revised:** September 22, 2017
Accepted: October 23, 2017

pISSN 2383-7837
eISSN 2383-7845

the LV demonstrated various morphologic spectrums, ranging from 1 to 14 days. The RV wall revealed granulation tissue with neovascularization and collagen deposition (Fig. 2B). The anterior wall of the LV and the interventricular septum were preserved. Microscopic examination of the LAD revealed mural lymphoplasmacytic infiltration, adventitial fibrosis, and neovascularization. The RCA showed polymorphonuclear leukocyte and lymphocyte infiltration with focal acute necrosis, which resulted in destruction of the internal elastic lamina (Fig. 3).

The cause of death was associated with acute and chronic ischemic injury of the heart muscle due to thrombotic coronary artery aneurysm (CAA), complicated by atypical KD.

Written informed consent was not required with a waiver by the Institutional Review Board of Kyungpook National University (KNUH 2018-04-015).

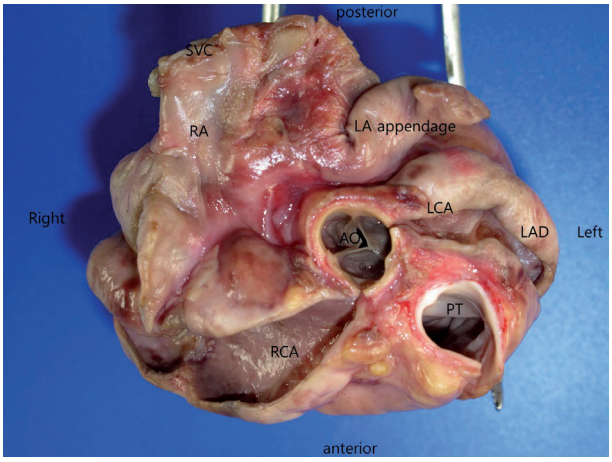

Fig. 1. Coronary artery aneurysms. The left main coronary artery (LCA), left anterior descending coronary artery (LAD), and right coronary artery (RCA) form giant aneurysms. Luminal thrombi were removed during examination. AO, aorta; LA appendage, left atrium appendage; PT, pulmonary trunk; RA, right atrium; SVC, superior vena cava.

DISCUSSION

KD is an acute inflammatory vasculitis of small- and medium-sized arteries.[1] It predominantly affects coronary arteries, resulting in weakening, aneurysm, and myocardial infarction. The diagnosis of KD is established by the presence of fever persisting for 5 days or more, along with at least four of the five principal

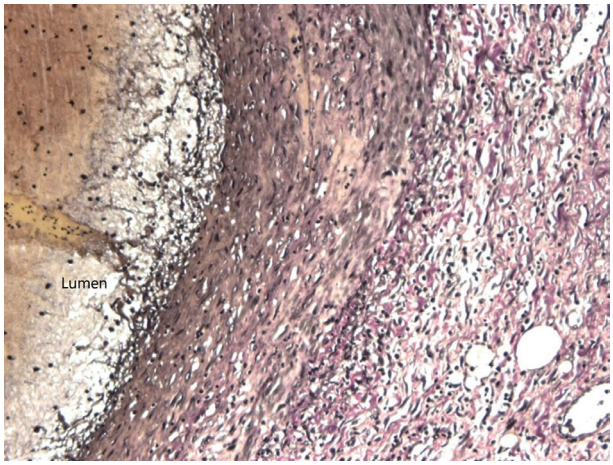

Fig. 3. Elastin stain. The right coronary artery shows destruction of internal elastic lamina and inflammatory cell infiltration.

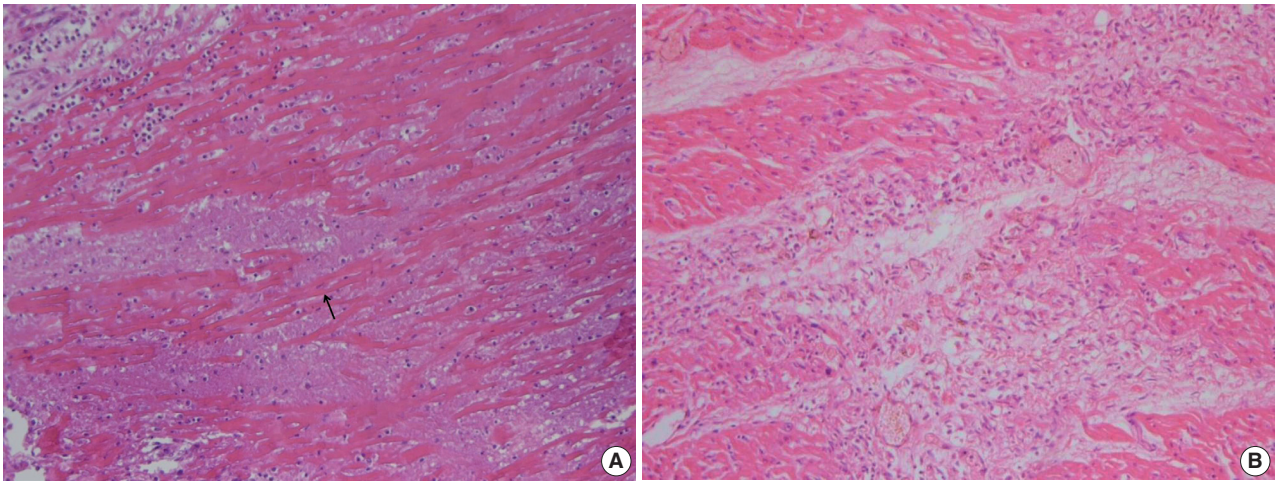

Fig. 2. Myocardial infarction of ventricular wall. (A) Posterior wall of left ventricle shows coagulative necrosis along with wavy fibers (arrow). Widened spaces between the dead myofibers contain edema fluid and scattered neutrophils. (B) Posterior wall of right ventricle reveals granulation tissue characterized by loose collagen and capillaries. Patchy fibrosis is observed, with compensatory hypertrophic changes in adjacent myocytes.

symptoms as follows: (1) bilateral bulbar conjunctival injection without exudates; (2) changes in the lips and oral cavity; (3) changes in the extremities, such as edema or erythema of hands and feet, or desquamation of the fingertips; (4) polymorphous exanthema; and (5) cervical lymphadenopathy. According to a large-scale retrospective review of KD, the majority of patients were 1 to 4 years old (62%).[4] In cases of children presenting fever and fewer than four of the other symptoms, diagnoses of "incomplete" or "atypical" KD were given. Atypical KD usually occurs in children younger than 6 months or older than 5 years.[2] Most reported cases of sudden unexpected death associated with incomplete or atypical KD were in infants less than 6 months of age.[5,6] The mortality peak for infants under 1-year-old occurs 15–45 days after the onset of symptoms.[5] In this case, death occurred one and a half months after the onset of symptoms, which was consistent with other cases. The diagnosis of KD in children is difficult because its presentation is usually similar to that of other viral or bacterial infections. In particular, atypical presentation may lead to delayed diagnosis and inappropriate therapy. In this case, the initial symptoms were obscure, without the typical manifestation of KD. First-line therapies for KD, such as aspirin and intravenous immunoglobulin, were not applied. In this case, the age at onset of atypical KD was older than usual, and the development of CAA progressed rapidly. The diagnosis was given at autopsy.

According to a review of studies about the distribution of CAA, the LAD is most commonly affected, followed by the RCA.[7] Characteristically, CAAs caused by KD are located in the proximal segments of coronary arteries. However, large CAAs (≥8 mm in diameter) were frequently found in the RCA rather than the LAD.[7] Aneurysm size is a major predictor for the development of myocardial infarction.[7,8] Larger CAAs indicated more extensive disease and an increased likelihood of bilateral CAAs. Furthermore, the outcome for patients with bilateral CAAs was worse than for patients with unilateral CAA.[7] In this case, there were bilateral giant coronary aneurysms involving the proximal LAD and the RCA. The pathologic features of cardiac complications from KD are rarely reported. Coronary vasculitis is pathognomonic for KD. A recently proposed model of coronary arteriopathy revealed three pathological processes, which include necrotizing arteritis, subacute/chronic vasculitis and luminal myofibroblastic proliferation.[8] Coronary arteritis results in rapid destruction of luminal endothelial cells, elastic lamina and medial smooth muscle cells. This causes loss of integrity of the arterial wall, eventually resulting in aneurysm formation. Giant CAAs larger than 8 mm in diameter do not resolve, regress or remodel.[8]

In adult patients, KD may remain clinically silent for decades after onset. On the other hand, atypical KD is more common in infants and poses a higher risk for developing CAA. KD continues to have a clinical diagnosis based on signs and symptoms without specific markers; this can result in diagnostic dilemmas, particularly in atypical cases. Atypical KD must be considered when prolonged fever is present in young infants or children who do not fulfill the classical KD diagnostic criteria. Supplemental laboratory findings, such as elevated erythrocyte sedimentation rate and C-reactive protein, and echocardiographic criteria, are recommended for evaluation of suspected atypical KD.

Herein, we report a case of atypical KD with bilateral giant aneurysms in the LAD and the RCA. This case, which occurred in a 23-month-old boy, developed at an unusual age and rapidly progressed to CAA, leading to death. The pathologic features of myocardial infarction can provide information to better understand the progression and severity of CAA.

ORCID

DongJa Kim: https://orcid.org/0000-0001-8462-3173
SangHan Lee: https://orcid.org/0000-0003-0390-3494

Conflicts of Interest

No potential conflict of interest relevant to this article was reported.

REFERENCES

1. Kato H, Sugimura T, Akagi T, *et al*. Long-term consequences of Kawasaki disease: a 10- to 21-year follow-up study of 594 patients. Circulation 1996; 94: 1379-85.
2. Singh S, Agarwal S, Bhattad S, *et al*. Kawasaki disease in infants below 6 months: a clinical conundrum? Int J Rheum Dis 2016; 19: 924-8.
3. Choi YS, Kwon T, Lee H, Lee SY, Lee WT. Medicolegal investigation of Kawasaki disease: three cases of sudden death by coronary artery lesions. Korean J Leg Med 2003; 27: 39-44.
4. Manlhiot C, Yeung RS, Clarizia NA, Chahal N, McCrindle BW. Kawasaki disease at the extremes of the age spectrum. Pediatrics 2009; 124: e410-5.
5. Pucci A, Martino S, Tibaldi M, Bartoloni G. Incomplete and atypical Kawasaki disease: a clinicopathologic paradox at high risk of sudden and unexpected infant death. Pediatr Cardiol 2012; 33: 802-5.
6. Diana MC, Villa G, Gattorno M, *et al*. Sudden death in an infant revealing atypical Kawasaki disease. Pediatr Emerg Care 2006; 22: 35-7.

7. Tsuda E, Tsujii N, Kimura K, Suzuki A. Distribution of Kawasaki disease coronary artery aneurysms and the relationship to coronary artery diameter. Pediatr Cardiol 2017; 38: 932-40.
8. McCrindle BW, Rowley AH, Newburger JW, *et al*. Diagnosis, treatment, and long-term management of Kawasaki disease: a scientific statement for health professionals from the American Heart Association. Circulation 2017; 135: e927-99.

Journal of Pathology and Translational Medicine 2018; 52: 252-256
https://doi.org/10.4132/jptm.2018.04.28

■ CASE STUDY ■

Hyalinizing Trabecular Tumor of the Thyroid Gland, a Diagnostic Challenge in Fine-Needle Aspiration Cytology: Case Report

Ye-Young Rhee · Hong Kyu Jung[1] Se Hoon Kim[2] · Soo Hee Kim

Pathology Center, Seegene Medical Foundation, Seoul; [1]Department of Surgery and Health Care Center, Seran Hospital, Seoul; [2]Department of Pathology, Yonsei University College of Medicine, Severance Hospital, Seoul, Korea

Received: March 16, 2018
Revised: April 18, 2018
Accepted: April 27, 2018

Corresponding Author
Soo Hee Kim, MD, PhD
Pathology Center, Seegene Medical Foundation, 320 Cheonho-daero, Seongdong-gu, Seoul 04805, Korea
Tel: +82-2-2218-9346
Fax: +82-2-2218-9310
E-mail: kshpath@gmail.com

Hyalinizing trabecular tumor (HTT) is a rare thyroid tumor with low to minimal malignant potential. HTT is often misinterpreted as other thyroid tumors, including papillary thyroid carcinoma (PTC) and medullary thyroid carcinoma (MTC), on fine-needle aspiration (FNA) cytology, because of its overlapping cytologic features, such as nuclear grooves and intranulcear pseudoinclusions. Although cytopathologists cannot definitely conclude HTT by FNA cytology, suspicion of HTT is necessary to avoid misdiagnosing HTT as PTC or MTC and to avoid unnecessary aggressive treatment. Here, we report a case of HTT with novel cytologic features in CellPrep liquid based cytology that was diagnosed as suspicious for papillary carcinoma by FNA and finally diagnosed as HTT in the surgical specimen.

Key Words: Hyalinizing trabecular tumor; Thyroid gland; Liquid-based cytology

Hyalinizing trabecular tumor (HTT) is an uncommon thyroid tumor that is usually benign and is, often misdiagnosed as another thyroid neoplasm, such as papillary thyroid carcinoma (PTC) or medullary thyroid carcinoma (MTC), by fine-needle aspiration (FNA) cytology, due to its similar nuclear features as PTC or the presence of hyaline material resembling amyloid in MTC.[1,2] Diagnosis of HTT in FNA specimens is challenging, as reported in Zipkin's first report in 1905,[3] and Carney's first detailed description in 1987,[4] because HTT has these overlapping cytologic features with PTC and MTC. There are several case reports of HTT and studies dealing with the pathologic features and biologic behavior of HTT, as well as diagnostic tools for accurate diagnosis of HTT.[5-7] Here, we report a case of HTT that includes several key features to remember for correct diagnosis.

CASE REPORT

A 63-year-old woman with history of breast cancer underwent a medical checkup. Ultrasound examination revealed one hypoechoic lesion measuring 0.6×0.4 cm in the left thyroid lobe (Fig. 1A) and two small cystic lesions in the right thyroid lobe. Liquid based cytology (LBC; CellPrep, Biodyne, Seongnam, Korea) FNA of the left lobe nodule showed features of PTC including overlapping enlarged nuclei, occasional nuclear grooves, and intranuclear pseudoinclusions. The lesion was diagnosed as suspicious for papillary carcinoma. Computed tomography revealed a 0.6 cm low density nodule with no evidence of extracapsular invasion and no significant lymph node enlargement (Fig. 1B). The surgeon decided to perform left lobectomy based on the assumption that the lesion could be a benign tumor in the final pathologic report, because of uncertain radiologic features.

On gross examination, one well circumscribed yellow to tan firm nodule measuring 0.6×0.5×0.4 cm was identified (Fig. 2A). Histologic examination revealed a well circumscribed nodule composed of trabecular and alveolar patterns of tumor cells. Hyalinization was observed between cell trabeculae. Tumor cells had abundant cytoplasm, low nuclear to cytoplasmic ratio, perinuclear clearing, nuclear grooves, and intranuclear pseudoinclusions (Fig. 2B, C).

Immunohistochemistry showed diffuse membrane positive

pISSN 2383-7837
eISSN 2383-7845

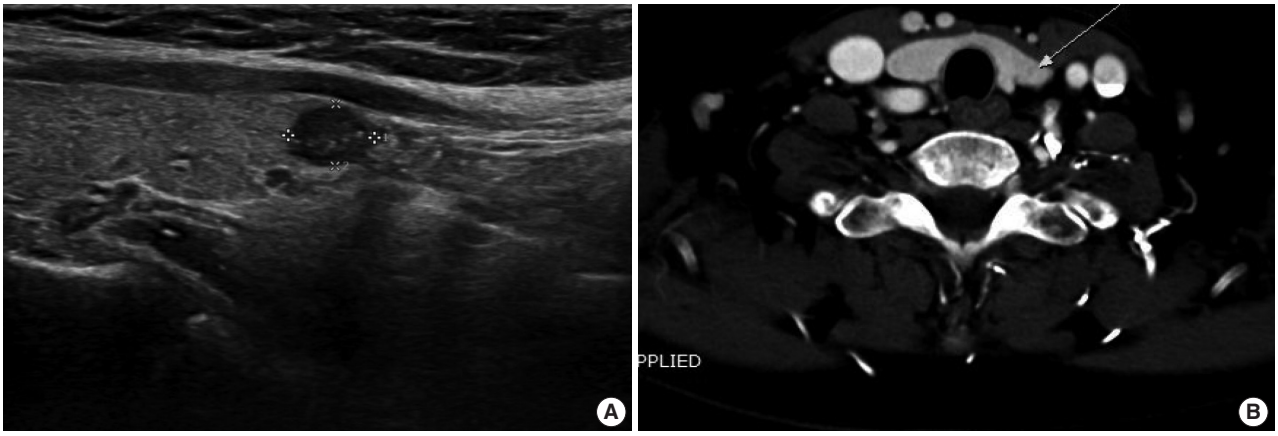

Fig. 1. Radiologic findings. (A) Ultrasonography shows a 0.6 cm hypoechoic nodule in the left lobe (longitudinal). (B) Computed tomography reveals a 0.6 cm low density nodule with no evidence of extracapsular invasion and no significant lymph node enlargement.

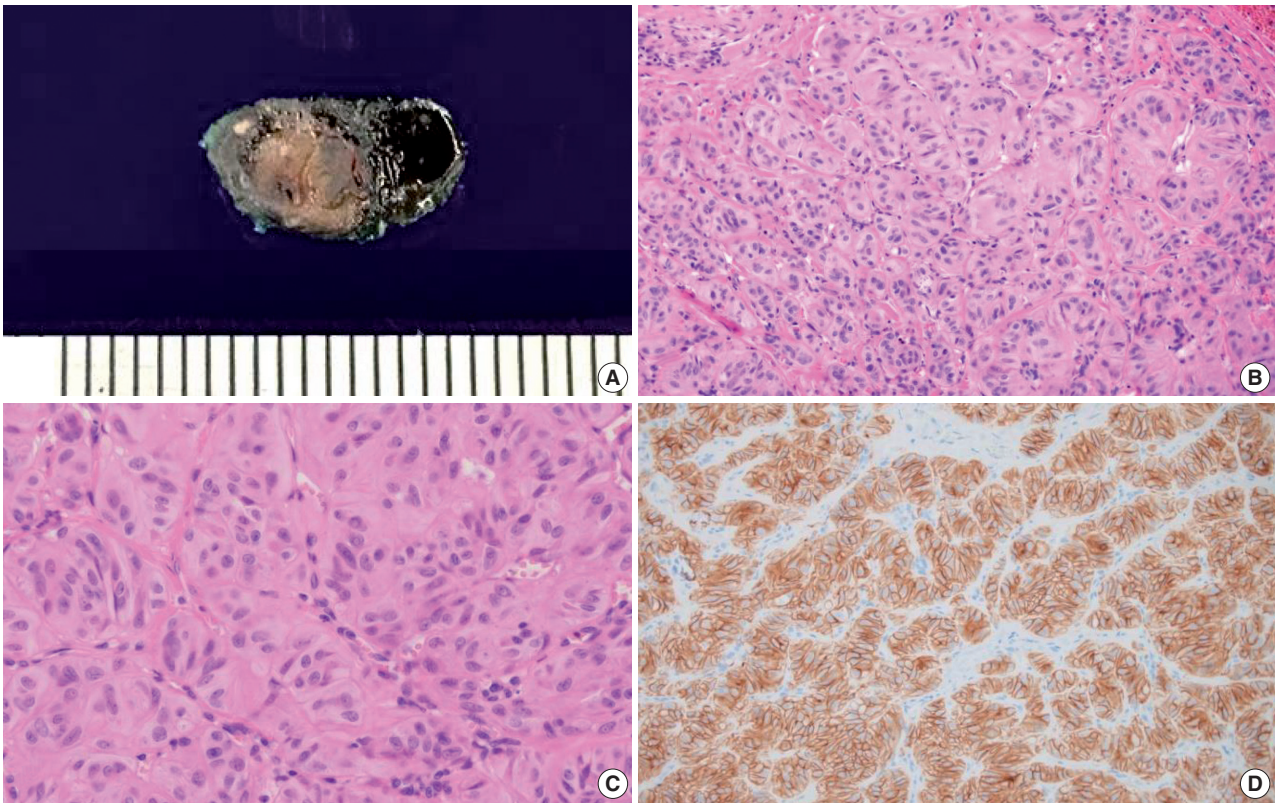

Fig. 2 . Gross specimen, microscopic findings (hematoxylin and eosin), and immunohistochemical staining of Ki-67 in the surgical specimen. (A) Gross specimen showing well circumscribed yellow to tan mass. (B, C) Histologic image shows trabecular pattern with oval to elongated tumor cells and intratrabecular hyalinization. (D) Ki-67 immunostaining using MIB1 monoclonal antibody shows characteristic peripheral membranous and cytoplasmic staining.

reactivity for Ki-67 (MIB1 clone) at room temperature, which is a distinct immunohistochemical characteristic of HTT (Fig. 2D). Immunohistochemical staining also revealed diffuse positivity for CD56, focal weak positivity for galectin 3, and negativity for cytokeratin 19. The lesion was diagnosed as HTT based on these histological and immunohistochemical features.

Retrospectively, there were several points that could have led to the suggestion or diagnosis of HTT on FNA cytology. Ultrasonographic findings are one clue because the lesion was well circumscribed, a benign feature, although it did show hypoechoic

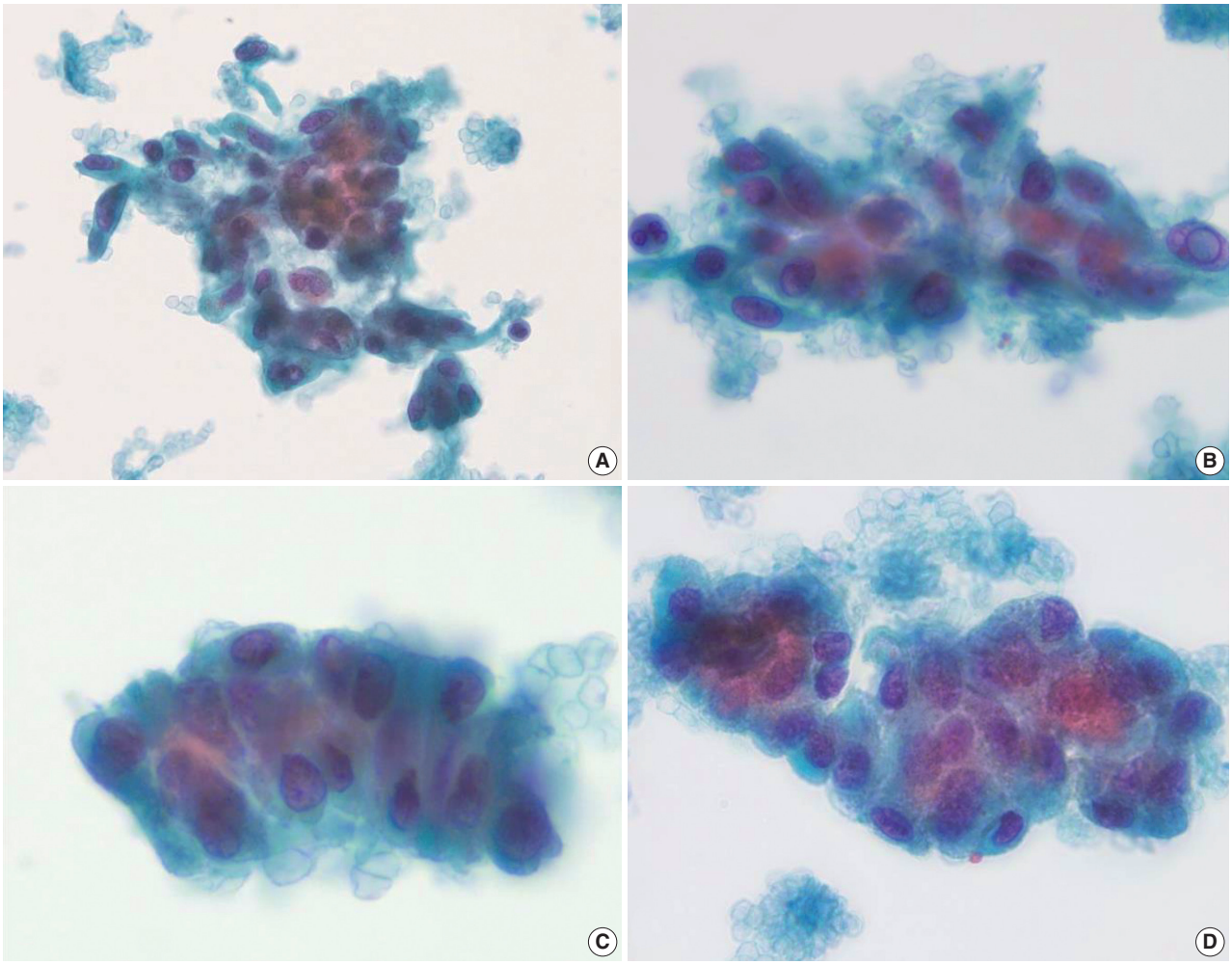

Fig. 3. Liquid based cytology (LBC; CellPrep) findings of hyalinizing trabecular tumor (HTT) (Papanicolaou). Cohesive aggregates or syncytial fragments of tumor cells around hyaline material. (A, B) Although oval to polygonal and occasionally elongated spindle-shaped tumor cells shows enlarged nuclei with hyperchromasia and occasional intranuclear pseudoinclusion as in papillary carcinoma, tumor cells in HTT shows dispersed fine chromatin rather than pale and clear chromatin, and had infrequent nuclear membrane irregularity. (C, D) Tumor cells were arranged in a more stratified trabecular pattern than in papillary carcinoma. Columnar character of tumor cells is observed in peripheral rims of clusters.

features with internal microcalcification. While the LBC of the FNA specimen had similar features to papillary carcinoma, such as occasional intranuclear pseudoinclusions and nuclear grooves, this case had some special cytological characteristics, as described below. Syncytial fragments or loosely cohesive groups of tumor cell clusters had cores of hyaline material among the cells. Tumor cells were usually oval to polygonal with pale to dense cytoplasm. However, spindle-shaped cells were occasionally observed. Unlike PTC, which has pale and clear chromatin, nuclei showed finely dispersed chromatin (Fig. 3A, B). Other than these general characteristics of HTT, more unique cytological features of this HTT case are frequent three-dimensional cell clusters and stratified columnar tumor cells in the peripheral rims of clusters. Although tumor cells of PTC also show nuclear overlapping, HTT tumor cells in this case are more often arranged in a ball-like structure. In addition to the distinct spindle-shaped tumor cells, cells with abundant cytoplasm and eccentrically located round nuclei with columnar features were frequently observed and arranged in a stratified trabecular pattern in this case (Fig. 3C, D).

This case study was approved by the Institutional Review Board of Seegene Medical Foundation (IRB No. SMF-IRB-2018-001). The need for informed consent was waived.

DISCUSSION

HTT is a rare thyroid tumor with low malignant potential

https://doi.org/10.4132/jptm.2018.04.28

often misdiagnosed as PTC or MTC by FNA cytology, because of their similar cytological features.[1,2] However, distinguishing characteristics of HTT must always be considered when diagnosing thyroid nodules, because diagnosis or suspicion of HTT on FNA is crucial to a correct therapeutic approach for a thyroid nodule that should not be overtreated with total or subtotal thyroidectomy.[5]

HTT could be considered a variant of PTC in that it has overlapping cytological features of PTC, *RET*/*PTC* rearrangement, and strong expression of galectin-3 in some cases.[8] However, HTT has unique characteristics that are described below. HTT does not show *BRAF* (V600E) mutation.[9] HTT has a unique immunohistochemical staining pattern for Ki-67 MIB1 monoclonal antibody, which is positive in peripheral tumor cell cytoplasm but expressed in the nuclei of most other tumors.[2,10]

Considering the characteristics of HTT mentioned above, Ki-67 immunohistochemistry of the FNA specimen,[2] and *RET*/*PTC* rearrangement, a *BRAF* mutation test[9] would be helpful to avoid over-diagnosis of HTT as PTC or suspicious for PTC. However, immunohistochemistry and mutation tests are difficult to perform on cytology specimen and are not sufficient to rule out PTC and diagnose HTT on FNA. General use of Ki-67 staining in HTT FNA specimens is also expensive; therefore, Ki-67 staining should be limited to carefully selected inconclusive cases, for example those cases showing nuclear features of PTC but with sparse hyaline material.[2,10,11]

HTT should be included in the differential diagnosis of solid tumors of the thyroid gland, especially thosee showing benign US features of marked hypoechogenecity with well circumscribed smooth margin and without internal microcalcification.[7,12-14]

Although cytopathologists cannot directly diagnose HTT on FNA, consideration of the possibility of HTT is important to avoid misdiagnosing HTT as a malignant thyroid neoplasm such as PTC or MTC and to avoid unnecessary overtreatment for HTT, especially when intraoperative frozen section evaluation could prevent patients from undergoing overtreatment.[14,15]

Cytologic findings such as bloody background, low nuclear to cytoplasmic ratio, cellular aggregates around the hyaline material, fine chromatin rather than clear chromatin, and numerous nuclear grooves and intranuclear inclusions should remind pathologists of HTT as a differential diagnosis.[4,16] The recognition of hyaline and colloid-like material in smears is also crucial to a correct diagnosis.[17]

The novel cytologic findings of our case including three-dimensional and stratified trabecular arrangement of tumor cells and columnar features of tumor cells at the periphery of cell clusters, are supportive of HTT by FNA cytology. These unique findings have never been described, especially in CellPrep LBC. Collective review of previously diagnosed HTT cases considering these unique cytologic features would be valuable to derive more exact criteria to diagnose HTT on FNA cytology.

ORCID

Soo Hee Kim: https://orcid.org/0000-0001-6715-8900

Conflicts of Interest

No potential conflict of interest relevant to this article was reported.

REFERENCES

1. Kim T, Oh YL, Kim KM, Shin JH. Diagnostic dilemmas of hyalinizing trabecular tumours on fine needle aspiration cytology: a study of seven cases with *BRAF* mutation analysis. Cytopathology 2011; 22: 407-13.
2. Casey MB, Sebo TJ, Carney JA. Hyalinizing trabecular adenoma of the thyroid gland identification through MIB-1 staining of fine-needle aspiration biopsy smears. Am J Clin Pathol 2004; 122: 506-10.
3. Zipkin R. Hyalinähnliche collagene Kugeln als Produkte epithelialer Zellen in malignen Strumen. Virchows Arch Pathol Anat Physiol Klin Med 1905; 182: 374-406.
4. Carney JA, Ryan J, Goellner JR. Hyalinizing trabecular adenoma of the thyroid gland. Am J Surg Pathol 1987; 11: 583-91.
5. Howard BE, Gnagi SH, Ocal IT, Hinni ML. Hyalinizing trabecular tumor masquerading as papillary thyroid carcinoma on fine-needle aspiration. ORL J Otorhinolaryngol Relat Spec 2013; 75: 309-13.
6. Jones DJ, Kieliszak CR, Patel SS, Selinsky CR. Hyalinizing trabecular tumor of the thyroid gland and its significant diagnostic issue. Thyroid Res 2017; 10: 7.
7. Saglietti C, Piana S, La Rosa S, Bongiovanni M. Hyalinizing trabecular tumour of the thyroid: fine-needle aspiration cytological diagnosis and correlation with histology. J Clin Pathol 2017; 70: 641-7.
8. Gaffney RL, Carney JA, Sebo TJ, *et al*. Galectin-3 expression in hyalinizing trabecular tumors of the thyroid gland. Am J Surg Pathol 2003; 27: 494-8.
9. Salvatore G, Chiappetta G, Nikiforov YE, *et al*. Molecular profile of hyalinizing trabecular tumours of the thyroid: high prevalence of *RET/PTC* rearrangements and absence of B-raf and N-ras point mutations. Eur J Cancer 2005; 41: 816-21.
10. Takada N, Hirokawa M, Ohbayashi C, *et al*. Re-evaluation of MIB-1 immunostaining for diagnosing hyalinizing trabecular tumour of the

thyroid: semi-automated techniques with manual antigen retrieval are more accurate than fully automated techniques. Endocr J 2018; 65: 239-44.
11. Park HS, Kim KM, Bae JS, *et al*. Diagnostic caveats of immunoreactivity for Ki67 and chromogranin A in hyalinizing trabecular tumour of the thyroid. J Clin Pathol 2014; 67: 835-9.
12. Lee S, Han BK, Ko EY, Oh YL, Choe JH, Shin JH. The ultrasonography features of hyalinizing trabecular tumor of the thyroid are more consistent with its benign behavior than cytology or frozen section readings. Thyroid 2011; 21: 253-9.
13. Choi WJ, Baek JH, Ha EJ, *et al*. The ultrasonography features of hyalinizing trabecular tumor of the thyroid gland and the role of fine needle aspiration cytology and core needle biopsy in its diagnosis. Acta Radiol 2015; 56: 1113-8.
14. Jang H, Park CK, Son EJ, *et al*. Hyalinizing trabecular tumor of the thyroid: diagnosis of a rare tumor using ultrasonography, cytology, and intraoperative frozen sections. Ultrasonography 2016; 35: 131-9.
15. Sung SY, Shen HY, Hsieh CB, *et al*. Hyalinizing trabecular tumor of thyroid: does frozen section prevent unnecessarily aggressive operation? Six new cases and a literature review. J Chin Med Assoc 2014; 77: 573-7.
16. Carney JA, Hirokawa M, Lloyd RV, Papotti M, Sebo TJ. Hyalinizing trabecular tumors of the thyroid gland are almost all benign. Am J Surg Pathol 2008; 32: 1877-89.
17. Bakula-Zalewska E, Cameron R, Gałczyński JP, Domanski HA. Hyaline matrix in hyalinizing trabecular tumor: findings in fine-needle aspiration smears. Diagn Cytopathol 2015; 43: 710-3.

 https://doi.org/10.4132/jptm.2018.04.28

Journal of Pathology and Translational Medicine 2018; 52: 257-261
https://doi.org/10.4132/jptm.2018.05.08

■ CASE STUDY ■

Malignant Pleural Effusion from Metastatic Prostate Cancer: A Case Report with Unusual Cytologic Findings

Jinyoung Jeon · Tae-Jung Kim[1]
Hong Sik Park · Kyo-Young Lee

Department of Hospital Pathology, Seoul St. Mary's Hospital, Seoul; [1]Department of Hospital Pathology, Yeouido St. Mary's Hospital, College of Medicine, The Catholic University of Korea, Seoul, Korea

Received: February 20, 2018
Revised: April 24, 2018
Accepted: May 8, 2018

Corresponding Author
Kyo-Young Lee, MD, PhD
Department of Hospital Pathology, Seoul St. Mary's Hospital, College of Medicine, The Catholic University of Korea, 222 Banpo-daero, Seocho-gu, Seoul 06591, Korea
Tel: +82-2-2258-1618
Fax: +82-2-2258-1627
E-mail: leekyoyo@catholic.ac.kr

We present a case of 55-year-old man who complained of dyspnea and sputum for a month. He was an ex-smoker with a history of prostate cancer and pulmonary tuberculosis. Chest radiographs revealed bilateral pleural effusions of a small to moderate amount. Pigtail catheters were inserted for drainage. The pleural fluid consisted of large clusters and tightly cohesive groups of malignant cells, which however could not be ascribed to prostate cancer with certainty. We performed immunocytochemical panel studies to determine the origin of cancer metastasis. The immunostaining results were positive for prostate-specific antigen, alpha-methylacyl-coenzyme A racemase, and Nkx 3.1, consistent with prostate cancer. Pleural effusion associated with prostate cancer is rare. To our knowledge, this is the first case report in Korea to describe cytologic features of malignant pleural effusion associated with prostate cancer.

Key Words: Prostatic neoplasms; Neoplasm metastasis; Pleural effusion, malignant

Malignant pleural effusion (MPE) is diagnosed by identifying malignant cells in pleural fluid or on pleural biopsy.[1,2] Metastatic adenocarcinoma is the most commonly found type of cancer in MPE; the most common causes of MPE are lung cancer, breast cancer, lymphoma, ovarian and gastric cancer in the descending order of occurrence.[3] Prostate cancer can metastasize to nearly every organ, but most frequently to bones and regional lymph nodes. The most frequent sites of atypical metastases are reported to be the lungs and pleura (40%), liver (37%), supradiaphragmatic lymph nodes (34%), and adrenal glands (15%).[4,5] Regardless of the location, whether pleural, pericardial or ascitic, malignant effusions are rather infrequent complication of prostate cancer.[6-11] There are few cytologic findings of pleural effusion due to prostate cancer described in the literature. Herein, we report a rare case of pleural effusion due to prostate cancer, showing unusually large cell-clusters.

CASE REPORT

A 55-year-old man was referred to the pulmonary clinic due to dyspnea and sputum for a month. He was an ex-smoker with a 45 pack-year history and had tuberculosis 25 years ago. Two years prior, the patient presented with a low back pain and anal incontinence. The tumor appeared to replace most of the prostate and spread to perirectal area and bilateral pelvic wall on computed tomography (CT) (Fig. 1A). Extensive pelvic lymphadenopathy and bone metastasis of the 11th thoracic vertebra were also found. He underwent a palliative transurethral resection of the prostate (TURP) and was diagnosed with prostate cancer of Gleason score 9 (4 + 5) on pathologic examination. He started receiving radiation therapy while taking leuprorelin, a gonadotropin-releasing hormone agonist. The prostate-specific antigen (PSA) levels dropped from 78.54 to 0.2 ng/mL and the androgen levels reached within castration concentrations (testosterone 0.13 ng/dL, free testosterone 0.58 ng/dL) for a year.

On chest radiographs, bilateral pleural effusions of a small to moderate amount were observed (Fig. 1B), with a larger amount on the right side (Fig. 1C). No mass-like lesion was found on thoracic CT scan. Bone scans showed newly noted multifocal uptakes in skull, rib cage, sacrum, pelvic bones, humeri, and

pISSN 2383-7837
eISSN 2383-7845

femurs. For reliable diagnosis and appropriate management, ultrasound-guided percutaneous pigtail catheters were inserted. The drained pleural fluid was turbid yellow with glucose 94 mg/dL, protein 4.4 g/dL, triglyceride 13 mg/dL, lactate dehydrogenase 1,113 U/L, and adenosine deaminase 17.1 IU/L. Its differential count was 7% lymphocytes, 41% macrophages, 5% mesothelial cells, and 47% malignant cells. PSA in pleural fluid and concomitant serum PSA were 21.50 and 44.71 ng/mL respectively.

The pleural fluid was prepared with routine conventional smear. The Papanicolaou stained smears showed groups of neoplastic cells arranged in large cell-clusters (Fig. 2A). Most of them formed large three-dimensional balls without glandular lumen (Fig. 2B), and they consisted of medium sized round to ovoid cells showing coarse, finely granular and vesicular chromatin. Most tumor cells showed smooth nuclear contours with large prominent nucleoli, but some showed irregular nuclear borders. They had hyperchromatic nuclei with a high nuclear to cytoplasmic (N/C) ratio (Fig. 2C). Nuclear pleomorphism was minimal to mild and mitosis was hardly found (less than 1/10 high-power field). The architectural and cytologic features were mostly similar on cell block, but a few glandular lumens were found. The tumor cells were in tightly cohesive groups without lumen (Fig. 2D). A very few of them had glandular lumen-like space with central necrosis (Fig. 2E). They had pale eosinophilic to clear cytoplasm, and the amount of cytoplasm was small to moderate. Based on these findings, the tumor cells were taken to be poorly differentiated carcinoma of unknown origin.

Immunocytochemical panel studies were performed on the cell block to determine the origin of cancer metastasis. The tumor cells were immunopositive for PSA (Fig. 2F), alpha-methylacyl-coenzyme A racemase (AMACR) (Fig. 2G), and Nkx 3.1 (Fig. 2H). They showed negative immunoreactivity for P40, cytokeratin 5/6 (Fig. 2I), thyroid transcription factor-1 and gross cystic disease fluid protein.

The patient was finally diagnosed with metastatic castration resistant prostate cancer. He was then treated with a second-line chemotherapeutic agent, biweekly docetaxel and oral dexamethasone.

This study was approved by the Institutional Review Board (IRB) of The Catholic University of Korea, Seoul St. Mary's Hospital (KC17ZESI0451) and was performed in accordance with the principles of the Declaration of Helsinki. The patient informed consent was waived.

DISCUSSION

Secondary pleural effusion from prostate cancer is a rare clinical manifestation. Moreover, it is even more rare to find malignant cells in pleural fluid on microscopic examination. So far, we have had a little more than 20 cases and fewer than 10 papers on MPE due to prostate cancer. Two of them are review papers including 10 and six cases, respectively (Table 1).[12,13] According to the literature, MPE caused by prostate cancer share several common characteristics: the patients are usually in high stage at the time of diagnosis, and the tumors are of high grade and unresectable.[13] the tumor cells have round to oval nuclei with large prominent nucleoli and scant cytoplasm: they show high N/C ratio, nuclear hyperchromasia and relatively smooth nuclear borders. Most tumor cells appear as isolated cells or in small, loosely cohesive

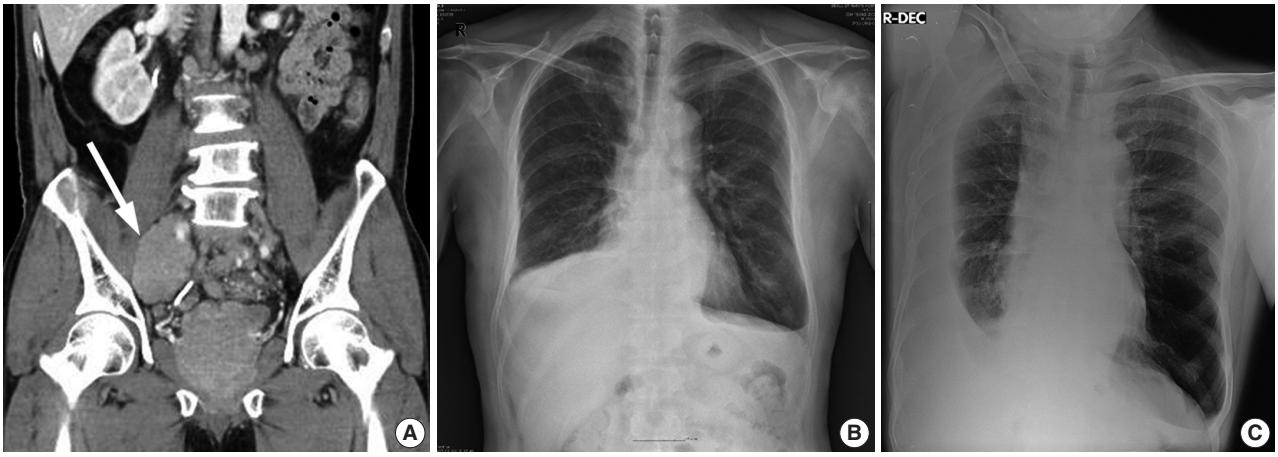

Fig. 1. Radiologic findings of the patient. (A) The tumor appears to replace most of the prostate and spread to perirectal area and bilateral pelvic wall on contrast-enhanced computed tomography. Extensive regional lymphadenopathy is observed (arrow). The chest X-ray reveals bilateral pleural effusions of a small to moderate amount (B) with a larger amount on the right side (C).

 https://doi.org/10.4132/jptm.2018.05.08

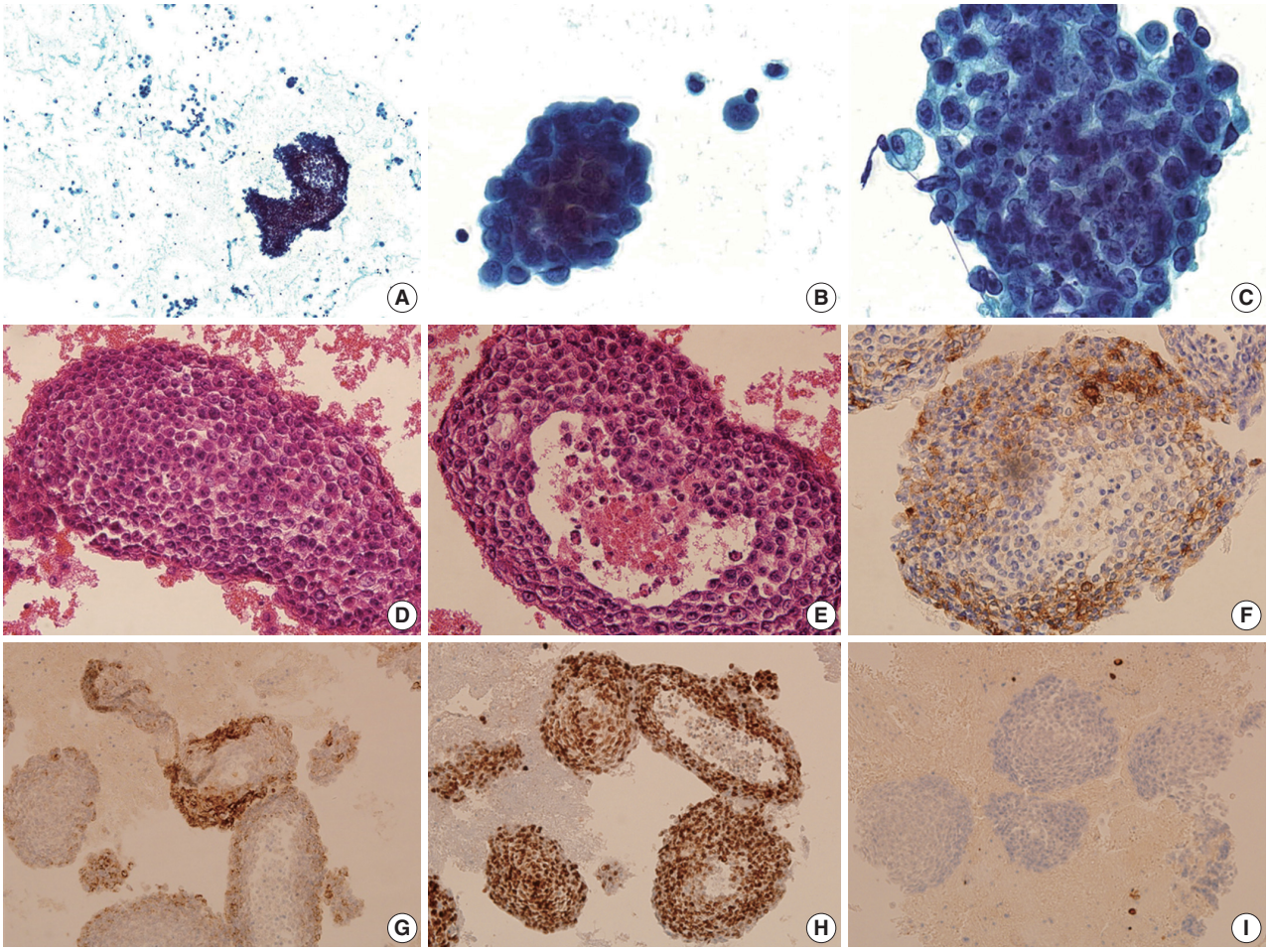

Fig. 2. Cytologic features of Papanicolaou smears (A–C), the cell block (D–F) and the result of immunocytochemical staining (G–I). (A) It shows a sheet-like cell group. (B) A large cell-cluster is noted, forming three-dimensional ball. Hyperchromatic nuclei and high nuclear to cytoplasmic ratio are also observed. (C) The tumor cells have coarse, finely granular and vesicular chromatin. (D) The majority are in tightly cohesive groups of cells. (E) Some groups have the glandular lumen-like structure with central necrosis. Tumor cells are immunopositive for prostate-specific antigen (F), alpha-methylacyl-coenzyme A racemase (G), and Nkx 3.1 (H). (I) They show negative immunoreactivity for cytokeratin 5/6.

groups.[12,13] There was only one exception to this consistent cytologic pattern, and that case showed the tumor cells arranged in large tightly cohesive balls.[13] Our case shared those unusual cytologic features, showing cytologic patterns that are more commonly seen in breast cancer. Three dimensional cell balls of various sizes with smooth outer contours, referred to as cannon balls, are well known as one of the common characteristics of malignant effusion from breast adenocarcinoma. The cytomorphologic pattern of malignant mesothelioma varies widely, which is well known to mimic other malignancies, the most common being adenocarcinoma. It should be kept in mind that the morphologic overlap may preclude an accurate identification of poorly differentiated metastatic adenocarcinoma.

The differential diagnosis included metastatic adenocarcinomas from the prostate, lung, breast, gastrointestinal tract, and thyroid gland. Prostate origin was most suspected due to the patient's past history. Metastatic non-keratinizing squamous cell carcinoma and primary malignant mesothelioma were also on the list to be excluded. Poorly differentiated squamous cell carcinoma in pleural effusion may resemble the cytomorphology of adenocarcinoma, however, most have been reported to have metastasized from the head and neck area or genital organs. Also, malignant mesothelioma was considered as the least likely because there was no mass-like lesion on imaging studies.

Hematoxylin and eosin stained sections of TURP specimen of the primary tumor were available for histological review, and were compared with the cytology. The primary tumor was a poorly differentiated carcinoma (Fig. 3A). Lymphovascular invasion

Table 1. Reported cases of malignant pleural effusion from prostate cancer

Author	Year	No. of cases	Age (yr)	Histologic differentiation	Effusion side	Intrathoracic cavity involvement	Pleural fluid cytology	PSA (ng/mL)	
								Fluid	Serum
Knight *et al.*[9]	2014	1	73	NS	Bilateral	Pleura with lung entrapment	Atypical cells	1,619	2,540
Bajpai *et al.*[7]	2014	1	84	GS 6	Right	Isolated PE	Adenocarcinoma	NS	>148
Mai *et al.*[12]	2007	6	77±8	GS 8.1±1.5	NS	NS	Adenocarcinoma	NS	4.1±2.3
Renshaw *et al.*[13]	1996	10	Mean 67	GS 7 (n=4), GS 8 (n=1), GS 9 (n=2), anaplastic small cell carcinoma (n=3)	NS	Lung (n=1), pleura (n=1), both lung and pleura (n=2)	Malignant cells	NS	NS
Carrascosa *et al.*[14]	1994	1	73	NS	Right	Suspected PLC	Adenocarcinoma	NS	197
Shimizu *et al.*[15]	1993	1	65	Poorly differentiated	Bilateral	Lung, PLC	Adenocarcinoma	NS	292
Mestitz *et al.*[16]	1989	2	67	Poorly differentiated	Bilateral	Lung, PLC, mediastinal LAP	Adenocarcinoma	NS	NS
			69	NS	Right	Isolated PE	Adenocarcinoma	NS	NS

PSA, prostate-specific antigen; NS, not stated; GS, Gleason score; PE, pleural effusion; PLC, pulmonary lymphangitis carcinomatosa; LAP, lymphadenopathy.

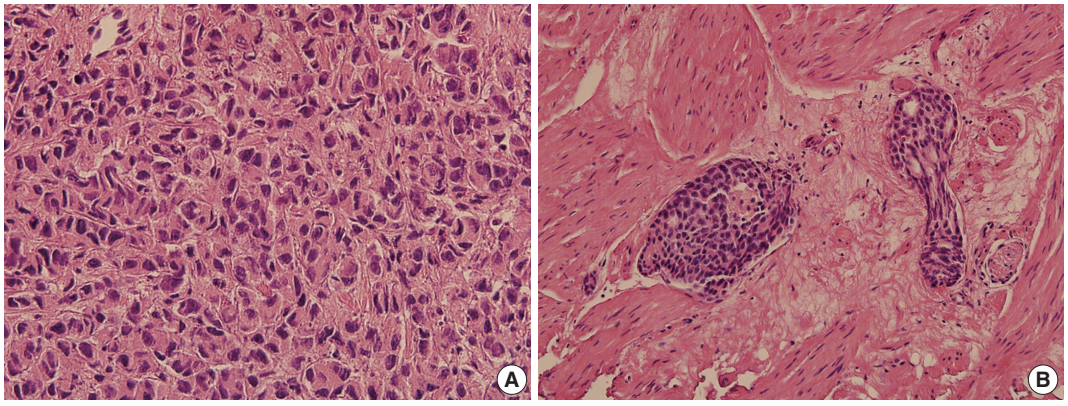

Fig. 3. The histological characteristics of transurethral resection of the prostate specimen. (A) The hematoxylin and eosin stained section shows a poorly differentiated carcinoma. (B) Lymphovascular invasion is observed with the tumor emboli forming well-demarcated ovoid masses.

was noted with the tumor emboli forming well-demarcated ovoid masses, usually in solid or cribriform architecture (Fig. 3B). These histologic features correlated well with the cytologic findings of pleural fluid. Since prostate cancer is famous for its various combinations of Gleason scores, it may not be surprising that the cytologic features also vary. Immunocytochemical staining is useful when cytologic findings are challenging. PSA is the most widely used biomarker for prostate cancer screening and treatment monitoring. Measurement of PSA in the pleural fluid is a useful adjunct test in the diagnosis of metastatic prostate cancer. However, immunocytochemical study of PSA displays negative, weak or focal staining in poorly differentiated carcinoma and in patients with prior hormone and/or radiation therapy.[12,13] As such, we recommend to use other prostatic markers, such as prostate alkaline phosphatase, AMACR, and Nkx 3.1 in combination with PSA.

In summary, we herein reported a rare case of MPE from prostate cancer, showing unusual cytologic characteristics that may require challenging differential diagnosis.

ORCID

Tae-Jung Kim: https://orcid.org/0000-0003-3140-3681
Kyo-Young Lee: https://orcid.org/0000-0001-9954-8583

Conflicts of Interest

No potential conflict of interest relevant to this article was reported.

REFERENCES

1. Egan AM, McPhillips D, Sarkar S, Breen DP. Malignant pleural effusion. QJM 2014; 107: 179-84.
2. Thomas JM, Musani AI. Malignant pleural effusions: a review. Clin Chest Med 2013; 34: 459-71.
3. Lim MH, Garrettc J, Mowlem L, Yap E. Diagnosing malignant

pleural effusions: how do we compare? N Z Med J 2013; 126: 42-8.
4. Bubendorf L, Schopfer A, Wagner U, *et al*. Metastatic patterns of prostate cancer: an autopsy study of 1,589 patients. Hum Pathol 2000; 31: 578-83.
5. Vinjamoori AH, Jagannathan JP, Shinagare AB, *et al*. Atypical metastases from prostate cancer: 10-year experience at a single institution. AJR Am J Roentgenol 2012; 199: 367-72.
6. Ani I, Costaldi M, Abouassaly R. Metastatic prostate cancer with malignant ascites: a case report and literature review. Can Urol Assoc J 2013; 7: E248-50.
7. Bajpai PA, Joshi P, Joseph D, Bajpai A. A case of recurrent massive right sided pleural effusion-an unusual presentation of carcinoma prostate. Lung India 2014; 31: 423-4.
8. dos Santos VM, Zembrzuski MM, Gouvea IP, Nery NS, dos Santos LA. Massive pleural effusion due to metastasis of prostate cancer. West Indian Med J 2011; 60: 690-3.
9. Knight JC, Ray MA, Benzaquen S. Malignant pleural effusion from prostate adenocarcinoma. Respir Med Case Rep 2014; 13: 24-5.
10. Saif MW. Malignant ascites associated with carcinoma of the prostate. J Appl Res 2005; 5: 305-11.
11. Saif MW, Figg WD, Hewitt S, Brosky K, Reed E, Dahut W. Malignant ascites as only manifestation of metastatic prostate cancer. Prostate Cancer Prostatic Dis 1999; 2: 290-3.
12. Mai KT, Roustan Delatour NL, Assiri A, Al-Maghrabi H. Secondary prostatic adenocarcinoma: a cytopathological study of 50 cases. Diagn Cytopathol 2007; 35: 91-5.
13. Renshaw AA, Nappi D, Cibas ES. Cytology of metastatic adenocarcinoma of the prostate in pleural effusions. Diagn Cytopathol 1996; 15: 103-7.
14. Carrascosa M, Perez-Castrillon JL, Mendez MA, Cillero L, Valle R. Malignant pleural effusion from prostatic adenocarcinoma resolved with hormonal therapy. Chest 1994; 105: 1577-8.
15. Shimizu T, Shibata Y, Uchida T, Satoh J. Severe flare-up in a prostate cancer patient treated with luteinizing hormone-releasing hormone analogue depot. Hinyokika Kiyo 1993; 39: 953-5.
16. Mestitz H, Pierce RJ, Holmes PW. Intrathoracic manifestations of disseminated prostatic adenocarcinoma. Respir Med 1989; 83: 161-6.

Journal of Pathology and Translational Medicine 2018; 52: 262-266
https://doi.org/10.4132/jptm.2018.05.15

■ CASE STUDY ■

Cytologic Diagnosis of Metastatic Alveolar Rhabdomyosarcoma in Cerebrospinal Fluid: A Case Report

Bobae Shim · Jiwon Koh · Ji Hye Moon · In Ae Park Han Suk Ryu

Department of Pathology, Seoul National University Hospital, Seoul, Korea

Received: May 14, 2018
Accepted: May 15, 2018

Corresponding Author
Han Suk Ryu, MD, PhD
Department of Pathology, Seoul National University Hospital, 101 Daehak-ro, Jongno-gu, Seoul 03080, Korea
Tel: +82-2-2072-3361
Fax: +82-2-743-5530
E-mail: karlnash@naver.com

Rhabdomyosarcoma is a malignant soft tissue tumor which shows skeletal muscle differentiation. Leptomeningeal metastasis can occur as a late complication, but currently there are no reports that have documented the cytologic features in cerebrospinal fluid (CSF). We report a case of metastatic alveolar rhabdomyosarcoma diagnosed in the CSF of a 28-year-old male who was originally diagnosed with rhabdomyosarcoma on the neck, and that went through systemic therapy. The tumor was positive for anaplastic lymphoma kinase, but progressed despite additional therapy with crizotinib. The CSF specimen revealed small round cells, large atypical cells with abundant cytoplasm and eccentric nuclei, and cells with horseshoe-shaped nuclei. These cytologic findings were in agreement with previous literature and well-correlated with histopathology. This is the first report to document the cytologic feature of rhabdomyosarcoma in CSF. In many cases it is difficult to perform ancillary tests in a CSF specimen and cytopathologists should be aware of the cytomorphologic characteristics to avoid misdiagnosis.

Key Words: Rhabdomyosarcoma; Cytology; Cerebrospinal fluid

Rhabdomyosarcoma (RMS) is a malignant soft tissue tumor with a skeletal muscle phenotype that mainly affects children and adolescents.[1] Among its subtypes, alveolar rhabdomyosarcoma (ARMS) is more common in adolescents and young adults and has a worse prognosis, compared to embryonal rhabdomyosarcoma (ERMS).[2] RMS frequently arises in the head and neck, genitourinary system and extremities and commonly metastasizes to lung and bone.[1] The central nervous system (CNS) can be involved by direct extension or distant metastasis, and CNS involvement may present either as a parenchymal lesion or leptomeningeal metastasis (LM).[3]

Although cerebrospinal fluid (CSF) cytology is considered as a gold standard for diagnosing LM, cytologic features of RMS in CSF has not been described to date, which makes it challenging for cytopathologists to recognize the involved CSF and further affects future therapeutic plans and prognosis. Here, we report a case of metastatic ARMS that was diagnosed by CSF cytology.

CASE REPORT

A 28-year-old man presented with a mass on the left side of the neck that had persisted for 4 months. On physical examination, a 3-cm firm, non-tender mass was palpated. Computed tomography showed multiple enlarged left cervical lymph nodes with homogeneous enhancement (Fig. 1A). An excisional biopsy of the cervical lymph node was performed. Microscopic examination revealed diffuse sheets of poorly differentiated cells with variable amounts of eosinophilic cytoplasm (Fig. 2A). A few cells showed abundant cytoplasm and eccentric nuclei, and multinucleated cells with peripherally located nuclei were observed (Fig. 2B, C). Immunohistochemistry (IHC) indicated that the tumor cells were negative for CD3, CD20, CD30, and cytokeratin and positive for vimentin and myogenin (Fig. 2E, G, H). The tumor was positive for anaplastic lymphoma kinase (ALK) (Fig. 2F). Diagnosis of metastatic ERMS was made, but the primary site of the tumor was not identified in positron emission tomography (Fig. 1B). Fluorescence *in situ* hybridization (FISH) did not reveal *ALK* gene rearrangement, however, a low-level gain of *ALK* gene copy number was observed.

The patient received two cycles of preoperative IA (ifosfamide, adriamycin) and neck dissection, followed by three cycles of VAC (vincristine, dactinomycin, cyclophosphamide) and five cycles of VC (vincristine, cyclophosphamide). He was in complete remission for 6 months before the tumor recurred in the bilateral

pISSN 2383-7837
eISSN 2383-7845

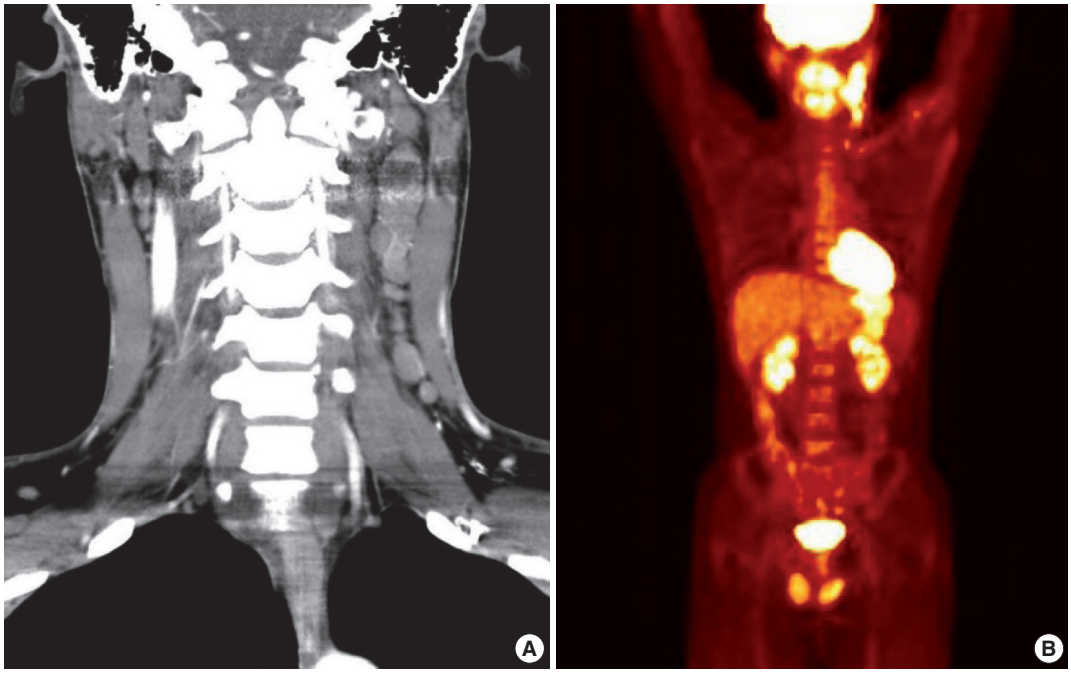

Fig. 1. Initial imaging studies. (A) Computed tomography shows multiple enlargements of left cervical lymph nodes. (B) Positron emission tomography reveals hypermetabolic lesion on the left side of the neck.

neck and left retropharyngeal space. Biopsy of the recurrent lesion showed the same histology as the previous specimen, but was diagnosed as ARMS based on diffuse, strong immunoreactivity for myogenin. The tumor progressed despite further treatment with crizotinib and the patient subsequently received palliative IA, radiation therapy and VIP (etoposide, ifosfamide, cisplatin).

After 10 months of palliative therapy, he developed seizure-like movement, nausea, and vomiting. Brain magnetic resonance imaging demonstrated leptomeningeal enhancement of the bilateral rectus gyri, left orbital gyrus and brainstem, with enhancing soft tissue in the left ethmoid sinus (Fig. 3A). A spinal tap was performed and a Papanicolaou-stained preparation of CSF revealed atypical small-sized cells, mostly individually scattered, with some forming clusters (Fig. 3B). Large atypical cells with eccentric nuclei and abundant cytoplasm were identified. The tumor cells showed nuclear pleomorphism with occasional horseshoe-shaped nuclei, and frequent karyorrhexis (Fig. 3C).

The CSF specimen was diagnosed as malignant tumor involvement. Intrathecal methotrexate was added but did not have an effect, and the patient refused further treatment.

This study was approved by the Institutional Review Board of the Seoul National University Hospital with a waiver of informed consent (IRB No. 1801-102-917).

DISCUSSION

LM usually occurs as a late-stage complication of malignancy, and due to development in systemic therapy and improved survival, the at-risk patient population has increased.[4] De *et al*.[3] reported 23 cases of RMS with CNS relapse, including 21 cases with LM. In their report, CNS relapse occurred from 1 to 23 months after initial diagnosis, with median of 12 months. LM results from dissemination of tumor cells in CSF, and tumor cells reach the CSF by hematogenous spread, direct extension or by growing along the blood vessel or nerve sheath.[4] In our case, the tumor was located in the cervical lymph node at initial diagnosis, but the metastatic lesion developed an intracranial extension and LM after going through multiple cycles of treatment and recurrence. Time from initial diagnosis to LM was 29 months.

To date, literature on cytologic feature of RMS has been mainly focused on fine-needle aspiration (FNA). There are few reports on body fluid cytology, and this is the first report on CSF. In previous studies on fluid cytology, RMS cells commonly appeared as single cells or as or clusters of small round cells with scant to moderate amounts of vacuolated cytoplasm.[5] Tumor cells show hyperchromatic and pleomorphic nuclei with occasional prominent nucleoli, and some authors have reported rhabdomyoblast-like, multinucleated or large pleomorphic cells with eccentric nuclei.[6-8] Cytoplasmic cross-striation is not recog-

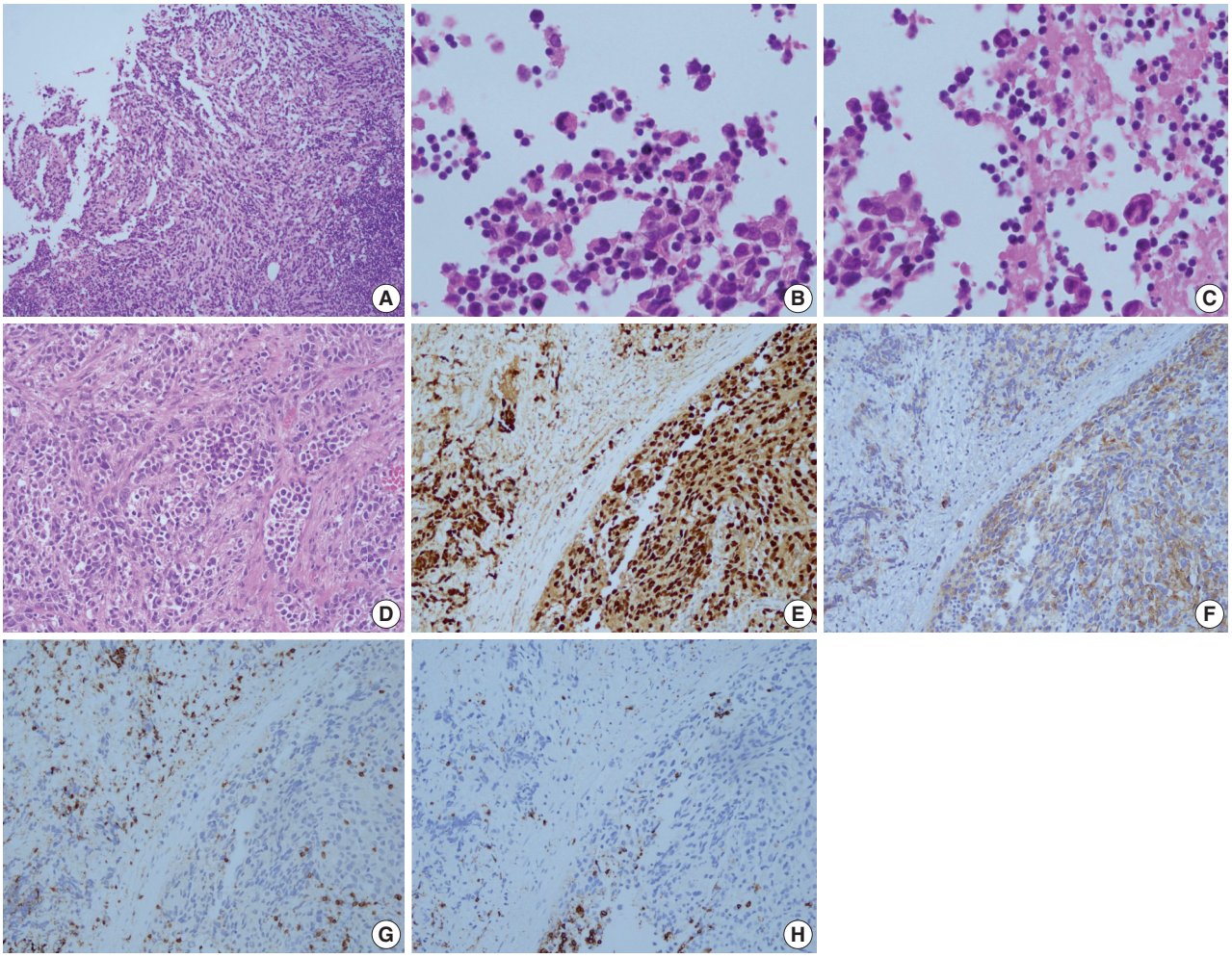

Fig. 2. Microscopic examination of the biopsied lymph node reveals malignant cells with a diffuse sheet-like pattern (A). A few cells show abundant cytoplasm and eccentric nuclei (B), and multinucleated cells are seen (C). Fibrovascular septa are observed in the neck dissection specimen (D). On immunohistochemistry, tumor cells are positive for myogenin (E) and anaplastic lymphoma kinase (F), and negative for CD3 (G) and CD20 (H).

nized in most cases. In immunocytochemistry, tumor cells show immunoreactivity for muscle-specific proteins such as myogenin, myoD1, desmin, and muscle-specific actin.[5,9] Electron microscopy and molecular study has also been reported to aid the diagnosis.[5,7,10]

The majority of cytomorphologic findings observed in our case were consistent with histopathology and previous literature, except for the horseshoe-shaped nuclei. These characteristics may cause concern about the possibility of malignant lymphoma, but they often appeared multilobated and peripherally located, sharing morphological similarity with multinucleated cells observed in the histology specimen and wreath-like nuclei reported in ARMS.[8] Karyorrhexis seemed to reflect the effect of prior therapy.

An ancillary study could not be performed in our case due to the limited amount and scarce cellularity of the CSF specimen, and attempt to destain and restain the cytology slides for muscle markers was unsuccessful. Nevertheless, the diagnosis of metastatic RMS could be made based on the patient's history, neuroimaging and CSF cytology which was well-correlated with the histopathology. In many cases, a CSF sample is of insufficient volume because the sample is small and often shared among laboratories for multiple tests.[11,12] Immunocytochemistry, electron microscopy or molecular study may aid the diagnosis of RMS with a cytology specimen, but the small sample size makes these tests difficult in CSF. Therefore, it is important to be aware of the cytomorphologic characteristics, compare with histology, and to consider clinical history and neuroimaging findings in making the diagnosis.

The present case was initially diagnosed as ERMS, but the biopsy from the recurrent lesion was diagnosed as ARMS based

 https://doi.org/10.4132/jptm.2018.05.15

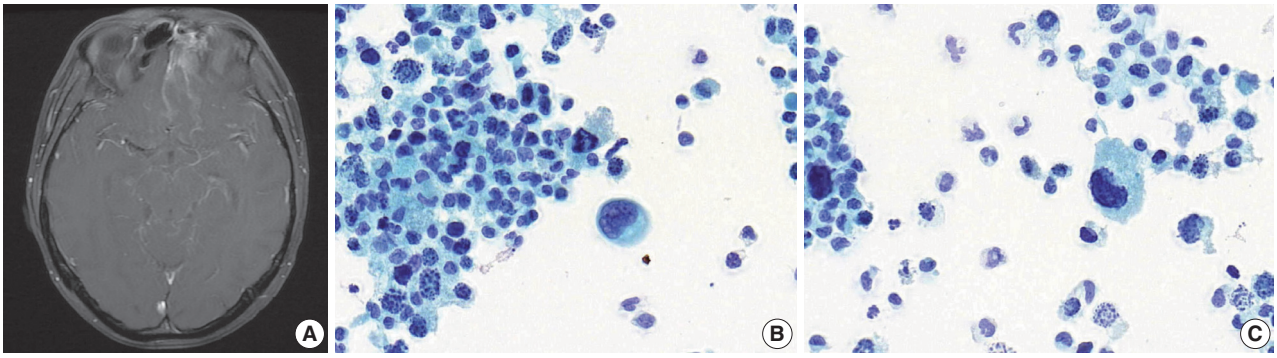

Fig. 3. Relapse in central nervous system. (A) Brain magnetic resonance imaging shows soft tissue lesion in the left ethmoid sinus and leptomeningeal enhancement. (B) In Papanicolau-staining of the cerebrospinal fluid specimen, small-sized cells and a large atypical cell with an eccentric nucleus are observed. (C) Peripherally located, horseshoe-shaped nuclei and frequent karryorhexis are noted.

on the IHC results. In the pathology review, myogenin showed diffuse strong immunoreactivity in both initial and recurrent lesions and features of ARMS, such as fibrovascular septa, were more evident in the neck dissection specimen (Fig. 2D, E). These findings support the diagnosis of ARMS over ERMS. A differential diagnosis of ARMS and ERMS can be challenging in small specimens or between solid variant of ARMS and ERMS with dense pattern, but myogenin immunostaining can provide diagnostic clues by showing diffuse, strong expression in ARMS and a more heterogeneous staining pattern in ERMS.[13,14]

The RMS subtype is closely related to the prognosis and there have been several attempts to subtype RMS cytologically, primarily in the FNA specimens. After studying 37 FNA and six touch imprint samples, Atahan *et al*.[15] reported that cells with abundant cytoplasm and eccentric nuclei, multinucleated cells and background mucoid substance support the diagnosis of ARMS while tadpole or ribbon-shaped cells and small round cells support the diagnosis of ERMS. Findings more suggestive of ARMS were observed in our case and several other reports regarding ARMS in body fluid.[5,8,10] However, elongated cells of ERMS are rarely appreciated in body fluid, and we were unable to find literature that documented mucoid substance in fluid cytology of RMS.[9] These findings suggest that cytologic features that are characteristic of specific RMS subtypes can be less evident, and subtyping of RMS might be more challenging in body fluid. Thiryayi *et al*.[5] reported a case of metastatic ARMS in pleural effusion that showed diffuse, strong nuclear positivity for myogenin, which was confirmed by *PAX3-FKHR* gene fusion in FISH, however this report was not within the context of subtyping. It seems likely that myogenin immunostaining may aid subtyping in cytology specimens as in histopathology, but the utility needs to be validated in further studies.

ALK aberration is reported in both ARMS and ERMS, and is known to be associated with metastatic disease and poor survival in ERMS.[16] In our case, the neoplastic cells showed ALK positivity in IHC which correlated with a gain of *ALK* gene copy number in FISH. The patient received crizotinib, the ALK inhibitor, but the disease markedly progressed despite therapy. Crizotinib is approved for the treatment of *ALK*-rearranged non-small cell lung cancer, but the majority of *ALK* gene aberration in RMS is copy number gain.[16] There are limited clinical trial data on the effect of crizotinib on ALK-positive RMS and its efficacy on RMS requires further investigation.[17]

Here we report a case of ALK-positive ARMS which invaded the CNS and developed multiple LMs. To our knowledge this is the first report to describe the cytologic features of RMS in CSF. RMS belongs to the small round blue cell tumors, and in the diagnostic process, the differential diagnosis of other small round blue cell tumors should be considered. Ancillary tests may aid in the diagnosis of RMS but are often difficult to perform in a CSF specimen. Therefore, it is crucial for cytopathologists to be aware of the cytologic features. It is also important to compare the cytology with histology, if available, and clinical history and neuroimaging findings should be considered in the diagnosis.

Conflicts of Interest

No potential conflict of interest relevant to this article was reported.

REFERENCES

1. Dagher R, Helman L. Rhabdomyosarcoma: an overview. Oncologist 1999; 4: 34-44.
2. Parham DM, Ellison DA. Rhabdomyosarcomas in adults and children: an update. Arch Pathol Lab Med 2006; 130: 1454-65.

3. De B, Kinnaman MD, Wexler LH, Kramer K, Wolden SL. Central nervous system relapse of rhabdomyosarcoma. Pediatr Blood Cancer 2017 Jul 11 [Epub]. htpps://doi.org/10.1002/pbc.26710.
4. Jaeckle KA. Neoplastic meningitis from systemic malignancies: diagnosis, prognosis and treatment. Semin Oncol 2006; 33: 312-23.
5. Thiryayi SA, Rana DN, Roulson J, *et al*. Diagnosis of alveolar rhabdomyosarcoma in effusion cytology: a diagnostic pitfall. Cytopathology 2010; 21: 273-5.
6. Thompson KS, Jensen JD, Bhoopalam N, Reyes CV. Pleural effusion cytology of embryonal rhabdomyosarcoma. Diagn Cytopathol 1997; 16: 270-3.
7. Hamada T, Tanimoto A, Kaido M, Matsumoto S, Iribe K, Koide O. Diffuse pleural rhabdomyosarcoma with persistent pleural effusion. Acta Pathol Jpn 1989; 39: 803-9.
8. Nelson AC, Singh C, Pambuccian SE. Cytological diagnosis of metastatic alveolar rhabdomyosarcoma in the ascitic fluid: report of a case highlighting the diagnostic difficulties. Cytojournal 2012; 9: 9.
9. Bhattacharya B, Sariya D, Reddy VB, Kluskens L, Gould VE, Gattuso P. Application of adjunct techniques in cytologic material in the diagnosis of rhabdomyosarcoma: case report and review of the literature. Diagn Cytopathol 2002; 26: 384-6.
10. Theunissen P, Cremers M, van der Meer S, Bot F, Bras J. Cytologic diagnosis of rhabdomyosarcoma in a child with a pleural effusion: a case report. Acta Cytol 2004; 48: 249-53.
11. Walts AE. Cerebrospinal fluid cytology: selected issues. Diagn Cytopathol 1992; 8: 394-408.
12. Chamberlain MC, Glantz M, Groves MD, Wilson WH. Diagnostic tools for neoplastic meningitis: detecting disease, identifying patient risk, and determining benefit of treatment. Semin Oncol 2009; 36(4 Suppl 2): S35-45.
13. Rudzinski ER, Teot LA, Anderson JR, *et al*. Dense pattern of embryonal rhabdomyosarcoma, a lesion easily confused with alveolar rhabdomyosarcoma: a report from the Soft Tissue Sarcoma Committee of the Children's Oncology Group. Am J Clin Pathol 2013; 140: 82-90.
14. Dias P, Chen B, Dilday B, *et al*. Strong immunostaining for myogenin in rhabdomyosarcoma is significantly associated with tumors of the alveolar subclass. Am J Pathol 2000; 156: 399-408.
15. Atahan S, Aksu O, Ekinci C. Cytologic diagnosis and subtyping of rhabdomyosarcoma. Cytopathology 1998; 9: 389-97.
16. van Gaal JC, Flucke UE, Roeffen MH, *et al*. Anaplastic lymphoma kinase aberrations in rhabdomyosarcoma: clinical and prognostic implications. J Clin Oncol 2012; 30: 308-15.
17. Felkai L, Bánusz R, Kovalszky I, *et al*. The presence of ALK alterations and clinical relevance of crizotinib treatment in pediatric solid tumors. Pathol Oncol Res 2017 Oct 28 [Epub]. https://doi.org/10.1007/s12253-017-0332-1.


JPTM
Journal of Pathology and
Translational Medicine